US 20180333456A1

(19) **United States**

(12) **Patent Application Publication**

Deisseroth et al.

(10) **Pub. No.: US 2018/0333456 A1**

(43) **Pub. Date: Nov. 22, 2018**

(54) **OPTICALLY-CONTROLLED CNS DYSFUNCTION**

(71) Applicant: **The Board of Trustees of the Leland Stanford Junior Universit**, Stanford, CA (US)

(72) Inventors: **Karl Deisseroth**, Stanford, CA (US); **Kay Tye**, Cambridge, MA (US); **Lief Fenno**, San Francisco, CA (US)

(21) Appl. No.: **15/957,608**

(22) Filed: **Apr. 19, 2018**

Related U.S. Application Data

(60) Continuation of application No. 15/194,379, filed on Jun. 27, 2016, now Pat. No. 9,968,652, which is a division of application No. 14/555,048, filed on Nov. 26, 2014, now Pat. No. 9,421,258, which is a division of application No. 13/882,719, filed on Jul. 29, 2013, now Pat. No. 8,932,562, filed as application No. PCT/US2011/059298 on Nov. 4, 2011.

(60) Provisional application No. 61/464,806, filed on Mar. 8, 2011, provisional application No. 61/410,748, filed on Nov. 5, 2010.

Publication Classification

(51) **Int. Cl.**

A61K 38/17	(2006.01)
A01K 67/027	(2006.01)
G01N 33/50	(2006.01)
A61K 9/00	(2006.01)
A61K 49/00	(2006.01)
C07K 14/705	(2006.01)
A61K 41/00	(2006.01)
C12N 15/85	(2006.01)
C12N 15/86	(2006.01)
C12N 7/00	(2006.01)
A61K 48/00	(2006.01)
A61N 5/06	(2006.01)
A61B 5/16	(2006.01)

(52) **U.S. Cl.**

CPC ***A61K 38/177*** (2013.01); *A01K 2267/0356* (2013.01); *C12N 2750/14143* (2013.01); ***G01N 33/5088*** (2013.01); ***A61K 9/0019*** (2013.01); ***A61K 49/0008*** (2013.01); ***C07K 14/705*** (2013.01); ***A61K 41/00*** (2013.01); *A01K 2217/072* (2013.01); ***C12N 15/8509*** (2013.01); ***C12N 15/86*** (2013.01); *C12N 2015/859* (2013.01); ***A01K 67/0278*** (2013.01); ***C12N 7/00*** (2013.01); ***A61K 48/0058*** (2013.01); *C12N 2799/025* (2013.01); ***A61N 5/062*** (2013.01); ***A61B 5/165*** (2013.01); ***A61K 49/0004*** (2013.01); *A01K 2267/0393* (2013.01); *A01K 2227/105* (2013.01); ***A01K 67/0275*** (2013.01)

(57) **ABSTRACT**

Provided herein are animals expressing light-responsive opsin proteins in the basal lateral amygdala of the brain and methods for producing the same wherein illumination of the light-responsive opsin proteins causes anxiety in the animal. Also provided herein are methods for alleviating and inducing anxiety in an animal as well as methods for screening for a compound that alleviates anxiety in an animal.

Specification includes a Sequence Listing.

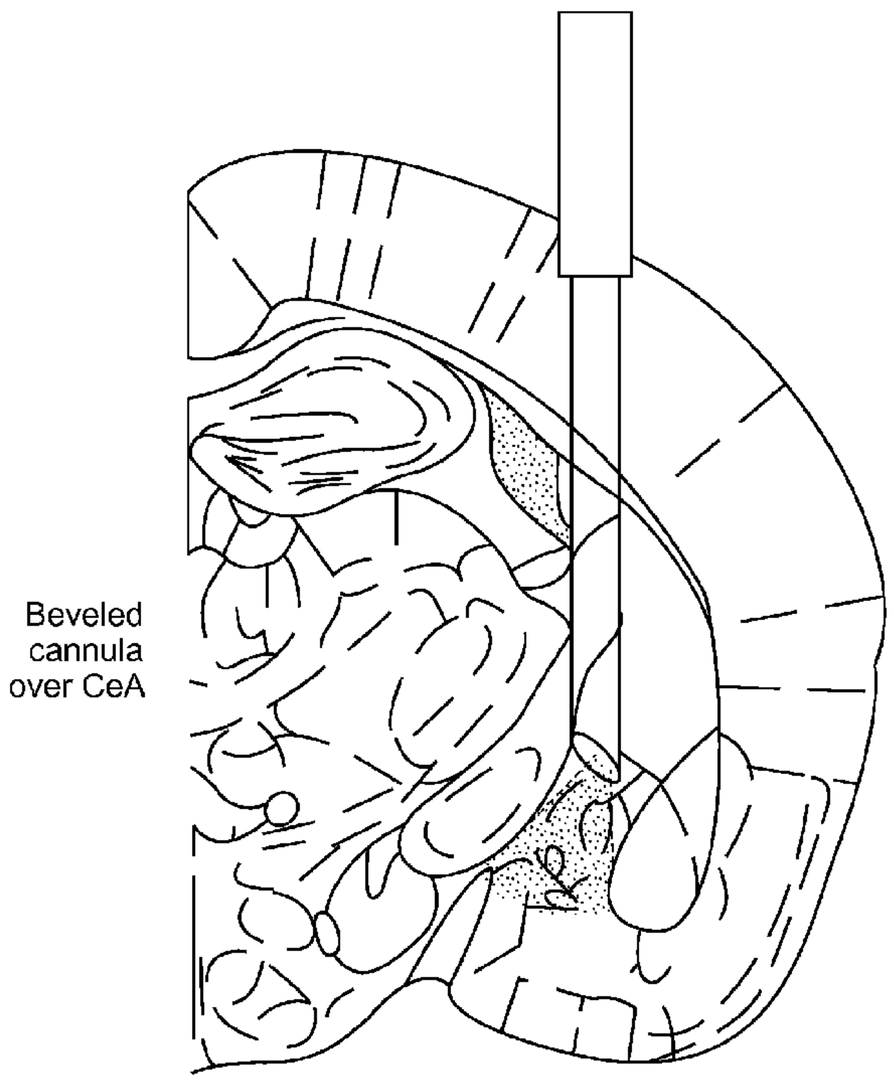

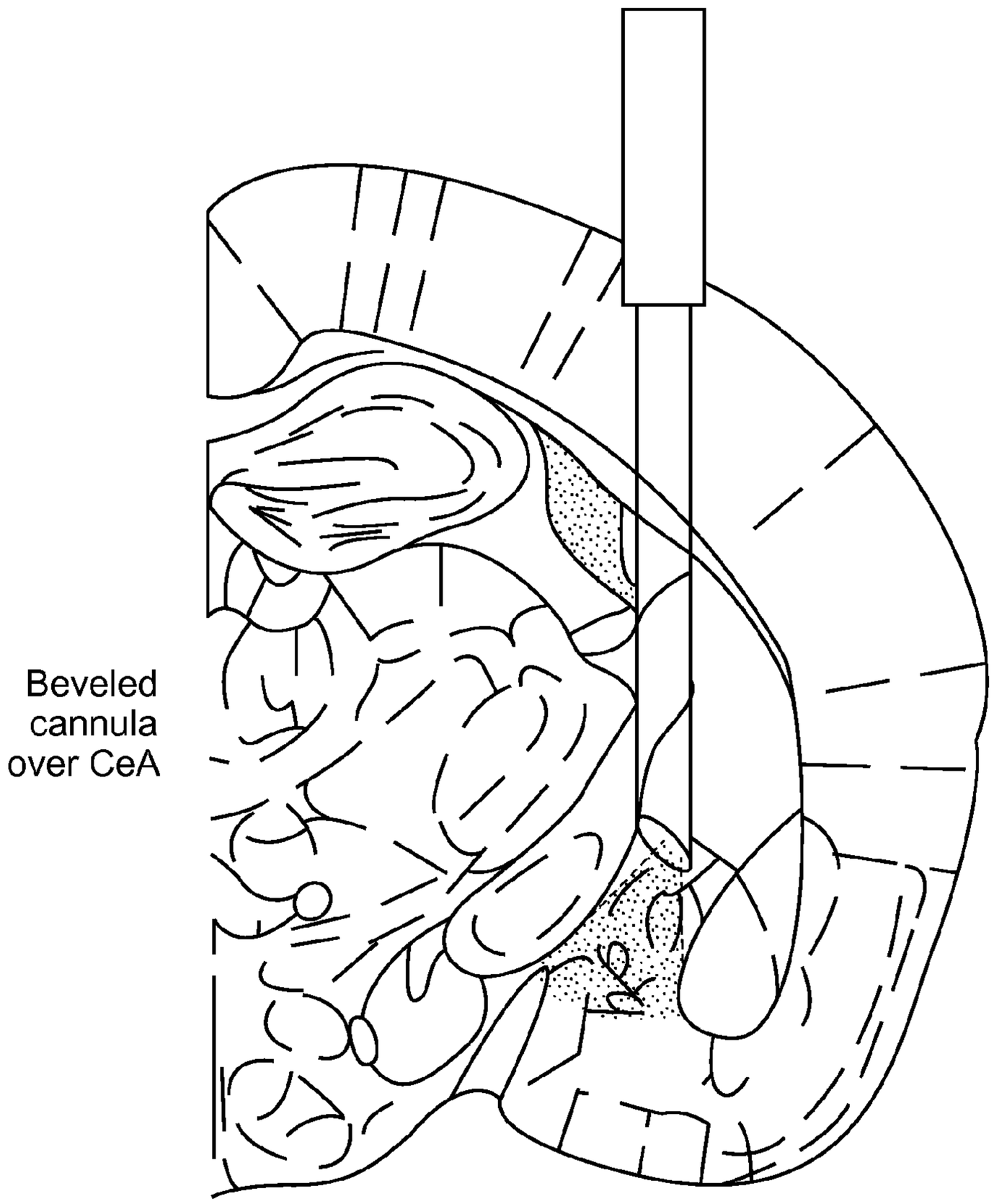

FIG. 1

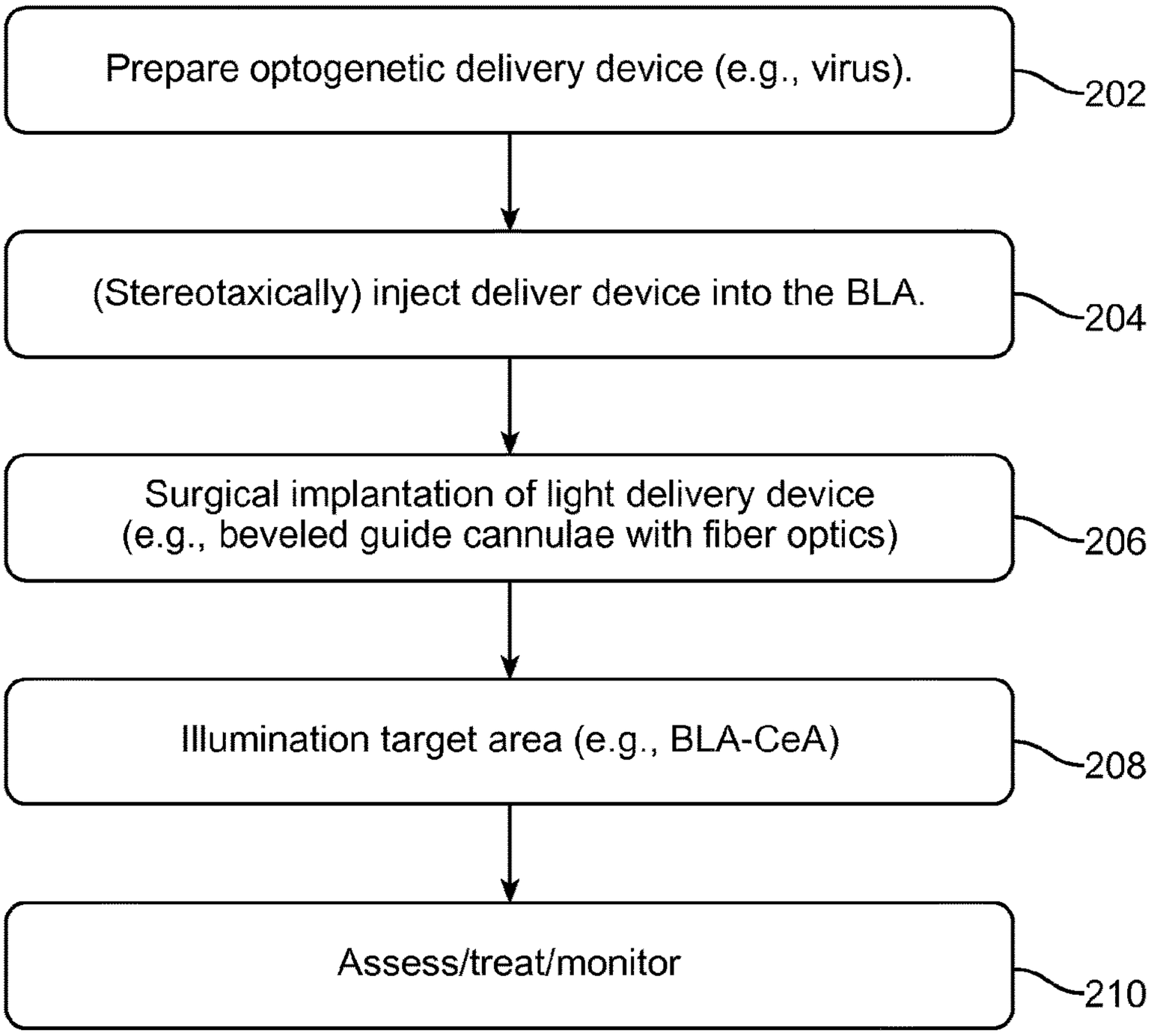
Prepare optogenetic delivery device (e.g., virus).
202
(Stereotaxically) inject deliver device into the BLA.
204
Surgical implantation of light delivery device
(e.g., beveled guide cannulae with fiber optics)
206
Illumination target area (e.g., BLA-CeA)
208
Assess/treat/monitor
210

FIG. 2

FIG. 3A

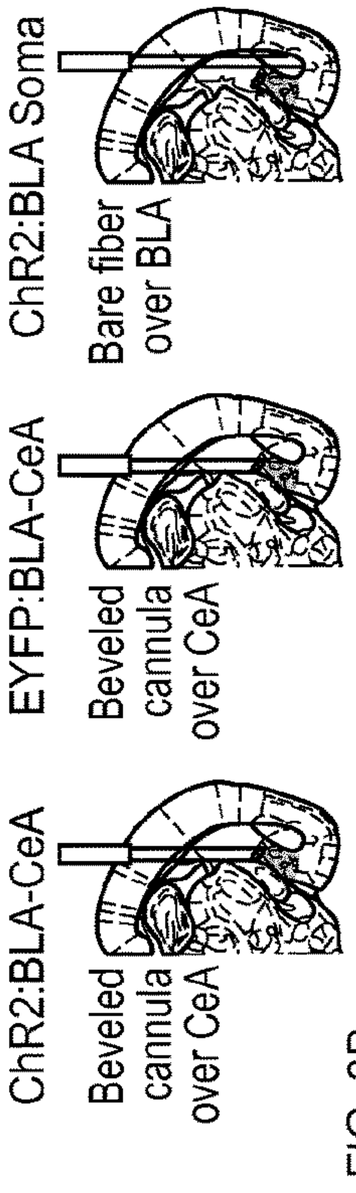

FIG. 3B

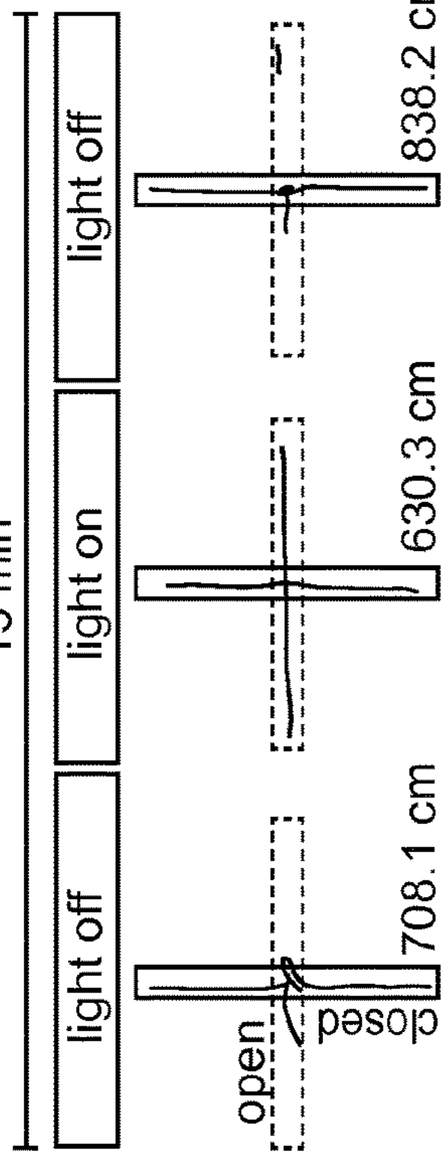

FIG. 3C

FIG. 3D

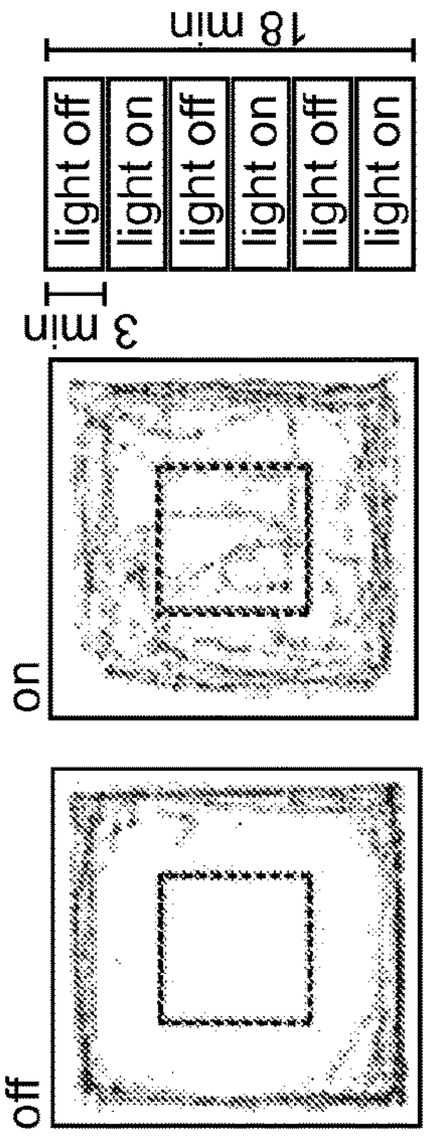

FIG. 3E

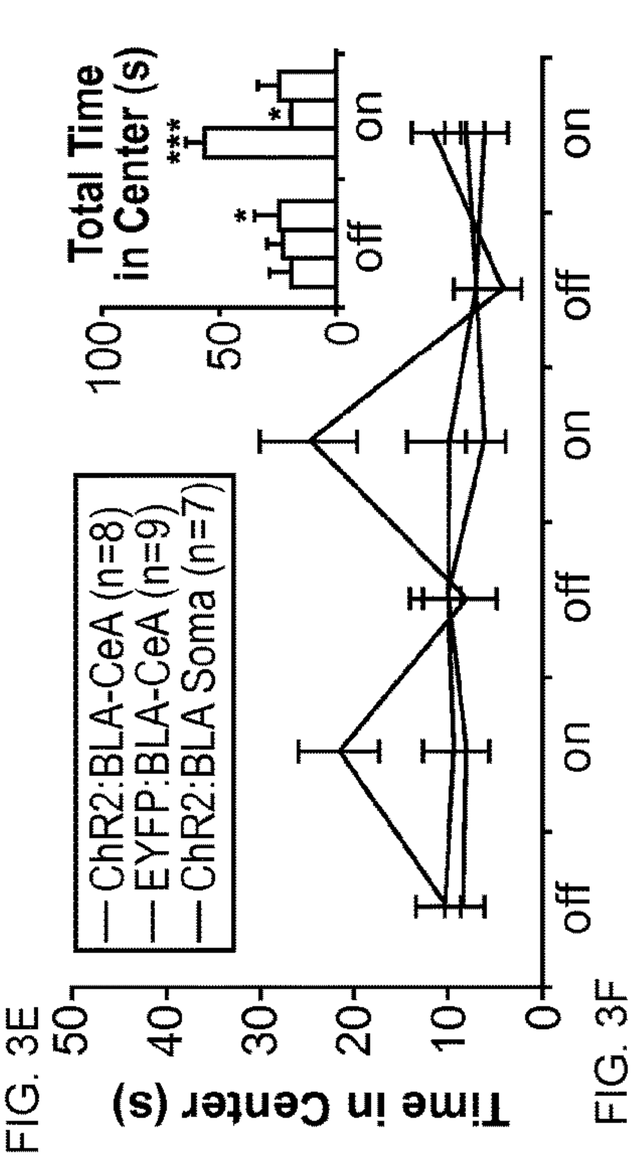

FIG. 3F

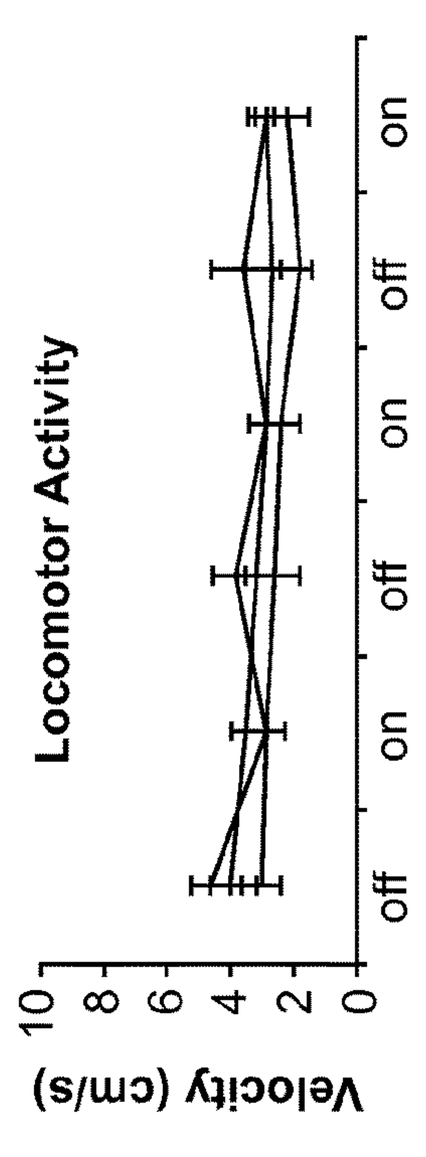

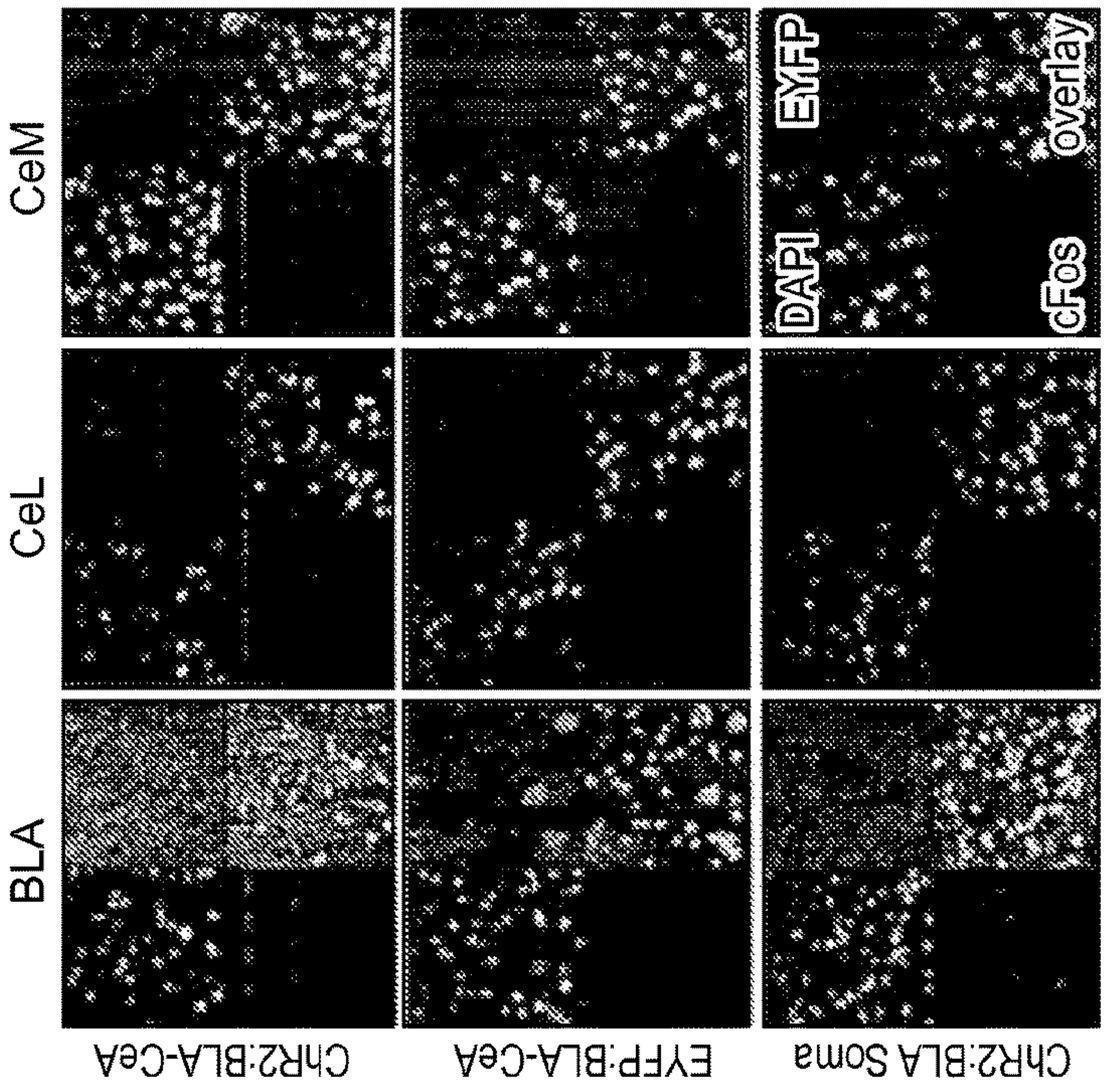

FIG. 3H

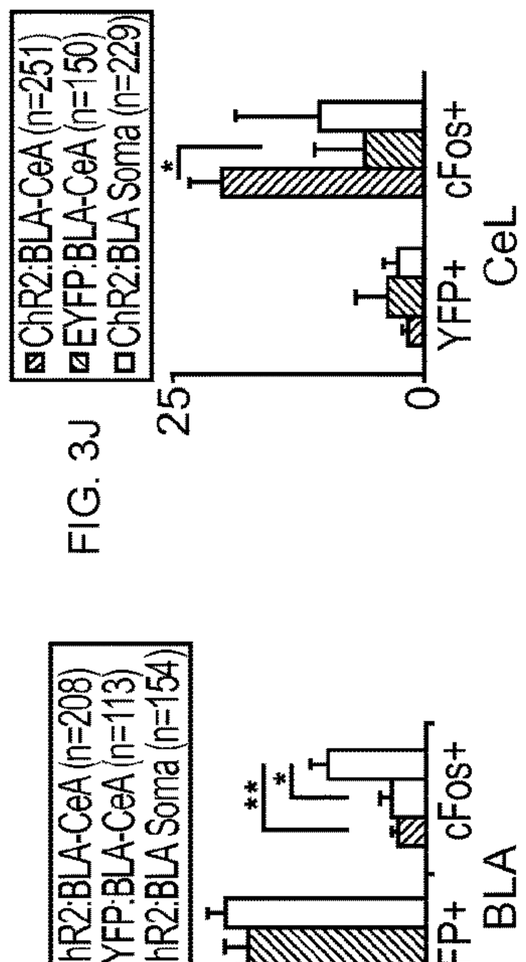

FIG. 3K

FIG. 3J

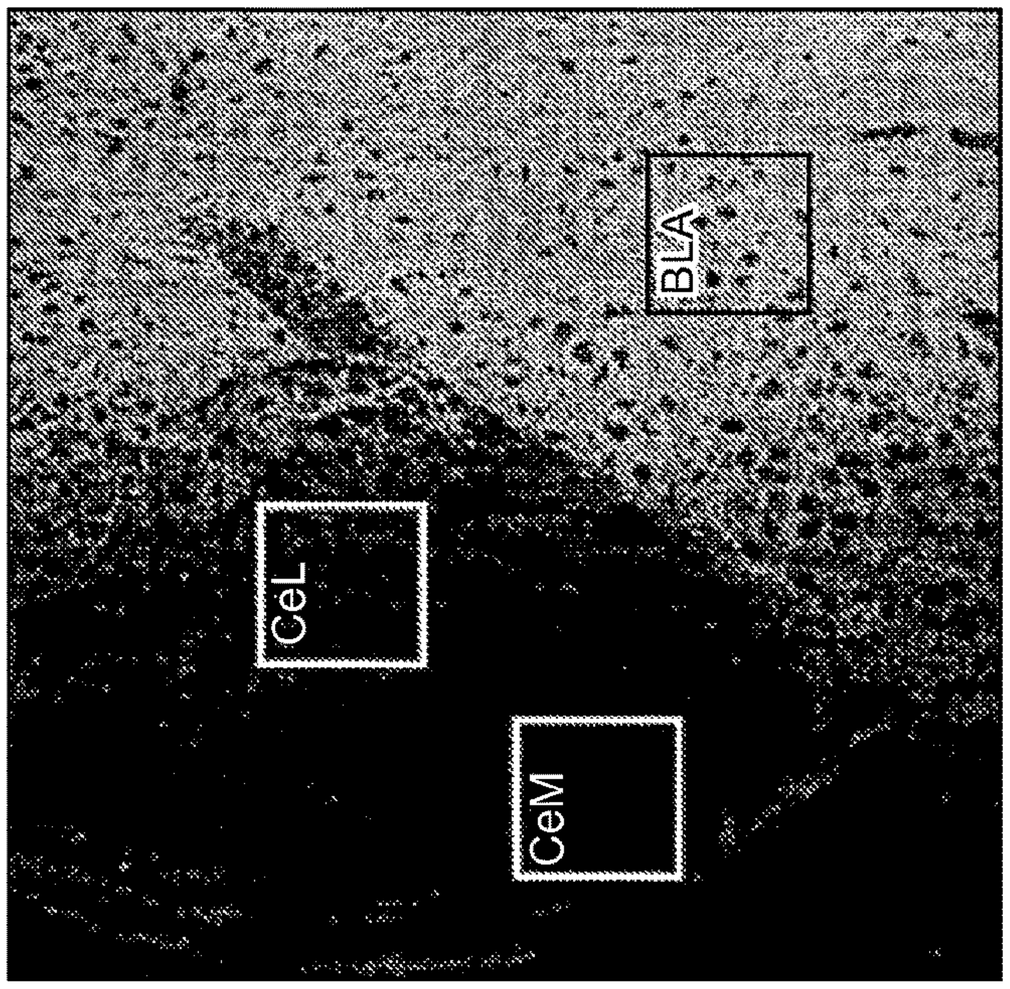

FIG. 3G

FIG. 3I

FIG. 4A

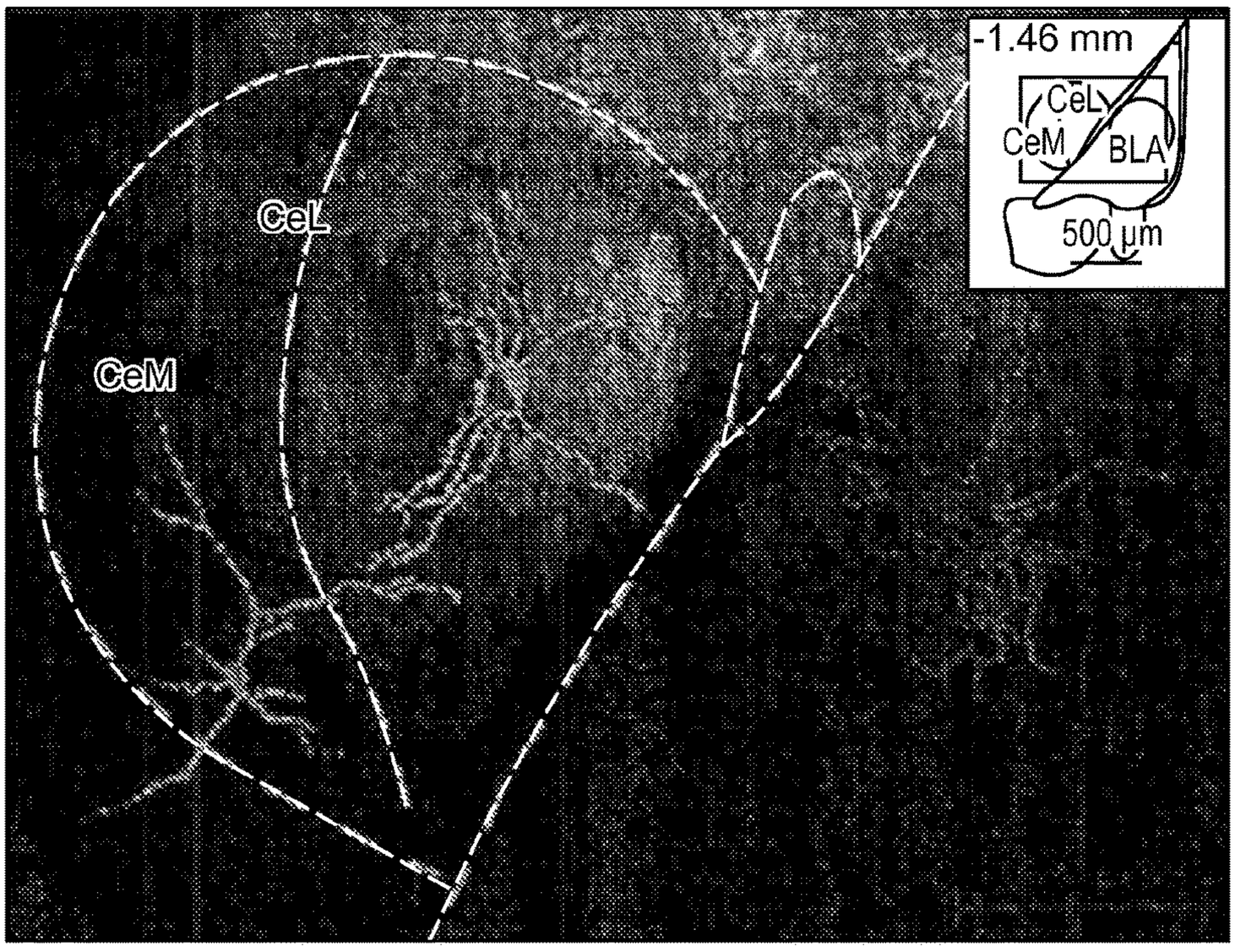

FIG. 4B

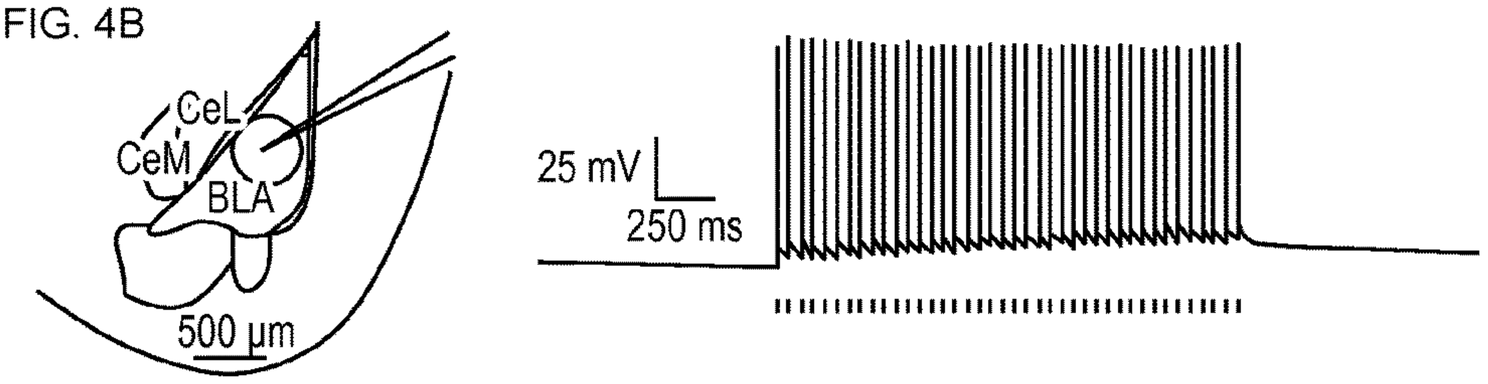

FIG. 4C

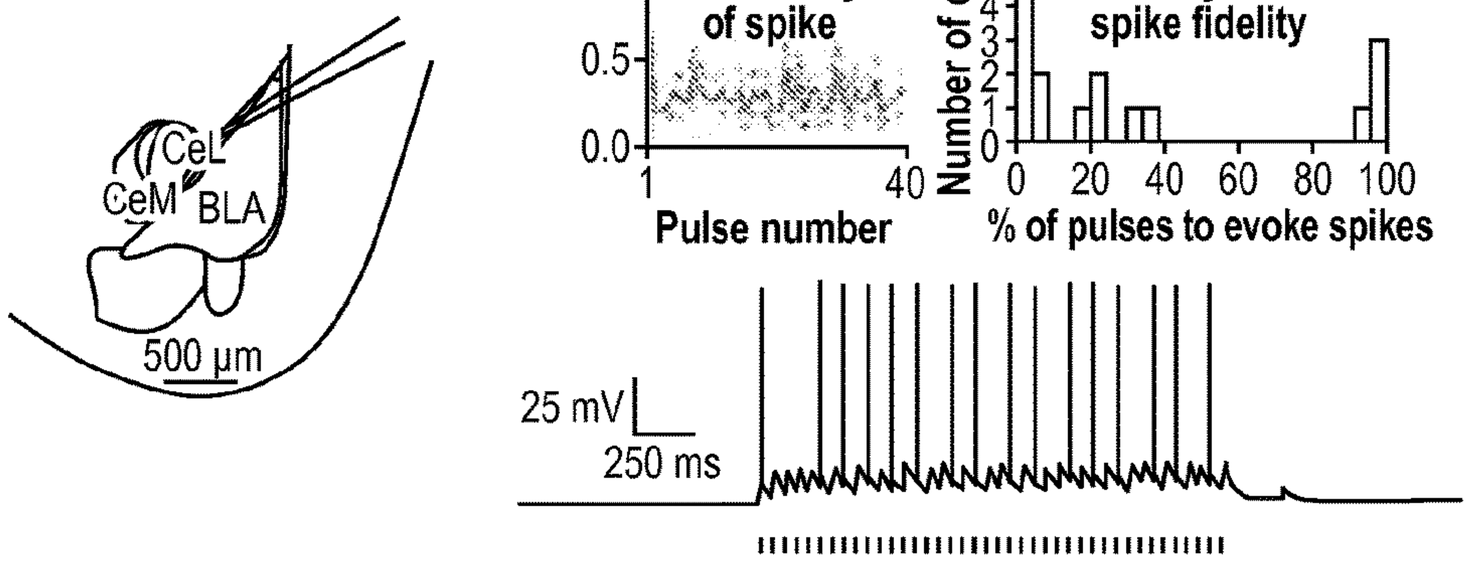

FIG. 4D

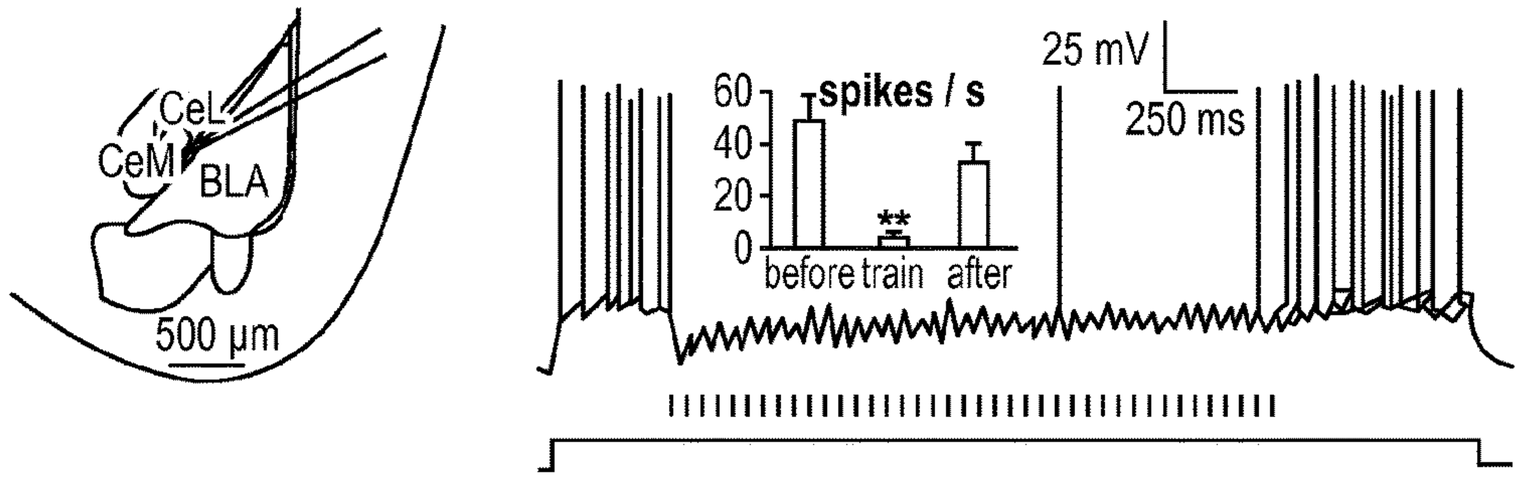

FIG. 4E

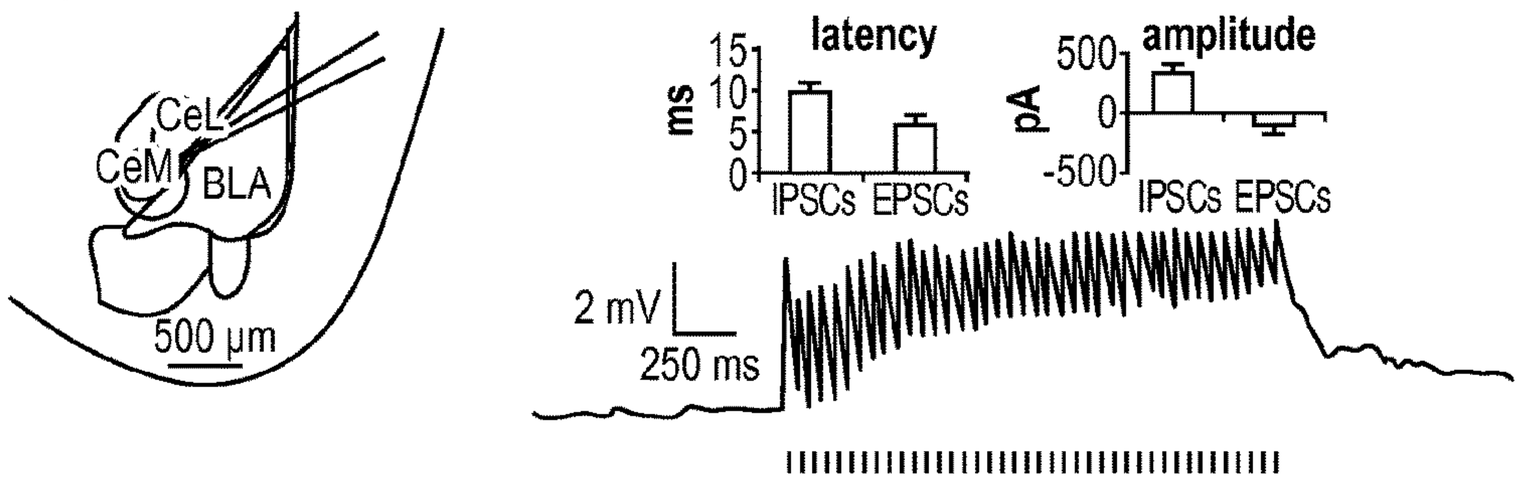

FIG. 4F

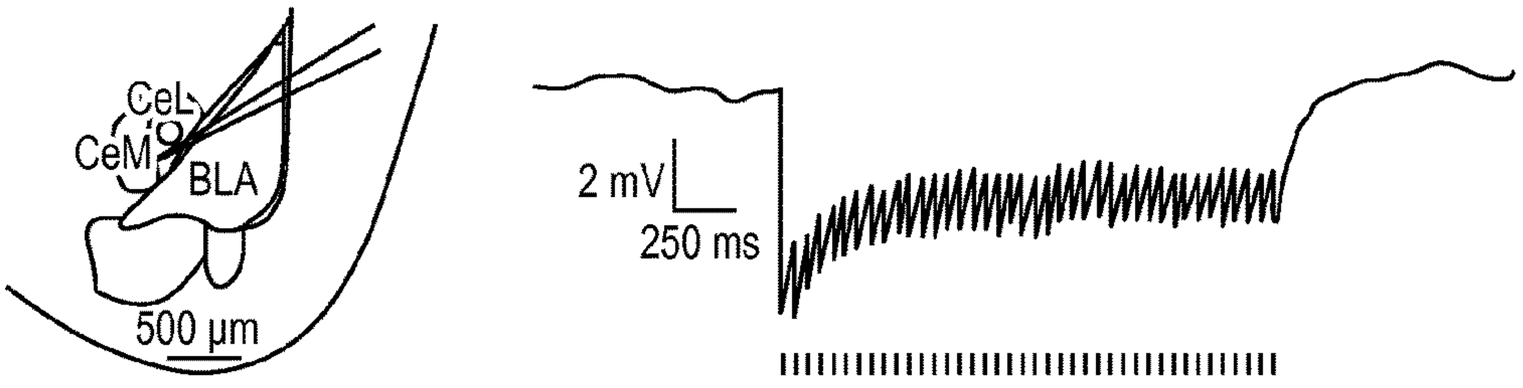

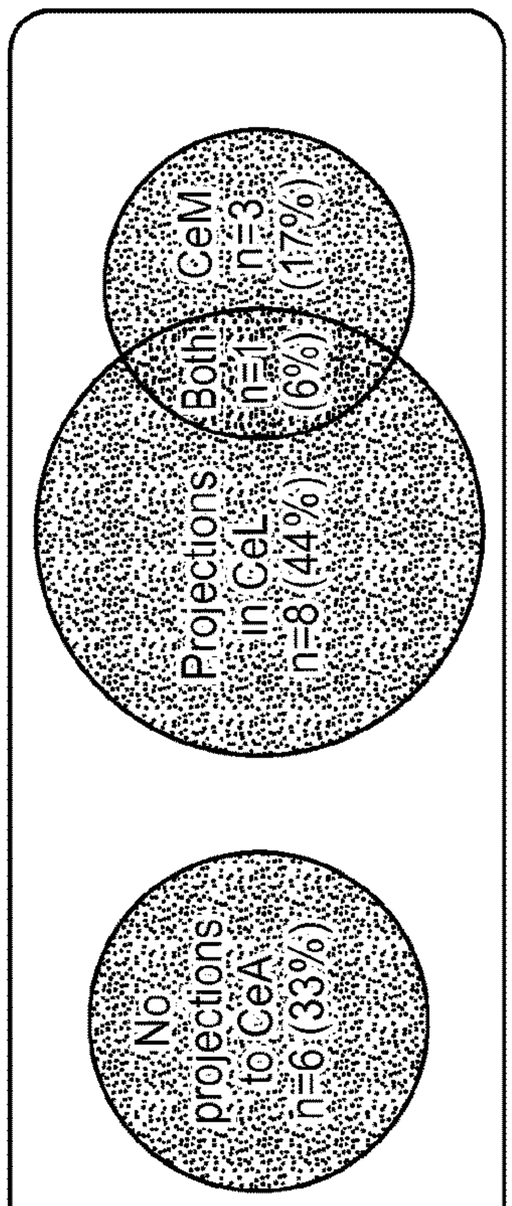

FIG. 5A

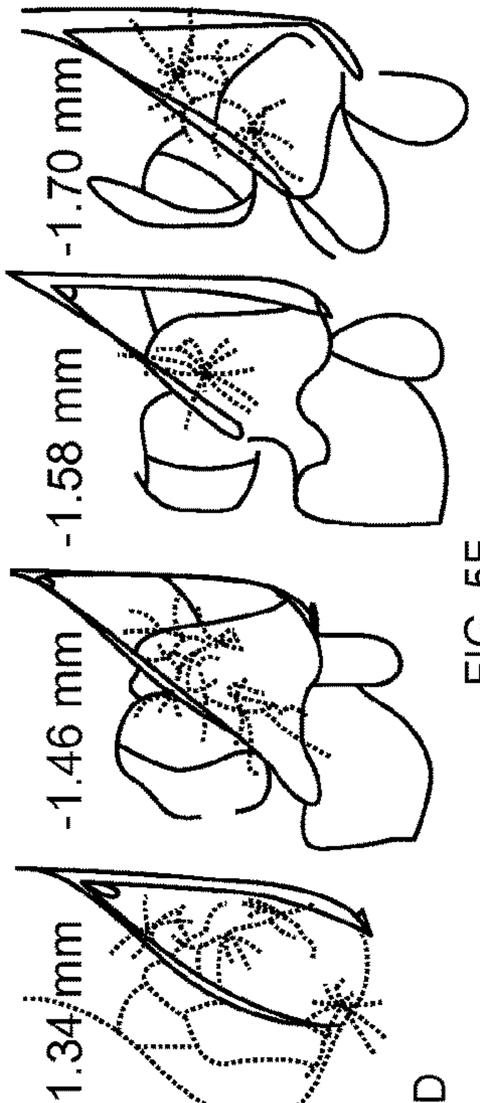

FIG. 5B

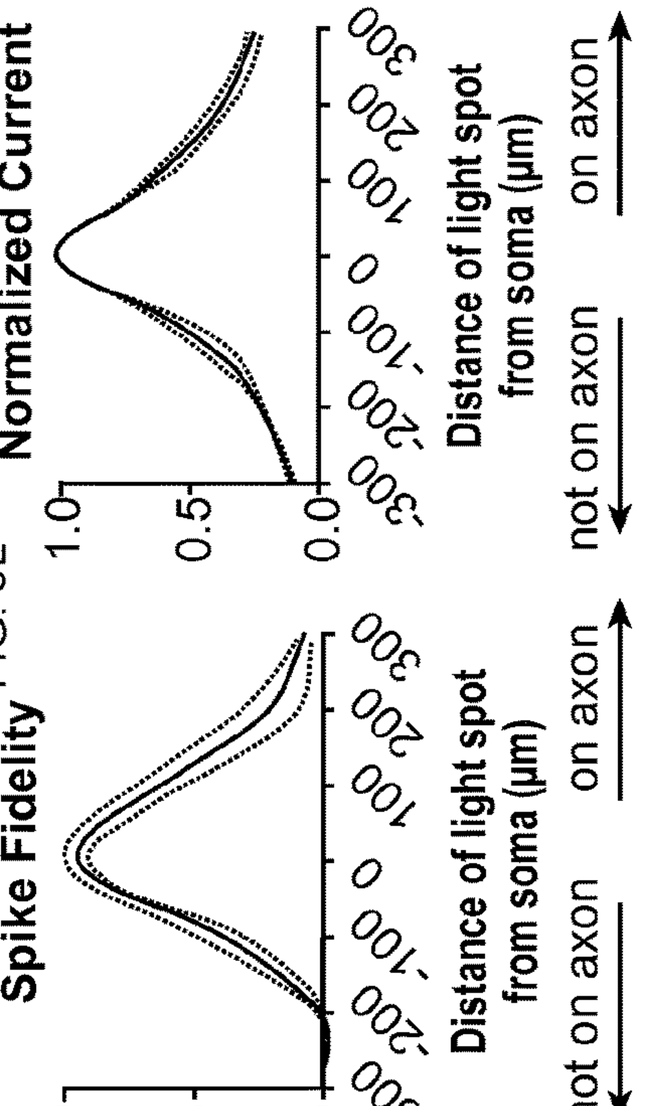

FIG. 5D FIG. 5E

FIG. 5C

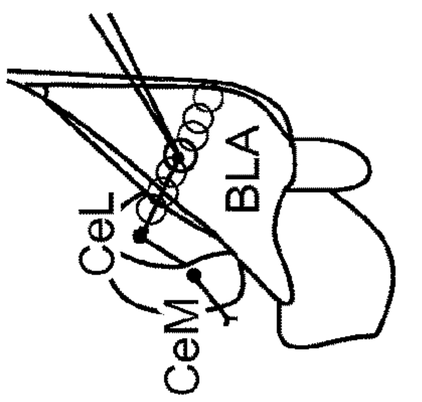

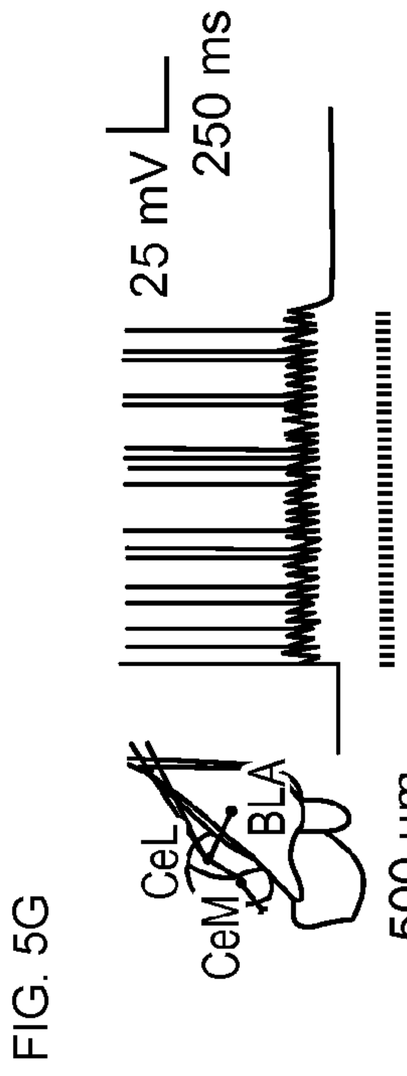

FIG. 5G

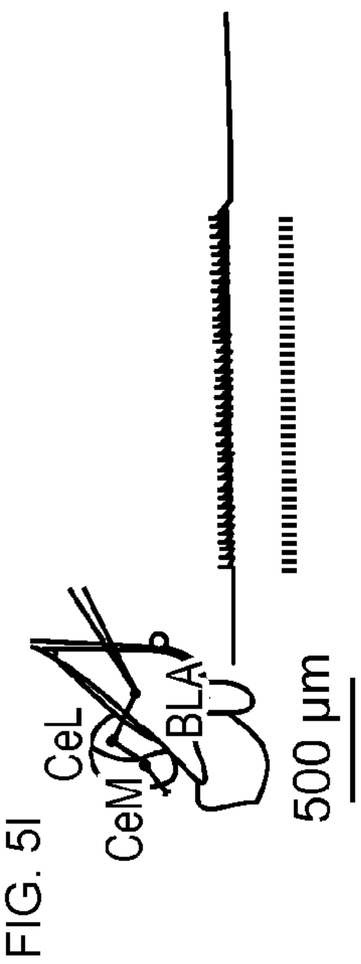

FIG. 5I

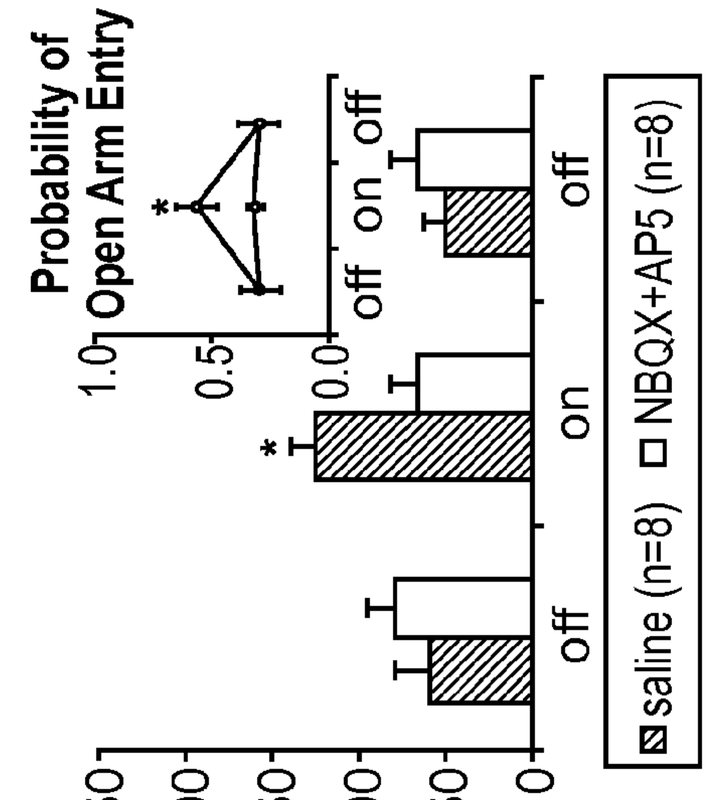

FIG. 5K

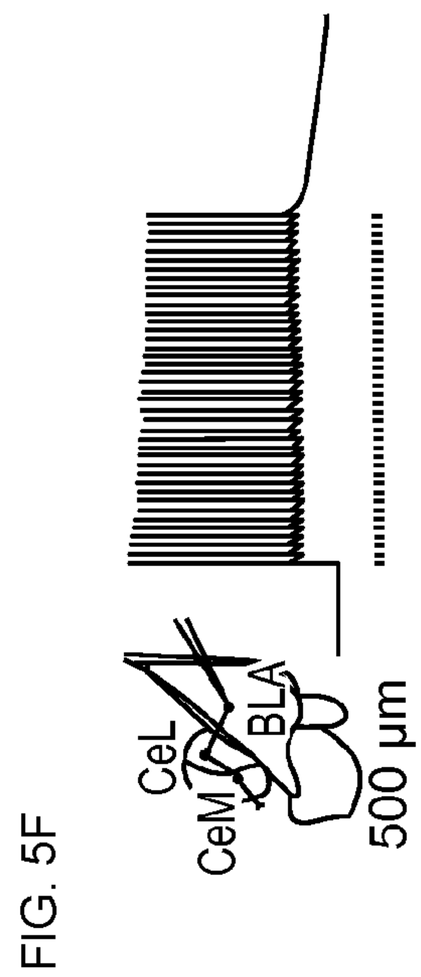

FIG. 5F

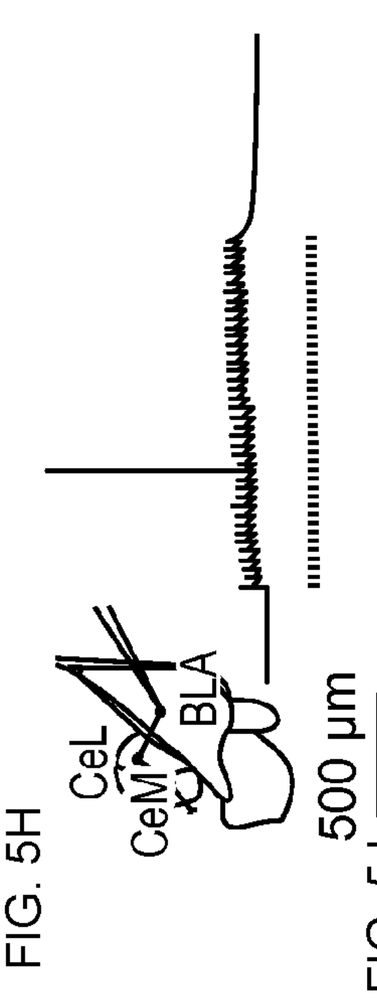

FIG. 5H

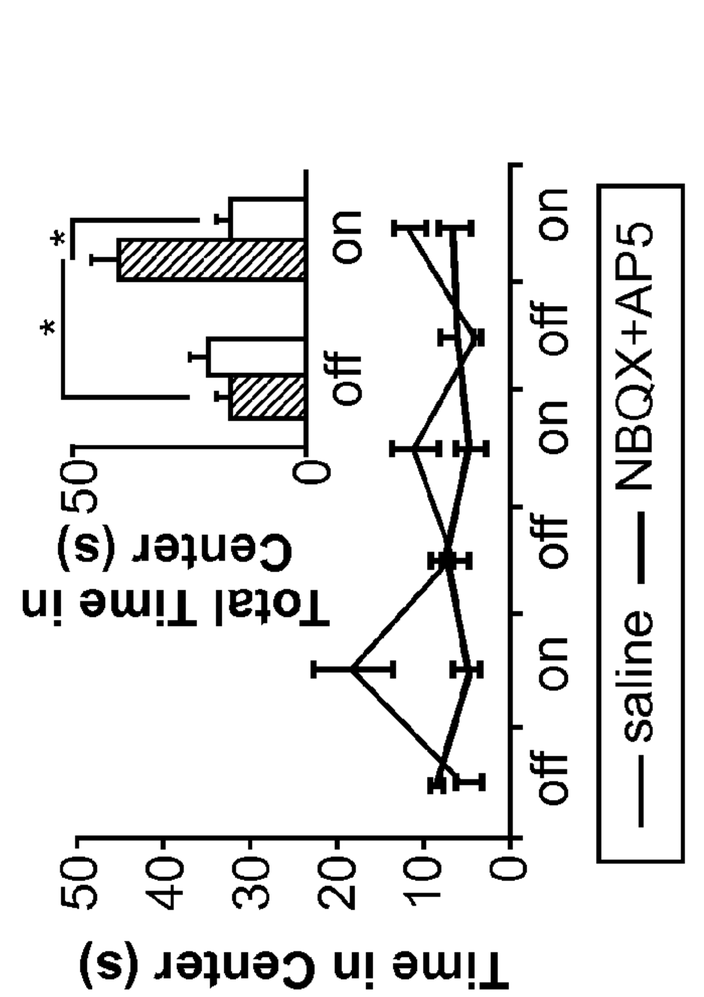

FIG. 5J

FIG. 6A

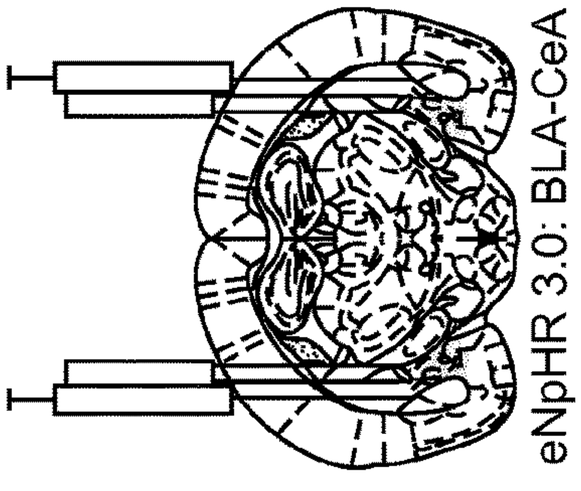

FIG. 6B

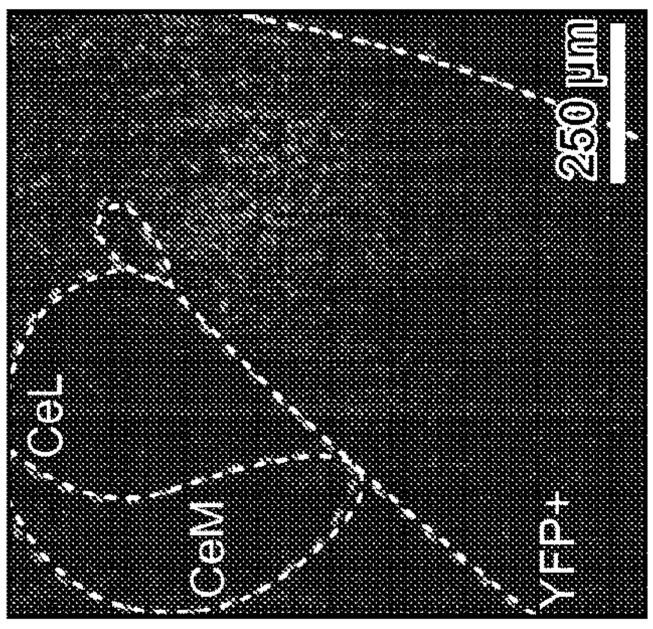

FIG. 6C

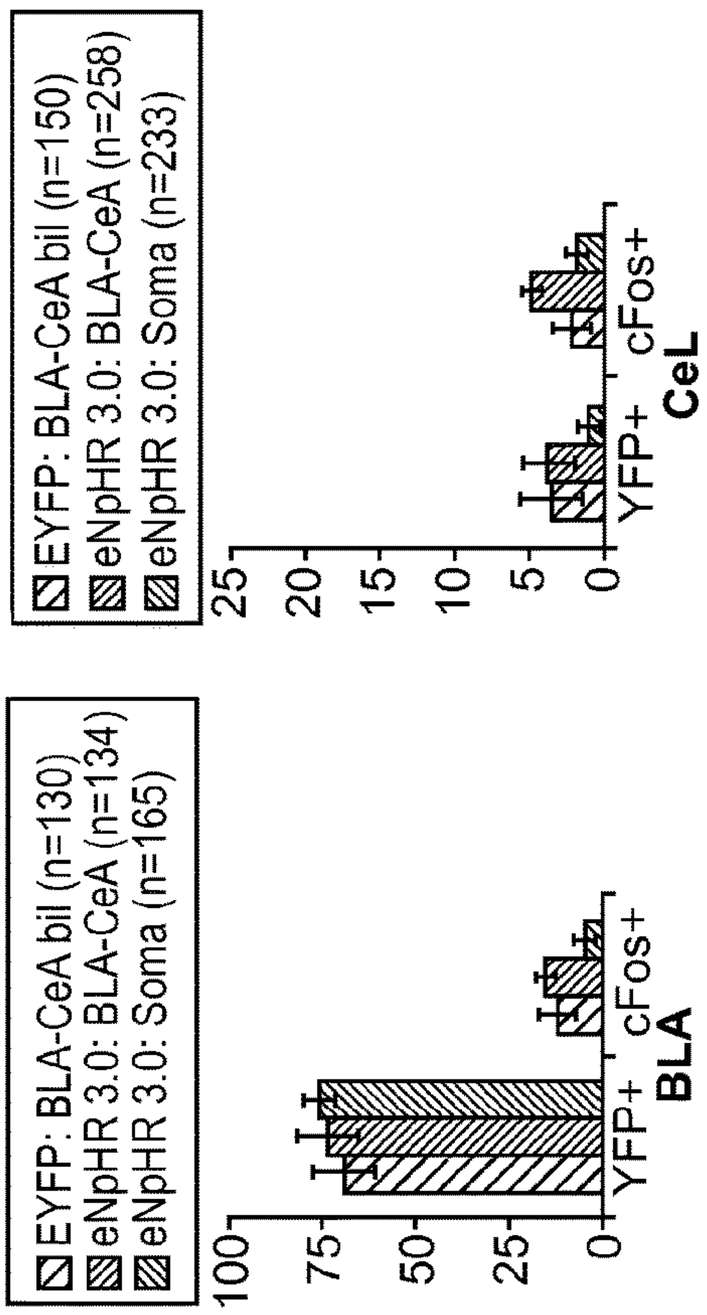

FIG. 6D

FIG. 6E

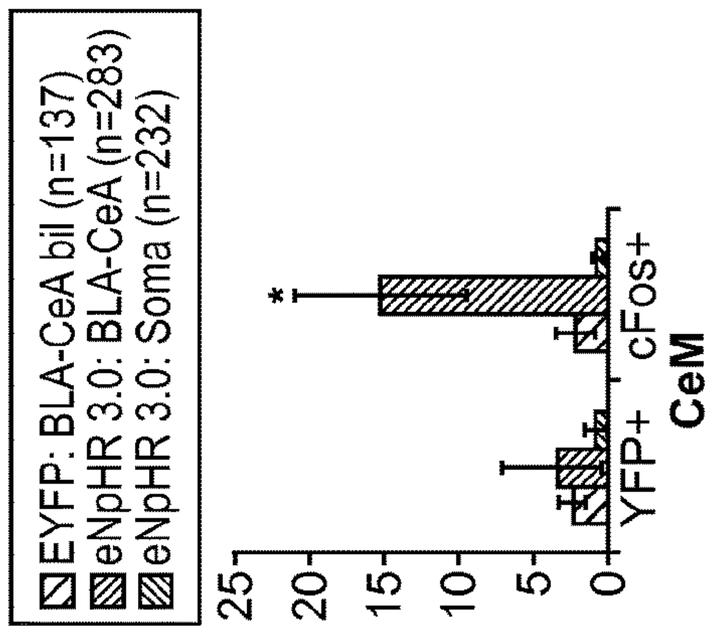

FIG. 6F

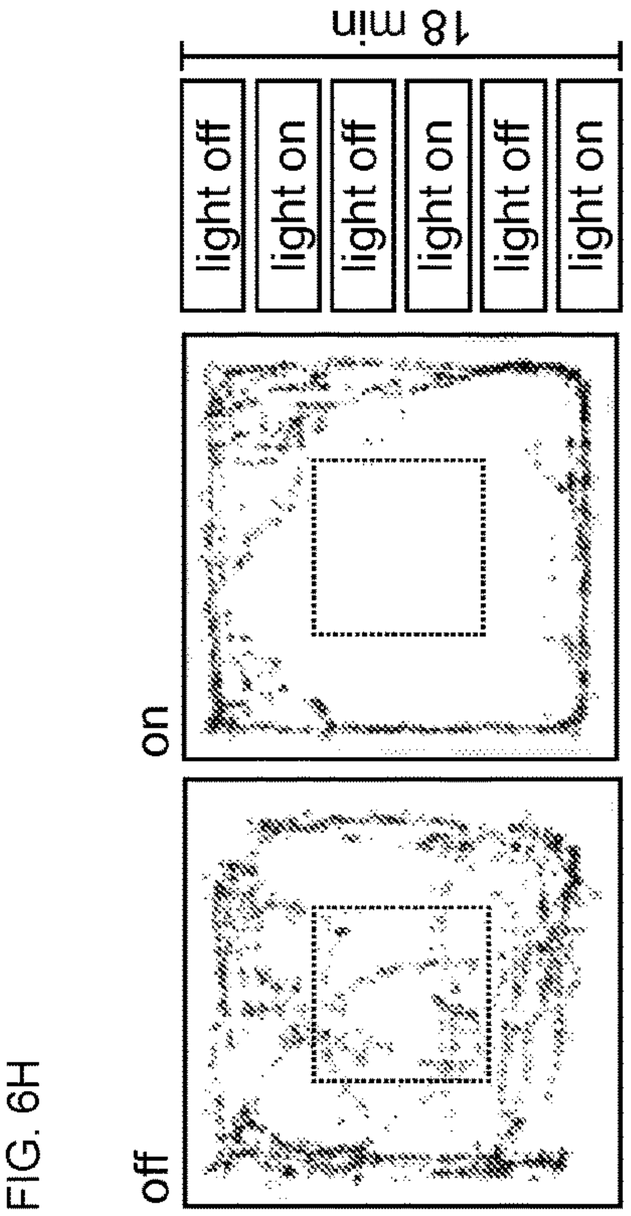

FIG. 6H

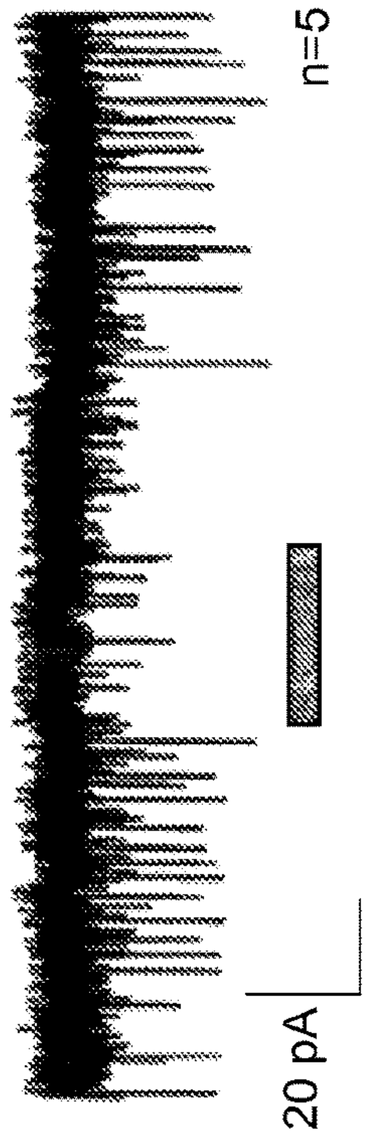

FIG. 6J
sEPSCs in 20 µm carbachol

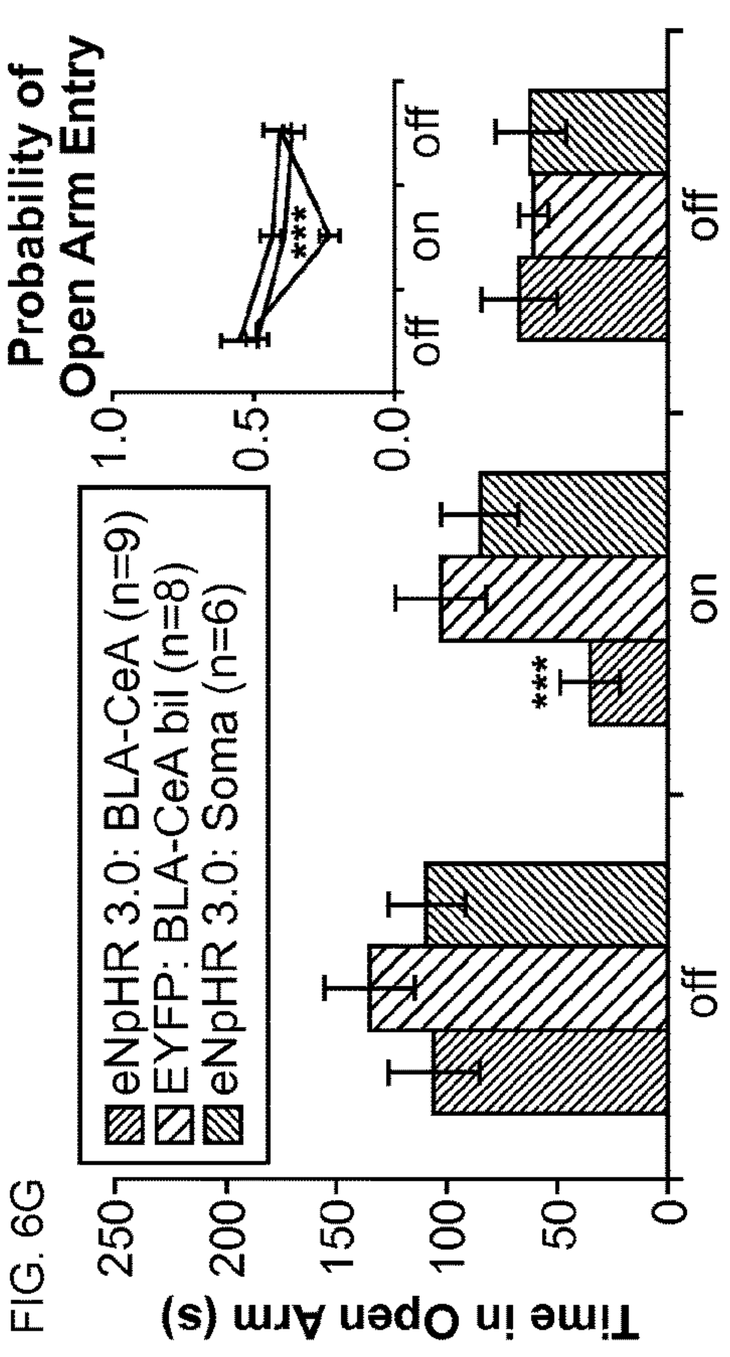

FIG. 6G

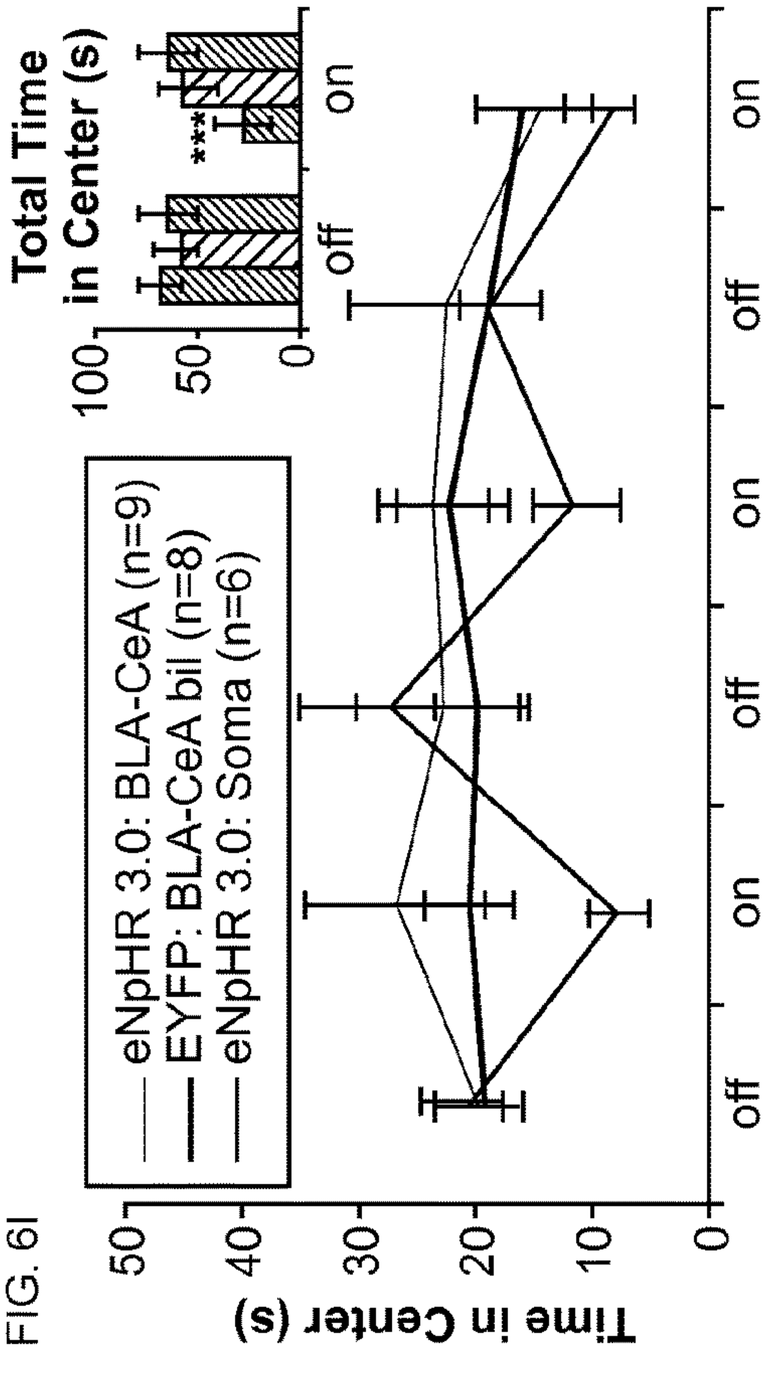

FIG. 6I

FIG. 6M

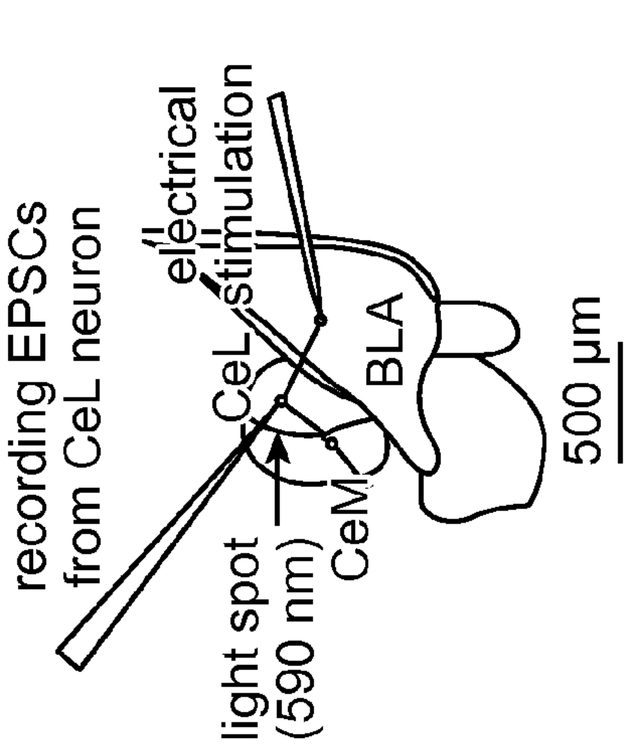

FIG. 6P

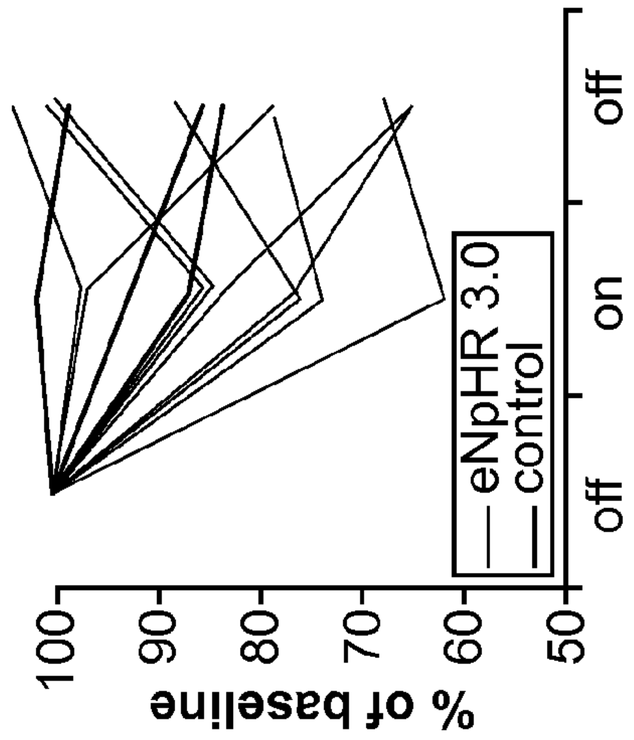

FIG. 6L

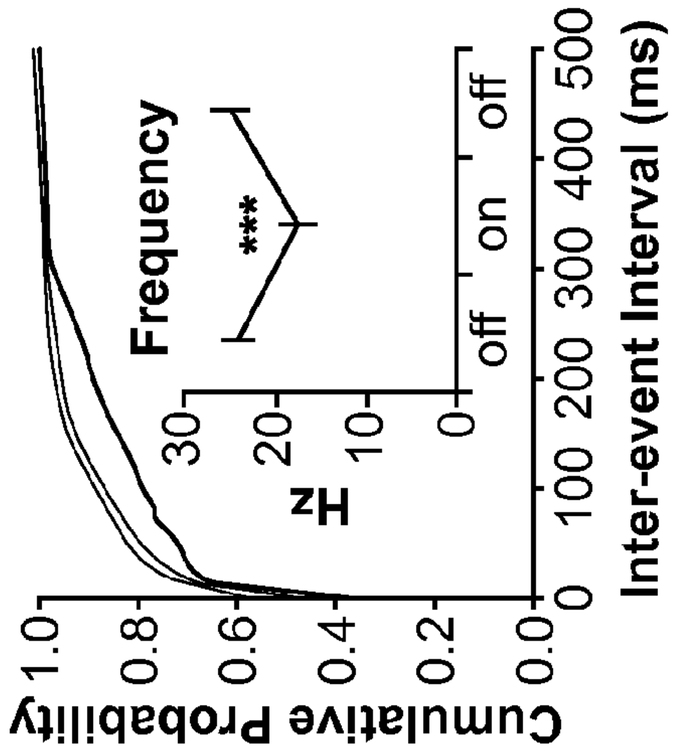

FIG. 6O

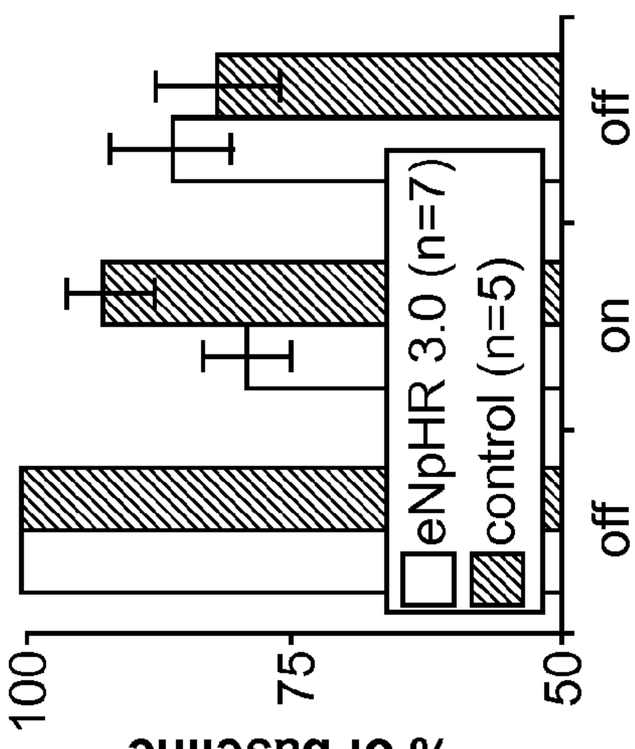

FIG. 6K

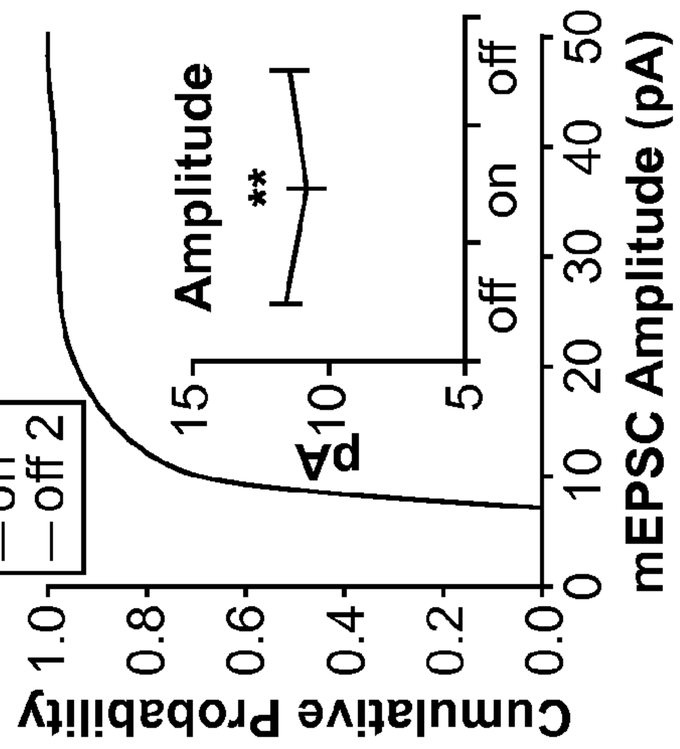

FIG. 6N

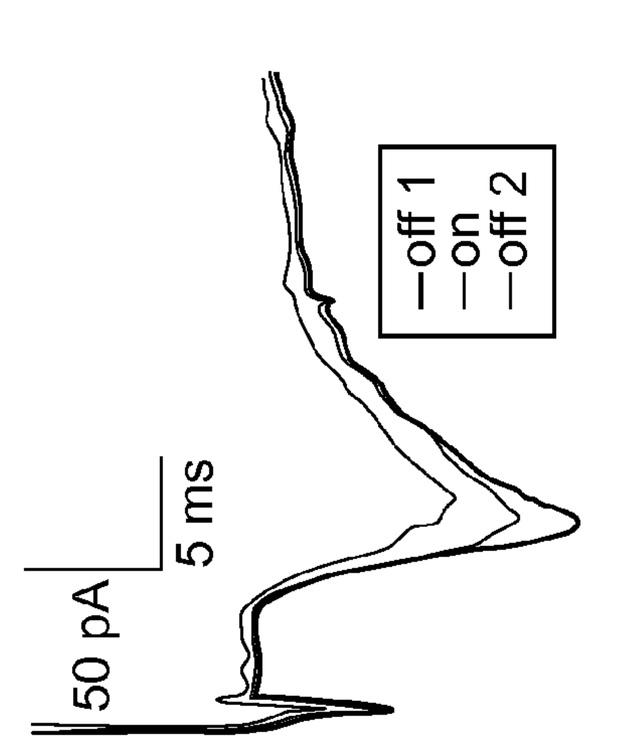

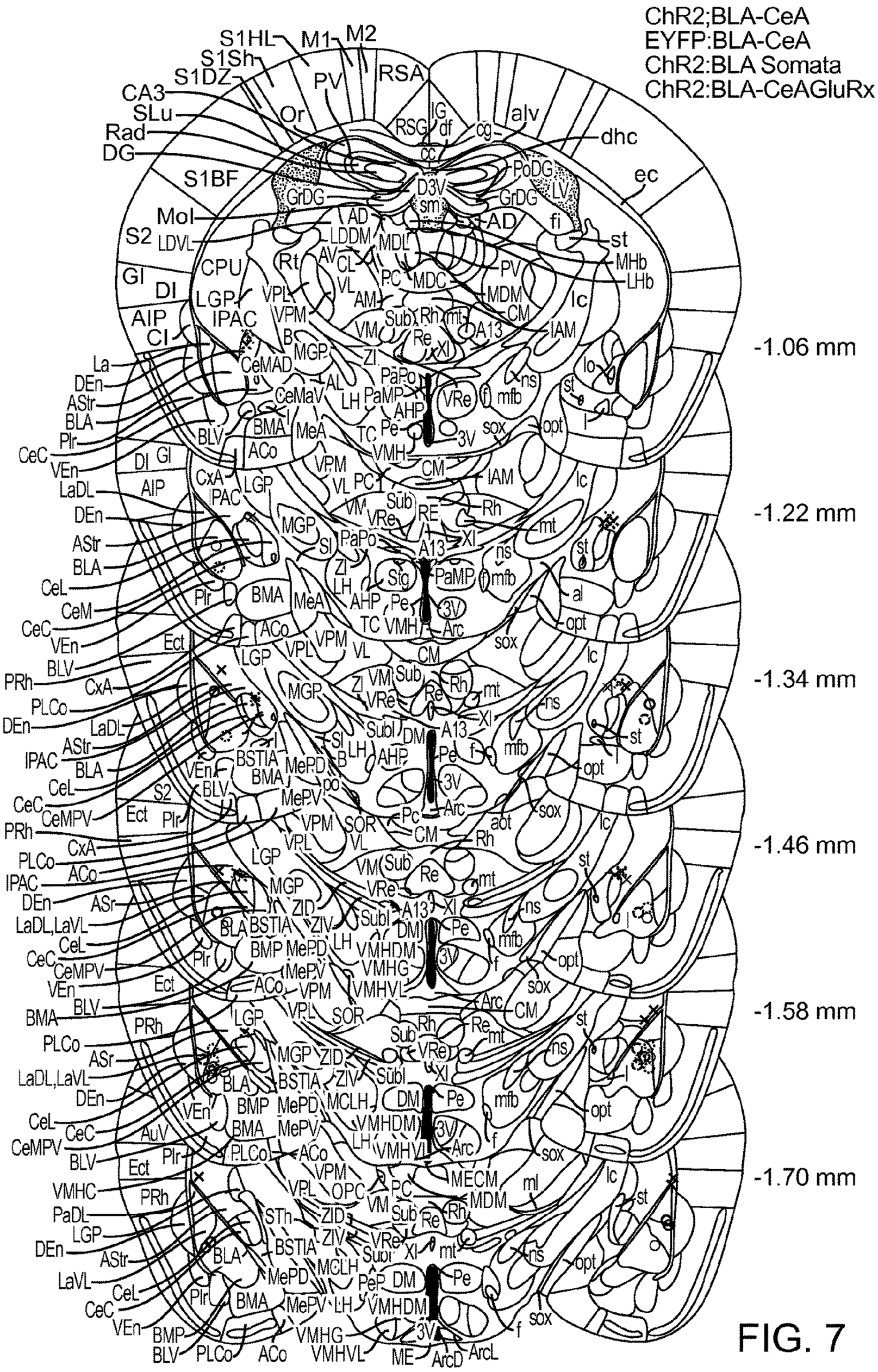
ChR2;BLA-CeA
EYFP:BLA-CeA
ChR2:BLA Somata
ChR2:BLA-CeAGluRx
-1.06 mm
-1.22 mm
-1.34 mm
-1.46 mm
-1.58 mm
-1.70 mm

FIG. 7

FIG. 8A

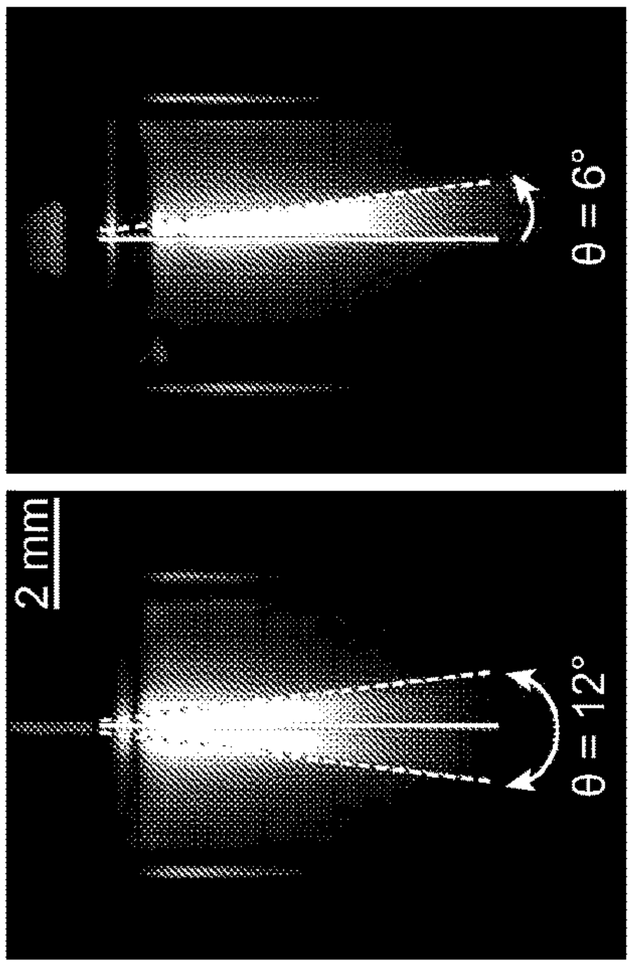

FIG. 8B

FIG. 8C

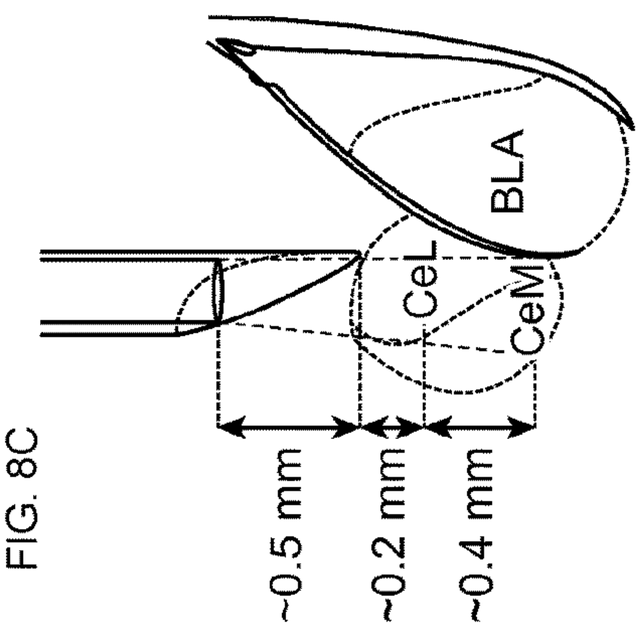

FIG. 8E

mW	mW/mm² at fiber tip	~mW/mm² at target depth: ~0.5 mm (BLA-CeL)	~0.7 mm (BLA-CeL)	~1.1 mm (BLA-CeM)
12	170	17.4	10.1	3.9
11	156	15.9	9.2	9.6
10	141	14.5	8.4	3.2
9	127	13	7.6	2.9
8	113	11.6	6.7	2.6
7	**99**	**10.1**	**5.9**	**2.2**
6	84	8.7	5.1	1.9
5	70	7.2	4.2	1.6
4	56	5.8	3.4	1.3
3	42	4.3	2.5	0.9
2	28	2.9	1.7	0.6
1	14	1.4	0.8	0.3
0	0	0	0	0

FIG. 8D

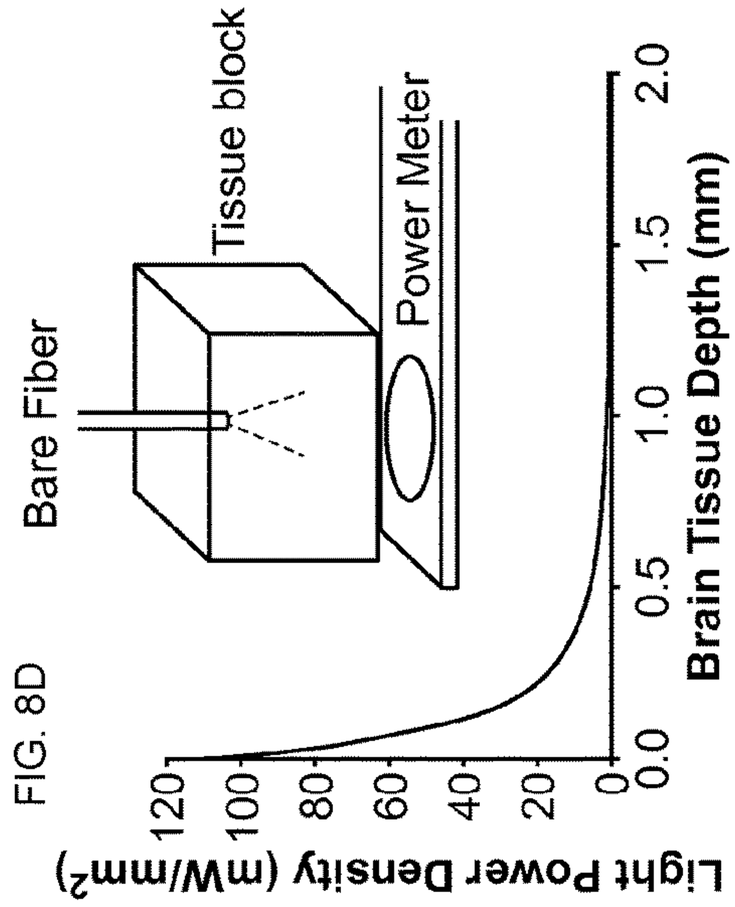

FIG. 9A

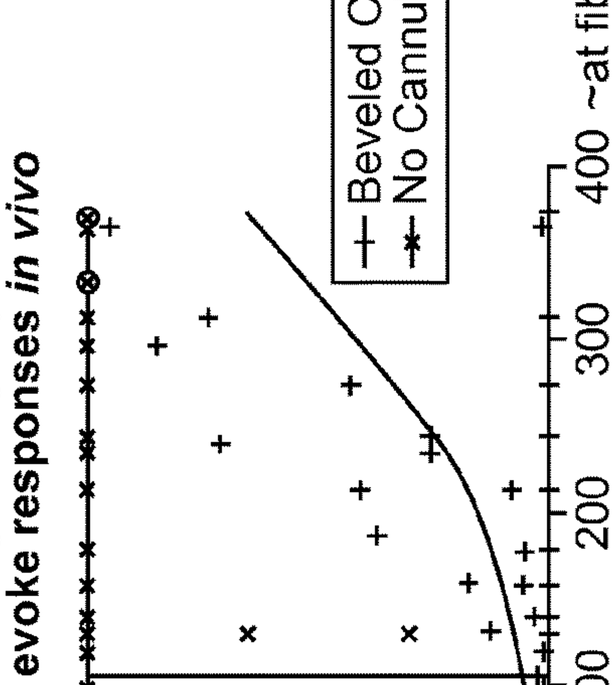

FIG. 9B

FIG. 9C

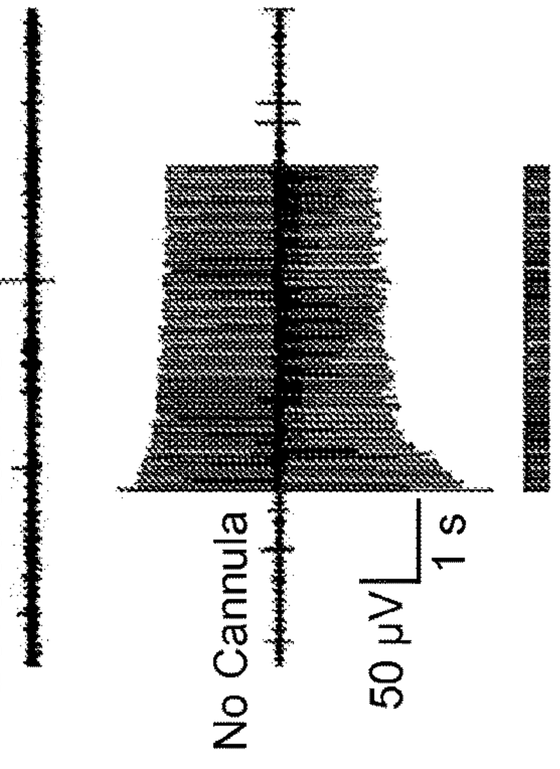

FIG. 9D

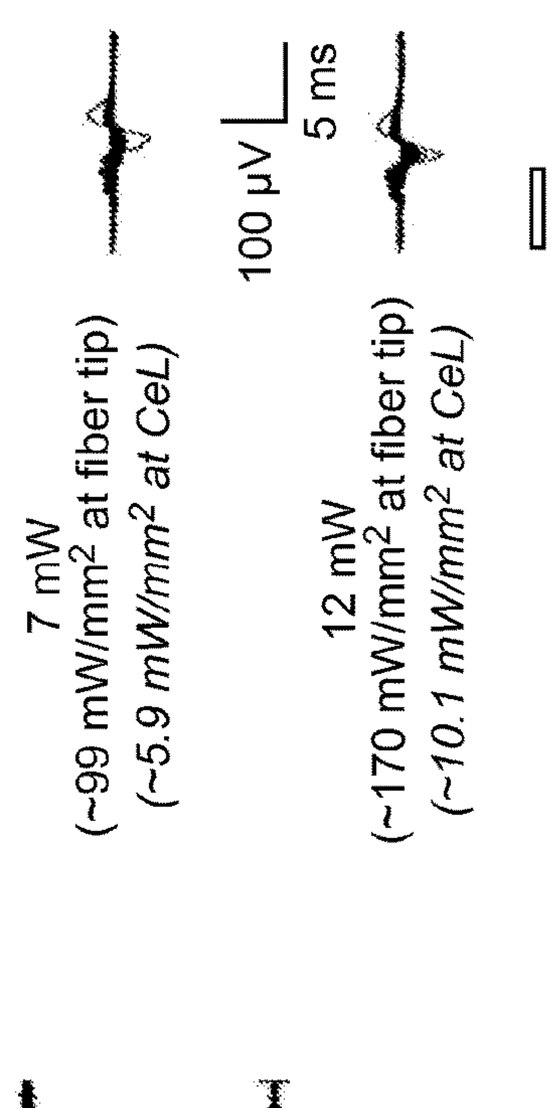

FIG. 10A
AAV_5-CaMKII-

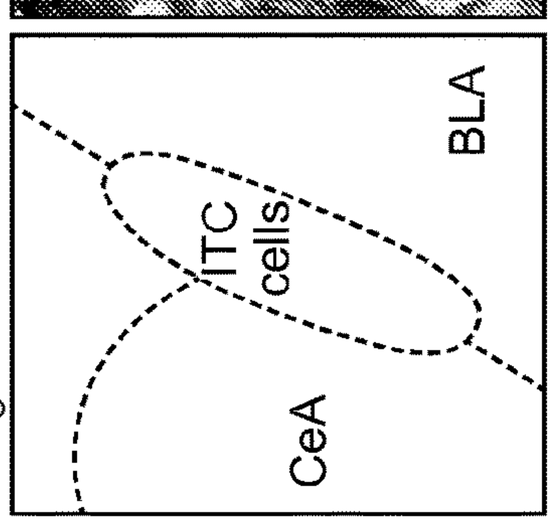

FIG. 10B
EYFP

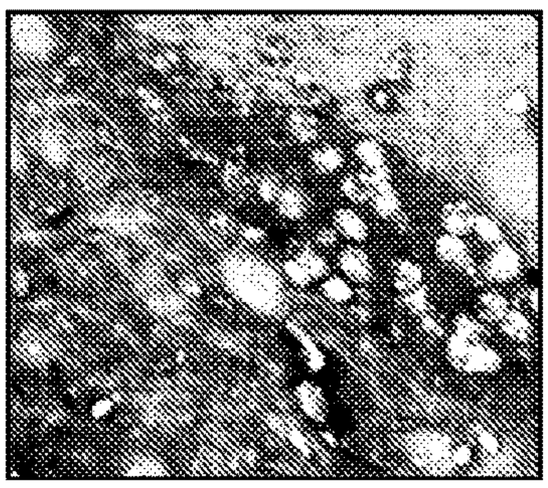

FIG. 10C
eNpHR 3.0

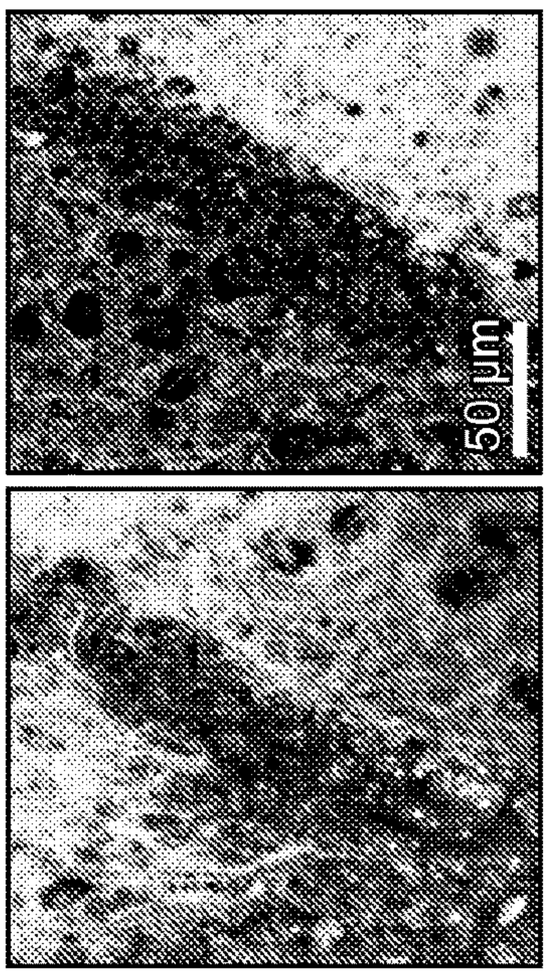

FIG. 10D
ChR2

FIG. 10E

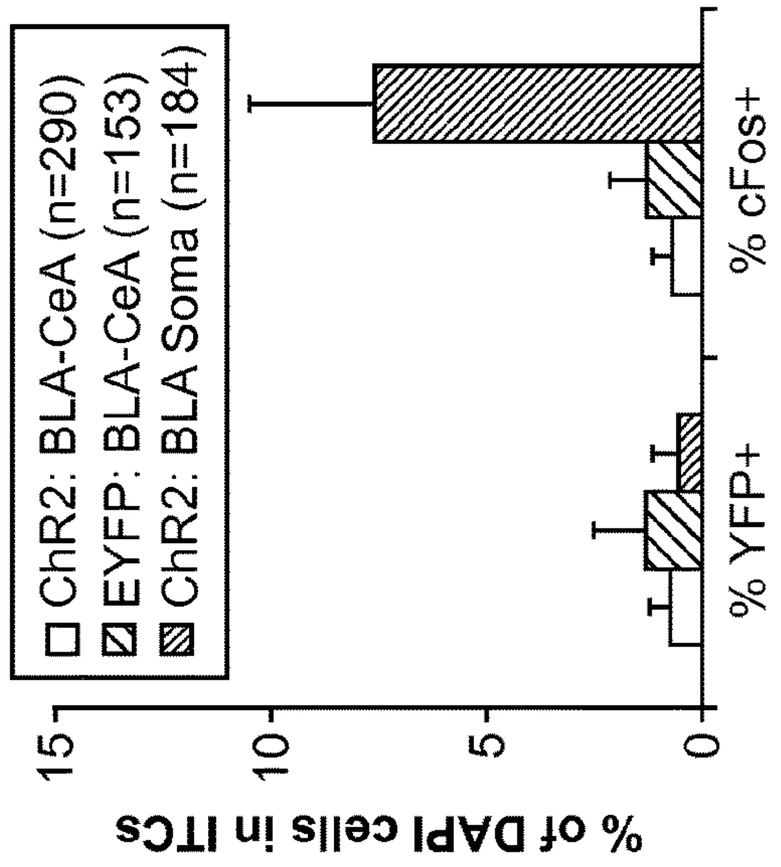

FIG. 10F

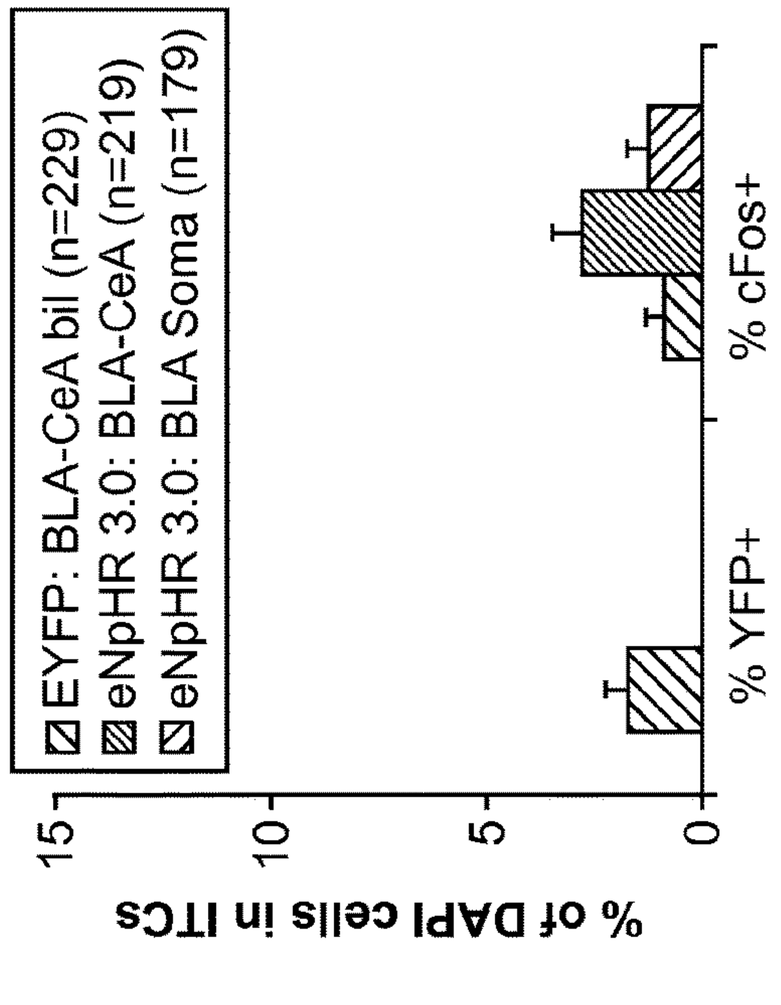

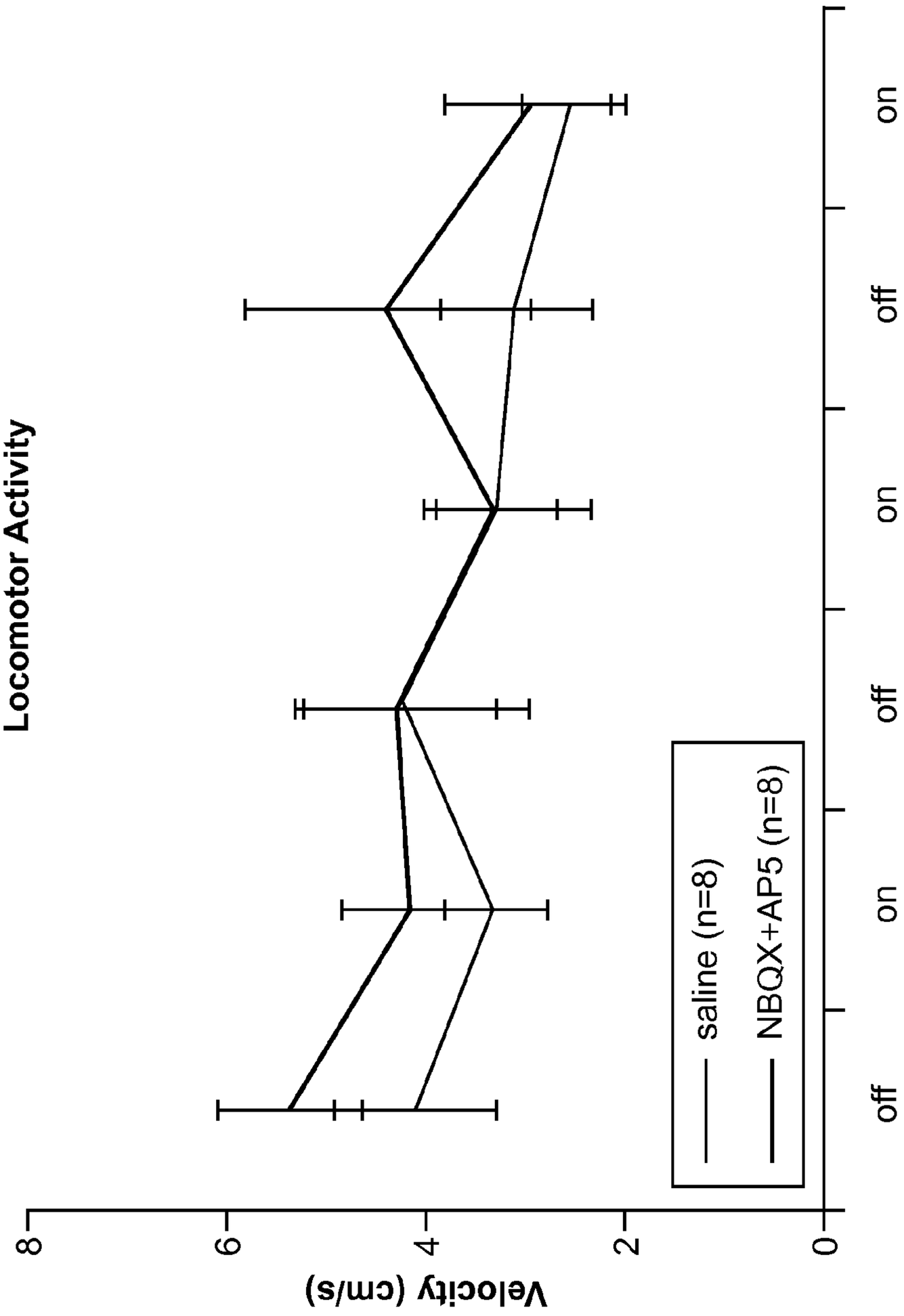
Locomotor Activity
Velocity (cm/s)
0
2
4
6
8
saline (n=8)
NBQX+AP5 (n=8)
off
on
off
on
off
on
off

FIG. 11

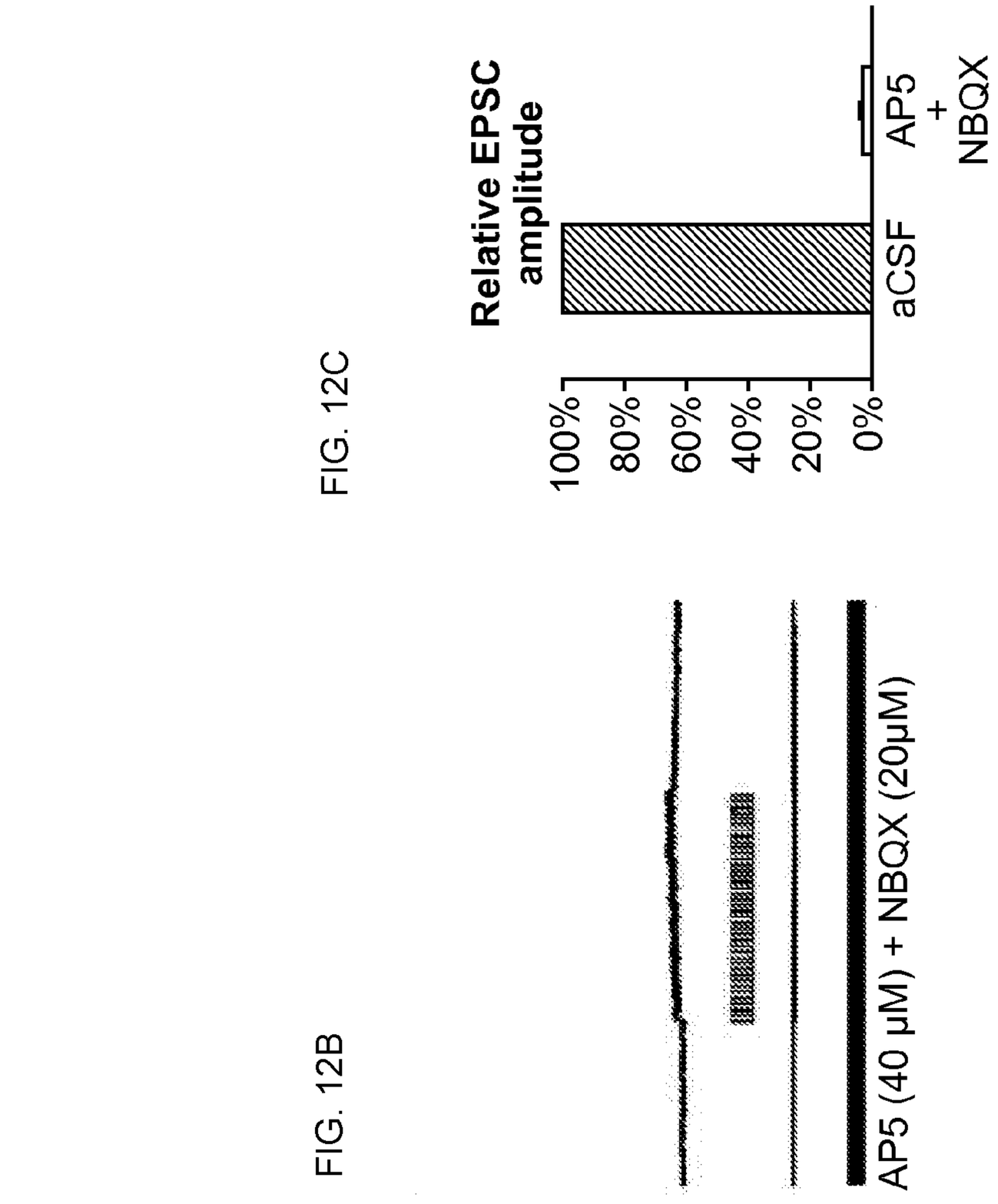

FIG. 12C

FIG. 12B

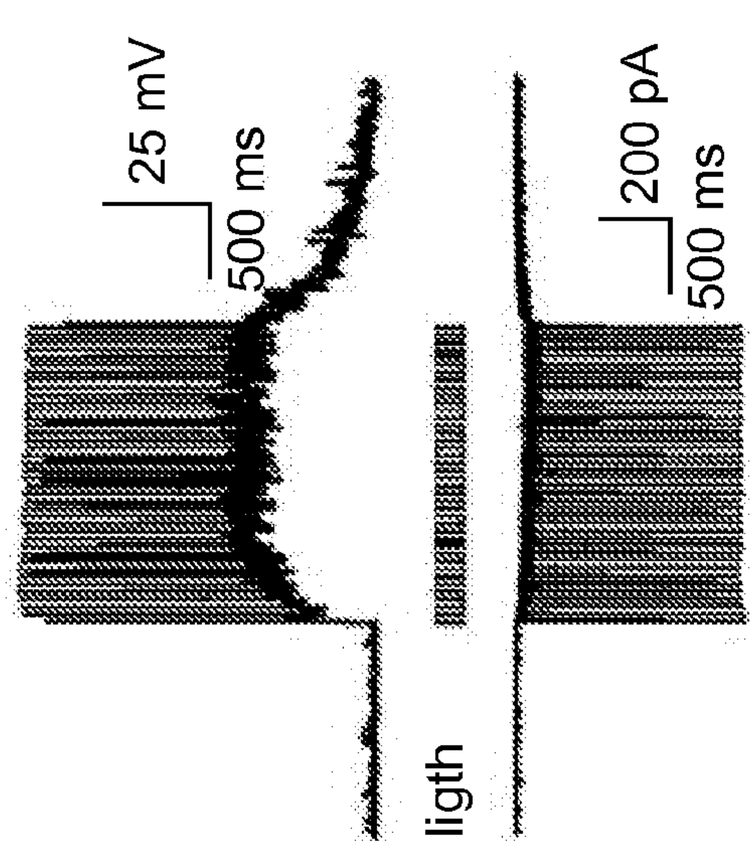

FIG. 12A

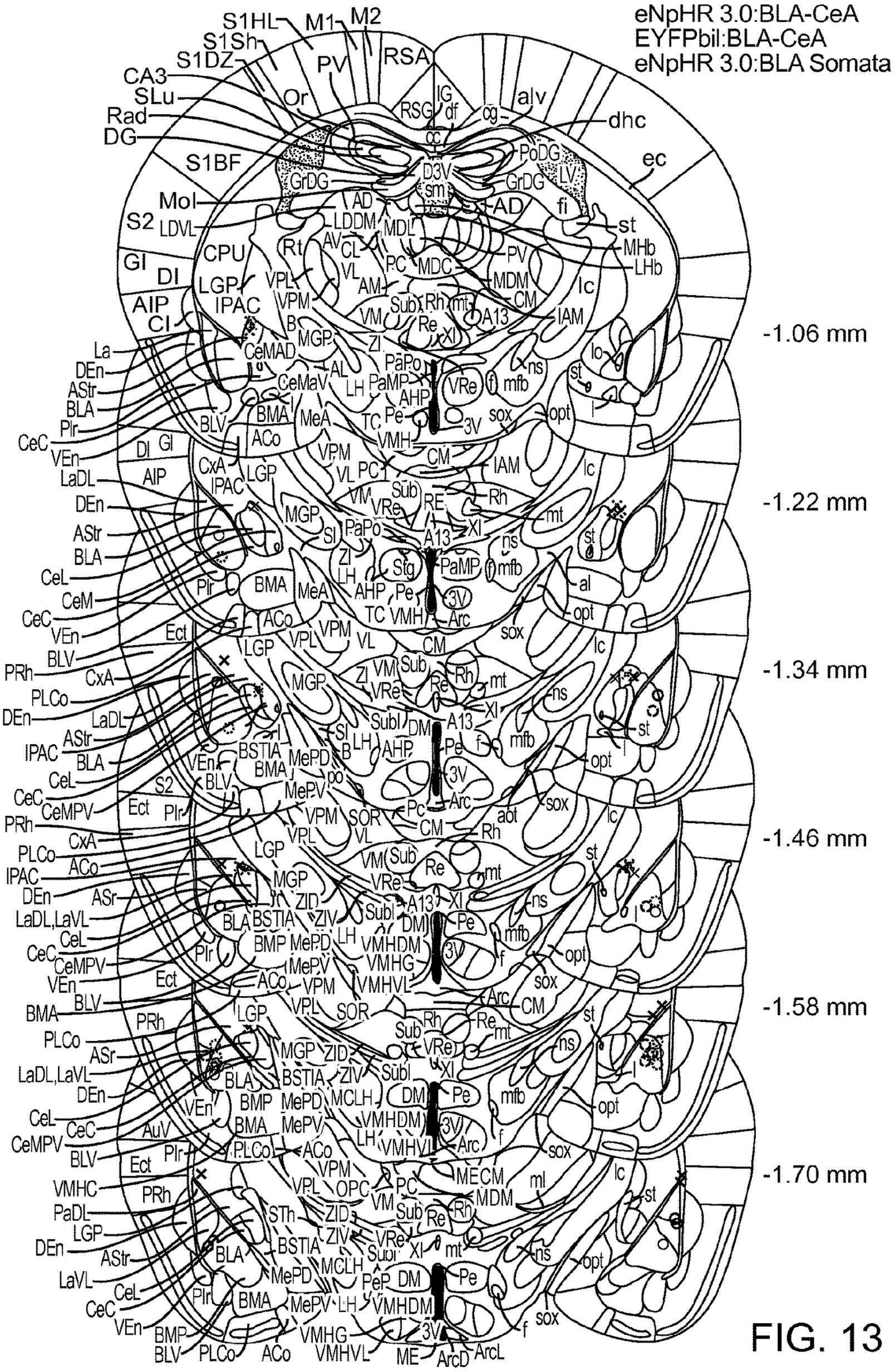
eNpHR 3.0:BLA-CeA
EYFPbil:BLA-CeA
eNpHR 3.0:BLA Somata
-1.06 mm
-1.22 mm
-1.34 mm
-1.46 mm
-1.58 mm
-1.70 mm

FIG. 13

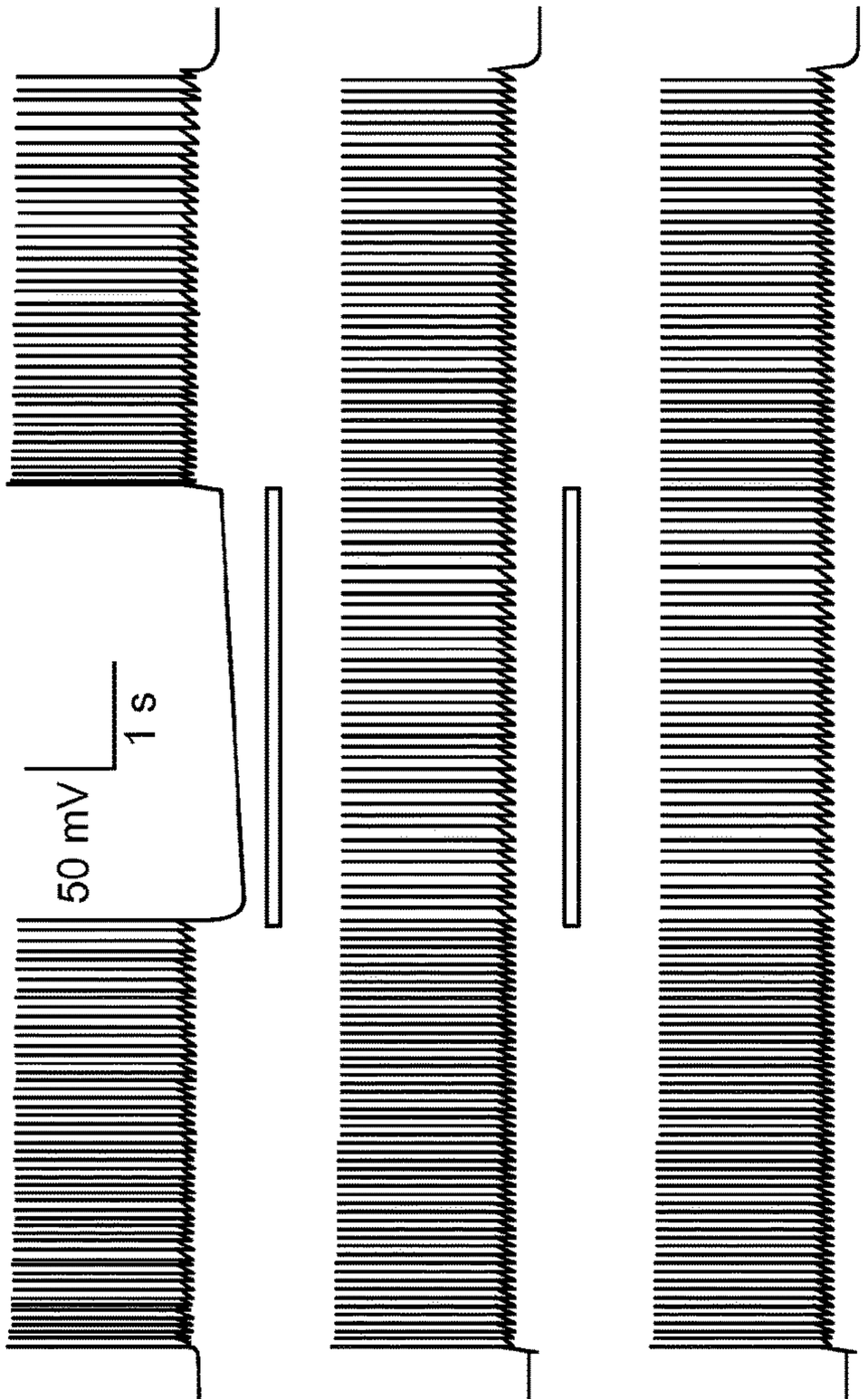

FIG. 14A

FIG. 14B

FIG. 14C

FIG. 14D

FIG. 14E

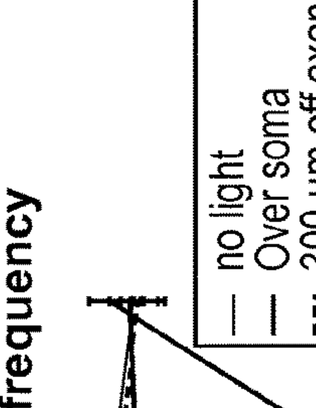

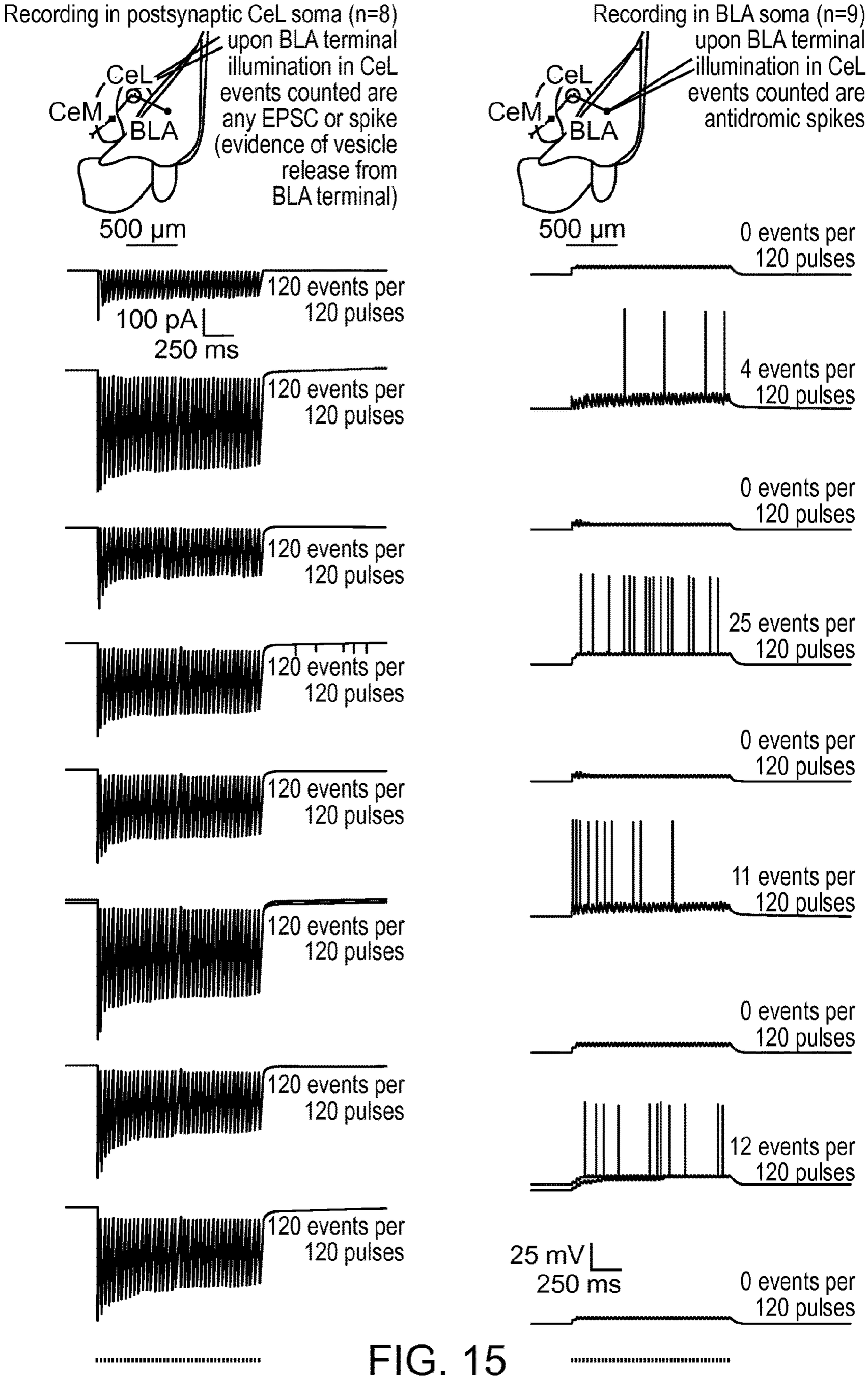
Recording in postsynaptic CeL soma (n=8)
upon BLA terminal illumination in CeL
events counted are any EPSC or spike (evidence of vesicle release from BLA terminal)
CeL
CeM
BLA
500 µm
120 events per 120 pulses
100 pA
250 ms
120 events per 120 pulses
120 events per 120 pulses
120 events per 120 pulses
120 events per 120 pulses
120 events per 120 pulses
120 events per 120 pulses
Recording in BLA soma (n=9)
upon BLA terminal illumination in CeL
events counted are antidromic spikes
CeL
CeM
BLA
500 µm
0 events per 120 pulses
4 events per 120 pulses
0 events per 120 pulses
25 events per 120 pulses
0 events per 120 pulses
11 events per 120 pulses
0 events per 120 pulses
12 events per 120 pulses
25 mV
250 ms
0 events per 120 pulses

FIG. 15

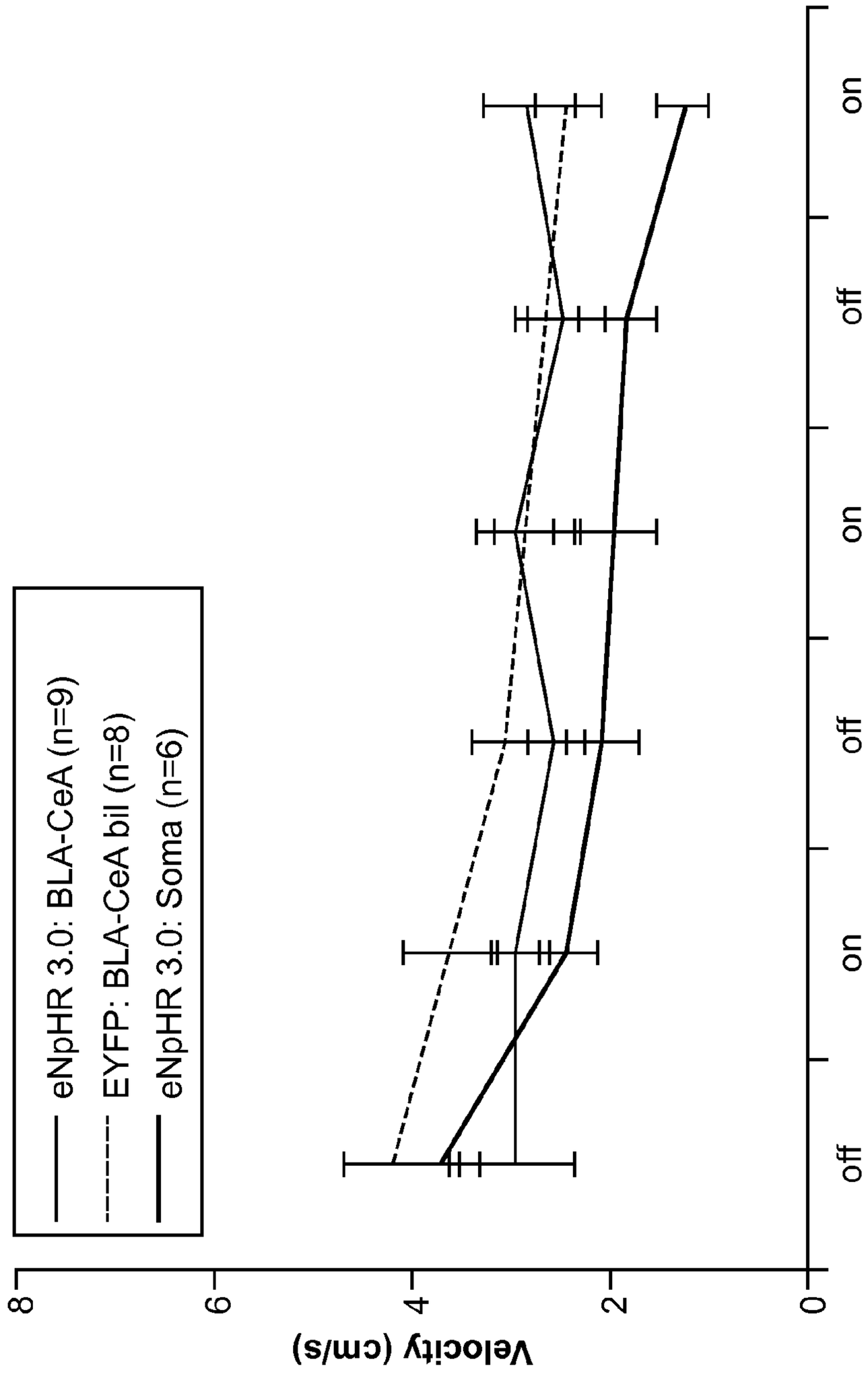
Locomotor Activity
eNpHR 3.0: BLA-CeA (n=9)
EYFP: BLA-CeA bil (n=8)
eNpHR 3.0: Soma (n=6)
Velocity (cm/s)
0
2
4
6
8
off
on
off
on
off
on

FIG. 16

OPTICALLY-CONTROLLED CNS DYSFUNCTION

CROSS REFERENCE TO RELATED APPLICATION

[0001] This application is a continuation of U.S. patent application Ser. No. 13/882,719, filed Jul. 29, 2013, now U.S. Pat. No. 8,932,562, which is a national stage filing under 35 U.S.C. § 371 of PCT/US2011/059298, filed Nov. 4, 2011, which claims the priority benefit of U.S. provisional application Ser. No. 61/410,748 filed on Nov. 5, 2010, and 61/464,806 filed on Mar. 8, 2011, the contents of each of which are incorporated herein by reference in their entirety.

BACKGROUND OF THE INVENTION

[0002] Anxiety is a sustained state of heightened apprehension in the absence of immediate threat, which in disease states becomes severely debilitating. Anxiety disorders represent the most common of the psychiatric diseases (with 28% lifetime prevalence), and have been linked to the etiology of major depression and substance abuse. While the amygdala, a brain region important for emotional processing, has long been hypothesized to play a role in anxiety, the neural mechanisms which control and mediate anxiety have yet to be identified. Despite the high prevalence and severity of anxiety disorders, the corresponding neural circuit substrates are poorly understood, impeding the development of safe and effective treatments. Available treatments tend to be inconsistently effective or, in the case of benzodiazepines, addictive and linked to significant side effects including sedation and respiratory suppression that can cause cognitive impairment and death. A deeper understanding of anxiety control mechanisms in the mammalian brain is necessary to develop more efficient treatments that have fewer side-effects. Of particular interest and novelty would be the possibility of recruiting native pathways for anxiolysis.

SUMMARY OF THE INVENTION

[0003] Provided herein is an animal comprising a light-responsive opsin expressed in glutamatergic pyramidal neurons of the basolateral amygdala (BLA), wherein the selective illumination of the opsin in the BLA-CeL induces anxiety or alleviates anxiety of the animal.

[0004] Provided herein is an animal comprising a light-responsive opsin expressed in glutamatergic pyramidal neurons of the BLA, wherein the opsin is an opsin which induces hyperpolarization by light, and wherein the selective illumination of the opsin in the BLA-CeL induces anxiety of the animal. In some embodiments, the opsin is NpHR, BR, AR, or GtR3. In some embodiments, the NpHR comprises the amino acid sequence of SEQ ID NO:1, 2, or 3. In some embodiments, the animal further comprises a second light-responsive opsin expressed in glutamatergic pyramidal neurons of the BLA, wherein the second opsin is an opsin that induces depolarization by light, and wherein the selective illumination of the second opsin in the BLA-CeL reduces anxiety of the animal. In some embodiments, the second opsin is ChR2, VChR1, or DChR. In some embodiments, the second opsin is a C1V1 chimeric protein comprising the amino acid sequence of SEQ ID NO:8, 9, 10, or 11. In some embodiments, the second opsin comprises the amino acid sequence of SEQ ID NO:6 or 7.

[0005] Provided herein is an animal comprising a light-responsive opsin expressed in the glutamatergic pyramidal neurons of the BLA, wherein the opsin is an opsin that induces depolarization by light, and wherein the selective illumination of the opsin in the BLA-CeL reduces anxiety of the animal. In some embodiments, the opsin is ChR2, VChR1, or DChR. In some embodiments, the opsin is a C1V1 chimeric protein comprising the amino acid sequence of SEQ ID NO:8, 9, 10, or 11. In some embodiments, the opsin comprises the amino acid sequence of SEQ ID NO:6 or 7.

[0006] Also provided herein is a vector for delivering a nucleic acid to glutamatergic pyramidal neurons of the BLA in an individual, wherein the vector comprises the nucleic acid encoding a light-responsive opsin and the nucleic acid is operably linked to a promoter that controls the specific expression of the opsin in the glutamatergic pyramidal neurons. In some embodiments, the promoter is a CaMKIIa promoter. In some embodiments, the vector is an AAV vector. In some embodiments, the opsin is an opsin that induces depolarization by light, and wherein selective illumination of the opsin in the BLA-CeL alleviates anxiety. In some embodiments, the opsin that induces depolarization by light is ChR2, VChR1, or DChR. In some embodiments, the opsin is a C1V1 chimeric protein comprising the amino acid sequence of SEQ ID NO:8, 9, 10, or 11. In some embodiments, the opsin comprises the amino acid sequence of SEQ ID NO:6 or 7. In some embodiments, the opsin is an opsin that induces hyperpolarization by light, and wherein selective illumination of the opsin in the BLA-CeL and induces anxiety. In some embodiments, the opsin that induces hyperpolarization by light is NpHR, BR, AR, or GtR3. In some embodiments, the NpHR comprises the amino acid sequence of SEQ ID NO:1, 2, or 3. In some embodiments, the individual is a mouse or a rat. In some embodiments, the individual is a human.

[0007] Also provided here is a method of delivering a nucleic acid to glutamatergic pyramidal neurons of the BLA in an individual, comprising administering to the individual an effective amount of a vector comprising a nucleic acid encoding a light-responsive opsin and the nucleic acid is operably linked to a promoter that controls the specific expression of the opsin in the glutamatergic pyramidal neurons. In some embodiments, the promoter is a CaMKIIα promoter. In some embodiments, the vector is an AAV vector. In some embodiments, the opsin is an opsin that induces depolarization by light, and wherein selective illumination of the opsin in the BLA-CeL alleviates anxiety. In some embodiments, the opsin that induces depolarization by light is ChR2, VChR1, or DChR. In some embodiments, the opsin is a C1V1 chimeric protein comprising the amino acid sequence of SEQ ID NO:8, 9, 10, or 11. In some embodiments, the opsin comprises the amino acid sequence of SEQ ID NO:6 or 7. In some embodiments, the opsin is an opsin that induces hyperpolarization by light, and wherein selective illumination of the opsin in the BLA-CeL and induces anxiety. In some embodiments, the opsin that induces hyperpolarization by light is NpHR, BR, AR, or GtR3. In some embodiments, the NpHR comprises the amino acid sequence of SEQ ID NO:1, 2, or 3. In some embodiments, the individual is a mouse or a rat. In some embodiments, the individual is a human.

[0008] Also provided herein is a coronal brain tissue slice comprising BLA, CeL, and CeM, wherein a light-responsive

opsin is expressed in the glutamatergic pyramidal neurons of the BLA. In some embodiments, the opsin is an opsin that induces depolarization by light. In some embodiments, the opsin that induces depolarization by light is ChR2, VChR1, or DChR. In some embodiments, the opsin is a C1V1 chimeric protein comprising the amino acid sequence of SEQ ID NO:8, 9, 10, or 11. In some embodiments, the opsin comprises the amino acid sequence of SEQ ID NO:6 or 7. In some embodiments, the opsin is an opsin that induces hyperpolarization by light. In some embodiments, the opsin that induces hyperpolarization by light is NpHR, BR, AR, or GtR3. In some embodiments, the NpHR comprises the amino acid sequence of SEQ ID NO:1, 2, or 3. In some embodiments, the tissue is a mouse or a rat tissue.

[0009] Also provided herein is a method for screening for a compound that alleviates anxiety, comprising (a) administering a compound to an animal having anxiety induced by selectively illumination of an opsin expressed in the glutamatergic pyramidal neurons of the BLA, wherein the animal comprises a light-responsive opsin expressed in the glutamatergic pyramidal neurons of the BLA, wherein the opsin is an opsin that induces hyperpolarization by light; and (b) determining the anxiety level of the animal, wherein a reduction of the anxiety level indicates that the compound may be effective in treating anxiety. In some embodiments, the opsin is NpHR, BR, AR, or GtR3. In some embodiments, the NpHR comprises the amino acid sequence of SEQ ID NO:1, 2, or 3.

[0010] Also provided herein is a method for alleviating anxiety in an individual, comprising: (a) administering to the individual an effective amount of a vector comprising a nucleic acid encoding a light-responsive opsin and the nucleic acid is operably linked to a promoter that controls the specific expression of the opsin in the glutamatergic pyramidal neurons of the BLA, wherein the opsin is expressed in the glutamatergic pyramidal neurons of the BLA, wherein the opsin is an opsin that induces depolarization by light; and (b) selectively illuminating the opsin in the glutamatergic pyramidal neurons in the BLA-CeL to alleviate anxiety. In some embodiments, the promoter is a CaMKIIα promoter. In some embodiments, the vector is an AAV vector. In some embodiments, the opsin is ChR2, VChR1, or DChR. In some embodiments, the opsin is a C1V1 chimeric protein comprising the amino acid sequence of SEQ ID NO:8, 9, 10, or 11. In some embodiments, the opsin comprises the amino acid sequence of SEQ ID NO:6 or 7.

[0011] Also provided herein is a method for inducing anxiety in an individual, comprising: (a) administering to the individual an effective amount of a vector comprising a nucleic acid encoding an opsin and the nucleic acid is operably linked to a promoter that controls the specific expression of the opsin in the glutamatergic pyramidal neurons of the BLA, wherein the opsin is expressed in the glutamatergic pyramidal neurons, wherein the opsin is an opsin that induces hyperpolarization by light; and (b) selectively illuminating the opsin in the glutamatergic pyramidal neurons in the BLA-CeL to induce anxiety. In some embodiments, the promoter is a CaMKIIα promoter. In some embodiments, the vector is an AAV vector. In some embodiments, the opsin is NpHR, BR, AR, or GtR3. In some embodiments, the NpHR comprises the amino acid sequence of SEQ ID NO:1, 2, or 3.

[0012] It is to be understood that one, some, or all of the properties of the various embodiments described herein may be combined to form other embodiments of the present invention. These and other aspects of the invention will become apparent to one of skill in the art.

BRIEF DESCRIPTION OF THE DRAWINGS

[0013] Various example embodiments may be more completely understood in consideration of the following description and the accompanying drawings, in which:

[0014] FIG. **1** shows a system for providing optogenetic targeting of specific projections of the brain, consistent with an embodiment of the present disclosure; and

[0015] FIG. **2** shows a flow diagram for use of an anxiety-based circuit model, consistent with an embodiment of the present disclosure.

[0016] FIGS. **3**A-**3**K show that projection-specific excitation of BLA terminals in the CeA induced acute reversible anxiolysis. FIG. **3**A: All mice were singly-housed in a high-stress environment for at least 1 week prior to behavioral manipulations and receive 5-ms light pulses at 20 Hz for all light on conditions. Mice in the ChR2:BLA-CeA group received viral transduction of ChR2 in BLA neurons under the CaMKII promoter and were implanted with a beveled cannula shielding light away from BLA somata to allow selective illumination of BLA terminals in the CeA, while control groups either received a virus including fluorophore only (EYFP:BLA-CeA group) or a light fiber directed to illuminate BLA somata (ChR2:BLA Somata group). FIG. **3**B-**3**C: Mice in the ChR2:BLA-CeA group (n=8) received selective illumination of BLA terminals in the CeA during the light on epoch during the elevated plus maze, as seen in this ChR2:BLA-CeA representative path FIG. **3**B, which induced a 5-fold increase in open arm time during the light on epoch relative to the light off epochs and EYFP:BLA-CeA (n=9) and ChR2:BLA Somata (n=7) controls FIG. **3**C, as well as a significant increase in the probability of entering the open arm (see inset). FIG. **3**D-**3**F: Mice in the ChR2:BLA-CeA group also showed an increase in the time spent in the center of the open field chamber, as seen in this representative trace (FIG. **3**D), during light on epochs relative to light off epochs and EYFP:BLA-CeA and ChR2:BLA Somata controls FIG. **3**E, but did not show a significant change in locomotor activity during light on epochs (FIG. **3**F). FIG. **3**G: Confocal image of a coronal slice showing the CeA and BLA regions from a mouse in the ChR2:BLA-CeA group wherein 125 μmx125 μm squares indicate regions used for quantification. FIG. **3**D-**3**H: Expanded regions are arranged in rows by group and in columns by brain region. FIG. **3**I-**3**K: Percent of EYFP-positive and c-fos-positive neurons of all DAPI-identified cells for all groups, by region. Numbers of counted per group and region are indicated in legends. None of the regions examined showed detectable differences in the proportion of EYFP-positive cells among groups. FIG. **31**: Proportion of BLA neurons that were EYFP-positive or c-fos-positive. The ChR2:BLA Somata group had a significantly higher proportion of c-fos-positive BLA neurons ($F_{2,9}$=10.12, $p<0.01$) relative to ChR2:BLA-CeA ($p<0.01$) or EYFP:BLA-CeA ($p<0.05$) groups. FIG. **3**J: The ChR2:BLA-CeA group had a significantly higher proportion of c-fos-positive cells in the CeL relative to the EYFP:BLA-CeA group ($p<0.05$), but not the ChR2:BLA Somata group.

FIG. **3**K:Summary data for CeM neurons show no detectable differences among groups.

[0017] FIGS. **4**A-**4**F show projection-specific excitation of BLA terminals in the CeA activates CeL neurons and elicits feed-forward inhibition of CeM neurons. FIG. **4**A: Live two-photon images of representative light-responsive BLA, CeL and CeM cells all imaged from the same slice, overlaid on a brightfield image. FIG. **4**B-**4**F: Schematics of the recording and illumination sites for the associated representative current-clamp traces (V_m=~70 mV). FIG. **4**B: Representative trace from a BLA pyramidal neuron expressing ChR2, all BLA neurons expressing ChR2 in the BLA spiked for every 5 ms pulse (n=4). FIG. **4**C: Representative trace from a CeL neuron in the terminal field of BLA projection neurons, showing both sub-threshold and supra-threshold excitatory responses to light-stimulation (n=16). Inset left, population summary of mean probability of spiking for each pulse in a 40-pulse train at 20 Hz, dotted lines indicate SEM. Inset right, frequency histogram showing individual cell spiking fidelity for 5 ms light pulses delivered at 20 Hz, y-axis is the number of cells per each 5% bin. FIG. **4**D: Six sweeps from a CeM neuron spiking in response to a current step (~60 pA; indicated in black) and inhibition of spiking upon 20 Hz illumination of BLA terminals in the CeL. Inset, spike frequency was significantly reduced during light stimulation of CeL neurons (n=4). FIG. **4**E-**4**F: Upon broad illumination of the CeM, voltage-clamp summaries show that the latency of EPSCs is significantly shorter than the latency of IPSCs, while there was a non-significant difference in the amplitude of EPSCs and IPSCs (n=11; *p=0.04, see insets). The same CeM neurons (n=7) showed either net excitation when receiving illumination of the CeM FIG. **4**E: or net inhibition upon selective illumination of the CeL (FIG. **4**F).

[0018] FIGS. **5**A-**5**K show light-induced anxiolytic effects were attributable to activation of BLA-CeL synapses alone. FIG. **5**A-**5**B: 2-photon z-stack images of 18 dye-filled BLA neurons were reconstructed, and their projections to the CeL and CeM are summarized in FIG. **5**A, with their images shown in FIG. **5**B wherein red indicates projections to CeL, blue indicates projections to CeM and purple indicates projections to both CeL and CeM. FIG. **5**C: Schematic of the recording site and the light spot positions, as whole-cell recordings were performed at each location of the light spot, which was moved in 100 um-steps away from the cell soma both over a visualized axon and in a direction that was not over an axon. FIG. **5**D: Normalized current-clamp summary of spike fidelity to a 20 Hz train delivered at various distances from the soma, showing that at ~300um away from the cell soma, illumination of an axon terminal results in low (<5%) spike fidelity. FIG. **5**E: Normalized voltage-clamp summary of depolarizing current seen at the cell soma upon illumination per distance from cell soma. FIG. **5**F-**5**I: Representative current-clamp traces upon illumination with a ~150 um-diameter light spot over various locations within each slice preparation (n=7). Illumination of the cell soma elicits high-fidelity spiking (FIG. **5**F). Illumination of BLA terminals in CeL elicits strong sub- and supra-threshold excitatory responses in the postsynaptic CeL neuron (FIG. **5**G), but does not elicit reliable antidromic spiking in the BLA neuron itself (FIG. **5**H), and light delivered off axon is shown for comparison as a control for light scattering (FIG. **5**I). FIG. **5**J-**5**K: A separate group of ChR2:BLA-CeL mice (n=8) were each run twice on the elevated plus maze and the open field test, one session preceded with intra-CeA infusions of saline (red) and the other session with the glutamate receptor antagonists NBQX and AP5 (purple), counterbalanced for order. FIG. **5**K: Glutamate receptor blockade in the CeA attenuated light-induced increases in both time spent in open arms as well as the probability of open arm entry (inset) on the elevated plus maze without impairing performance during light off epochs. FIG. FIG. **5**J: Local glutamate receptor antagonism significantly attenuated light-induced increases in center time on the open field test, inset shows pooled summary.

[0019] FIGS. **6**A-**6**P show that selective inhibition of BLA terminals in the CeA induced an acute and reversible increase in anxiety. FIG. **6**A: All mice were group-housed in a low-stress environment and received bilateral constant 591 nm light during light on epochs. Mice in the eNpHR3.0: BLA-CeA group (n=9) received bilateral viral transduction of eNpHR3.0 in BLA neurons under the CaMKII promoter and were implanted with a beveled cannula shielding light away from BLA somata to allow selective illumination of BLA terminals in the CeA, while control groups either received bilateral virus transduction of a fluorophore only (EYFP:BLA-CeA bil group; n=8) or a light fiber directed to illuminate BLA somata (eNpHR3.0:BLA Somata group; n=6). FIG. **6**B: Confocal image of the BLA and CeA of a mouse treated with eNpHR3.0. FIG. **6**C-**6**E: In the same animals used in anxiety assays below, a significantly higher proportion of neurons in the CeM (FIG. **6**E) from the eNpHR3.0 group expressed c-fos relative to the EYFP group (*p<0.05). FIG. **6**F: Representative path of a mouse in the eNpHR3.0:BLA-CeA group, showing a decrease in open arm exploration on the elevated plus maze during epochs of selective illumination of BLA terminals in the CeA. FIG. **6**G: eNpHR3.0 mice showed a reduction in the time spent in open arms and probability of open arm entry (inset) during light stimulation, relative to controls. FIG. **6**H: Representative path of a mouse from the eNpHR3.0:BLA-CeA group during pooled light off and on epochs in the open field test. FIG. **61**: Significant reduction in center time in the open field chamber for the eNpHR3.0:BLA-CeA group during light on, but not light off, epochs as compared to controls, inset shows pooled data summary. FIGS. **6**J-L: Selective illumination of eNpHR3.0-expressing BLA terminals is sufficient to reduce spontaneous vesicle release in the presence of carbachol. Representative trace of a CeL neuron (FIG. **6**J) from an acute slice preparation in which BLA neurons expressed eNpHR 3.0, shows that when BLA terminals ~300 μm away from the BLA soma are illuminated, there is a reduction in the amplitude (k) and frequency (l) of sEPSCs seen at the postsynaptic CeL neuron. Cumulative distribution frequency of the amplitude (k) and frequency (l) of sEPSCs recorded at CeL neurons (n=5) upon various lengths of illumination 5-60 s, insets show respective mean+SEM in the epochs of matched duration before, during and after illumination (**p<0.01; ***p<0.001). FIG. **6**M-6P: Selective illumination of BLA terminals expressing eNpHR 3.0 suppresses vesicle release evoked by electrical stimulation in the BLA. FIG. **6**M: Schematic indicating the locations of the stimulating electrode, the recording electrode and the ~150 μm diameter light spot. FIG. **6**N: Representative traces of EPSCs in a CeL neuron before (OM), during (On) and after (Off_2) selective illumination of BLA terminals expressing eNpHR3.0. Normalized EPSC amplitude summary data (FIG. **6**O) and individual cell data (FIG. **6**P) from slice

preparations containing BLA neurons expressing eNpHR 3.0 (n=7) and non-transduced controls (n=5) show that selectively illuminating BLA terminals in the CeL significantly (*p=0.006) reduces the amplitude of electrically-evoked EPSCs in postsynaptic CeL neurons.

[0020] FIG. **7** is a diagram showing the histologically verified placements of mice treated with 473 nm light. Unilateral placements of the virus injection needle (circle) and the tip of beveled cannula (x) are indicated, counterbalanced for hemisphere. Colors indicate treatment group, see legend. Coronal sections containing the BLA and the CeA are shown here, numbers indicate the anteroposterior coordinates from bregma (Aravanis et al., *J Neural Eng*, 4:S143-156, 2007).

[0021] FIGS. **8**A-**8**E show the beveled cannula and illumination profile design. FIG. **8**A:Light cone from bare fiber emitting 473 nm light over cuvette filled with fluorescein in water. The angle of the light cone is approximately 12 degrees. FIG. **8**B: Light cone from the same fiber and light ensheathed in a beveled cannula. The beveled cannula blocks light delivery to one side, without detectably altering perpendicular light penetrance. FIG. **8**C: Diagram of light delivery via the optical fiber with the beveled cannula over CeA. FIG. **8**D: Chart indicating estimated light power density seen at various distances from the fiber tip in mouse brain tissue when the light power density seen at the fiber tip was 7 mW (~99 mW/mm^2). Inset, cartoon indicating the configuration. Optical fiber is perpendicular and aimed at the center of the power meter, through a block of mouse brain tissue. FIG. **8**E: Table showing light power (mW) as measured by a standard power meter and the estimated light power density (mW/mm^2) seen at the tip, at the CeL (~0.5-0.7 mm depth in brain tissue) and at the CeM (~1.1 mm depth in brain tissue).

[0022] FIGS. **9**A-**9**D demonstrate that the beveled cannula prevented light delivery to BLA and BLA spiking at light powers used for behavioral assays. FIG. **9**A: Schematic indicating the configuration of light delivery by optical fiber to the CeA and recording electrode (red) in the BLA. FIG. **9**B: Scatterplot summary of recordings in the BLA with various light powers delivered to the CeA with and without the beveled cannula (n=4 sites). For each site, repeated alternations of recordings were made with and without the beveled cannula. The x-axis shows both the light power density at the fiber tip (black) and the estimated light power density at the CeL (grey). The blue vertical or shaded region indicates the range of light power densities used for behavioral assays (~7 mW; ~99 mW/mm^2 at the tip of the fiber). Reliable responses from BLA neurons were not observed in this light power density range. FIG. **9**C: Representative traces of BLA recordings with 20 Hz 5 ms pulse light stimulation at 7mW (~99 mW/mm^2 at fiber tip; ~5.9 mW/mm^2 at CeL) at the same recording site in the CeA. FIG. **9**D: Population spike waveforms in response to single pulses of light reveal substantial light restriction even at high 12 mV power (~170 mW/mm^2 at the tip of the fiber; ~10.1 mW/mm^2 at CeL).

[0023] FIGS. **10**A-**10**F demonstrate that viral transduction excluded intercalated cell clusters. FIG. **10**A: Schematic of the intercalated cells displayed in subsequent confocal images. FIG. **10**B-**10**D: Representative images of intercalated cells from mice that received EYFP (FIG. **10**B) , eNpHR 3.0 (FIG. **10**C) and ChR2 (FIG. **10**D) injections into the BLA that were used for behavioral manipulations. Viral expression was not observed in intercalated cell clusters. FIG. **10**E-**10**F: There were very low (<2%) levels of YFP expression in intercalated cell clusters for all 6 groups used in behavioral assays. There were no statistically significant differences among groups in c-fos expression.

[0024] FIG. **11** shows that unilateral intra-CeA administration of glutamate antagonists did not alter locomotor activity. Administration of NBQX and AP5 prior to the open field test did not impair locomotor activity (as measured by mean velocity) relative to saline infusion ($F_{1,77}$=2.34, p=0.1239).

[0025] FIGS. **12**A-**12**C demonstrate that bath application of glutamate antagonists blocked optically-evoked synaptic transmission. 4-6 weeks following intra-BLA infusions of AAV5-CAMKII-ChR2-EYFP into the BLA of wild-type mice, we examined the ability of the glutamate receptor antagonists NBQX and AP5 to block glutamatergic transmission. FIG. **12**A: Representative current-clamp (top) and voltage-clamp (bottom) traces of a representative CeL neuron upon a 20 Hz train of 473 nm light illumination of BLA terminals expressing ChR2. FIG. **12**B:The same cell's responses following bath application of NBQX and AP5 show abolished spiking and EPSCs. FIG. **12**C: Population summary (n=5) of the depolarizing current seen before and after bath application of NBQX and AP5, normalized to the pre-drug response.

[0026] FIG. **13** is a diagram depicting the histologically verified placements of mice treated with 594 nm light. Bilateral placements of virus injection needle (circle) and tip of beveled cannula (x) are indicated. Colors indicate treatment group, see legend. Coronal sections containing BLA and CeA are shown; numbers indicate AP coordinates from bregma (Aravanis et el., *J Neural Eng,* 4:S143-156, 2007).

[0027] FIGS. **14**A-**14**E show that light stimulation parameters used in the eNpHR 3.0 terminal inhibition experiments does not block spiking at the cell soma. FIG. **14**A-**14**C: Schematics of the light spot location and recording sites alongside corresponding representative traces upon a current step lasting the duration of the spike train, paired with yellow light illumination at each location during the middle epoch (indicated by yellow horizontal bar). FIG. **14**A: Representative current-clamp trace from a BLA neuron expressing eNpHR 3.0 upon direct illumination shows potent inhibition of spiking during illumination of cell soma. FIG. **14**B: Representative current-clamp trace from a BLA neuron expressing eNpHR 3.0 when a ~125 um diameter light spot is presented ~300 um away from the cell soma without illuminating an axon. FIG. **14**C: Representative current-clamp trace from a BLA neuron expressing eNpHR 3.0 when a ~125 μm diameter light spot is presented ~300 μm away from the cell soma when illuminating an axon. FIG. **14**D:While direct illumination of the cell soma induced complete inhibition of spiking that was significant from all other conditions ($F_{3,9}$=81.50, p<0.0001; n=3 or more per condition), there was no significant difference among the distal illumination ~300 um away from the soma of BLA neurons expressing eNpHR 3.0 conditions and the no light condition ($F_{2,7}$=0.79, p=0.49), indicating that distal illumination did not significantly inhibit spiking at the cell soma. FIG. **14**E: Schematic indicating light spot locations relative to recording site, regarding the population summary shown to the right. Population summary shows the normalized

hyperpolarizing current recorded from the cell soma per distance of light spot from cell soma, both on and off axon collaterals (n=5).

[0028] FIG. **15** demonstrates that selective illumination of BLA terminals induced vesicle release onto CeL neurons without reliably eliciting antidromic action potentials. Schematics and descriptions refer to the traces below, and trace color indicates cell type. Light illumination patterns are identical for both series of traces. Left column, CeL traces for three overlaid sweeps of a 40-pulse light train per cell (n=8). Here, both time-locked EPSCs indicate vesicle release from the presynaptic ChR2-expressing BLA terminal, and for all postsynaptic CeL cells, there were excitatory responses to 100% of light pulses. Right column, BLA traces for three overlaid 40-pulse sweeps per cell (n=9), with the mean number of light pulses delivered at the axon terminal resulting in a supra-threshold antidromic action potential (5.4% ±2%, mean±SEM).

[0029] FIG. **16** is a graph demonstrating that light stimulation did not alter locomotor activity in eNpHR 3.0 and control groups. There were no detectable differences in locomotor activity among groups nor light epochs ($F_{1,20}$=0.023, p=0.3892; $F_{1,100}$=3.08, p=0.086).

DETAILED DESCRIPTION

[0030] The present disclosure relates to control over nervous system disorders, such as disorders associated with anxiety and anxiety symptoms, as described herein. While the present disclosure is not necessarily limited in these contexts, various aspects of the invention may be appreciated through a discussion of examples using these and other contexts.

[0031] Various embodiments of the present disclosure relate to an optogenetic system or method that correlates temporal control over a neural circuit with measurable metrics. For instance, various metrics or symptoms might be associated with a neurological disorder exhibiting various symptoms of anxiety. The optogenetic system targets a neural circuit within a patient for selective control thereof. The optogenetic system involves monitoring the patient for the metrics or symptoms associated with the neurological disorder. In this manner, the optogenetic system can provide detailed information about the neural circuit, its function and/or the neurological disorder.

[0032] Consistent with the embodiments discussed herein, particular embodiments relate to studying and probing disorders. Other embodiments relate to the identification and/or study of phenotypes and endophenotypes. Still other embodiments relate to the identification of treatment targets.

[0033] Aspects of the present disclosure are directed to using an artificially-induced anxiety state for the study of anxiety in otherwise healthy animals. This can be particularly useful for monitoring symptoms and aspects that are poorly understood and otherwise difficult to accurately model in living animals For instance, it can be difficult to test and/or study anxiety states due to the lack of available animals exhibiting the anxiety state. Moreover, certain embodiments allow for reversible anxiety states, which can be particularly useful in establishing baseline/control points for testing and/or for testing the effects of a treatment on the same animal when exhibiting the anxiety state and when not exhibiting the anxiety state. The reversible anxiety states of certain embodiments can also allow for a reset to baseline between testing the effects of different treatments on the same animal

[0034] Certain aspects of the present disclosure are directed to a method related to control over anxiety and/or anxiety symptoms in a living animal In certain more specific embodiments, the monitoring of the symptoms also includes assessing the efficacy of the stimulus in mitigating the symptoms of anxiety. Various other methods and applications exist, some of which are discussed in more detail herein.

[0035] Light-responsive opsins that may be used in the present invention includes opsins that induce hyperpolarization in neurons by light and opsins that induce depolarization in neurons by light. Examples of opsins are shown in Tables 1 and 2 below.

[0036] Table 1 shows identified opsins for inhibition of cellular activity across the visible spectrum:

TABLE 1

Fast optogenetics: inhibition across the visible spectrum

Opsin Type	Biological Origin	Wavelength Sensitivity	Defined action
NpHR	*Natronomonas pharaonis*	589 nm max	Inhibition (hyperpolarization)
BR	*Halobacterium helobium*	570 nm max	Inhibition (hyperpolarization)
AR	*Acetabulaira acetabulum*	518 nm max	Inhibition (hyperpolarization)
GtR3	*Guillardia theta*	472 nm max	Inhibition (hyperpolarization)
Mac	*Leptosphaeria maculans*	470-500 nm max	Inhibition (hyperpolarization)
NpHr3.0	*Natronomonas pharaonis*	680 nm utility 589 nm max	Inhibition (hyperpolarization)
NpHR3.1	*Natronomonas pharaonis*	680 nm utility 589 nm max	Inhibition (hyperpolarization)

[0037] Table 2 shows identified opsins for excitation and modulation across the visible spectrum:

TABLE 2

Fast optogenetics: excitation and modulation across the visible spectrum

Opsin Type	Biological Origin	Wavelength Sensitivity	Defined action
VChR1	*Volvox carteri*	589 nm utility 535 nm max	Excitation (depolarization)
DChR	*Dunaliella salina*	500 nm max	Excitation (depolarization)

TABLE 2-continued

Fast optogenetics: excitation and modulation across the visible spectrum

Opsin Type	Biological Origin	Wavelength Sensitivity	Defined action
ChR2	*Chlamydomonas reinhardtii*	470 nm max 380-405 nm utility	Excitation (depolarization)
ChETA	*Chlamydomonas reinhardtii*	470 nm max 380-405 nm utility	Excitation (depolarization)
SFO	*Chlamydomonas reinhardtii*	470 nm max 530 nm max	Excitation (depolarization) Inactivation
SSFO	*Chlamydomonas reinhardtii*	445 nm max 590 nm; 390-400 nm	Step-like activation (depolarization) Inactivation
C1V1	*Volvox carteri* and *Chlamydomonas reinhardtii*	542 nm max	Excitation (depolarization)
C1V1 E122	*Volvox carteri* and *Chlamydomonas reinhardtii*	546 nm max	Excitation (depolarization)
C1V1 E162	*Volvox carteri* and *Chlamydomonas reinhardtii*	542 nm max	Excitation (depolarization)
C1V1 E122/E162	*Volvox carteri* and *Chlamydomonas reinhardtii*	546 nm max	Excitation (depolarization)

[0038] As used herein, a light-responsive opsin (such as NpHR, BR, AR, GtR3, Mac, ChR2, VChR1, DChR, and ChETA) includes naturally occurring protein and functional variants, fragments, fusion proteins comprising the fragments or the full length protein. For example, the signal peptide may be deleted. A variant may have an amino acid sequence at least about any of 90%, 91%, 92%, 93%, 94%, 95%, 96%, 97%, 98%, 99%, or 100% identical to the naturally occurring protein sequence. A functional variant may have the same or similar hyperpolarization function or depolarization function as the naturally occurring protein.

[0039] In some embodiments, the NpHR is eNpHR3.0 or eNpHR3.1 (See www.stanford.edu/group/dlab/optogenetics/sequence_info.html). In some embodiments, the light-responsive opsin is a C1V1 chimeric protein or a C1V1-E162 (SEQ ID NO:10), C1V1-E122 (SEQ ID NO:9), or C1V1-E122/E162 (SEQ ID NO:11) mutant chimeric protein (See, Yizhar et al, *Nature,* 2011, 477(7363):171-78 and www.stanford.edu/group/dlab/optogenetics/sequence_info.html). In some embodiments, the light-responsive opsin is a SFO (SEQ ID NO:6) or SSFO (SEQ ID NO:7) (See, Yizhar et al, *Nature,* 2011, 477(7363):171-78; Berndt et al., *Nat. Neurosci.,* 12(2):229-34 and www.stanford.edu/group/dlab/optogenetics/sequence_info.htme.

[0040] In some embodiments, the light-activated protein is a NpHR opsin comprising an amino acid sequence at least 95%, at least 96%, at least 97%, at least 98%, at least 99% or 100% identical to the sequence shown in SEQ ID NO:1. In some embodiments, the NpHR opsin further comprises an endoplasmic reticulum (ER) export signal and/or a membrane trafficking signal. For example, the NpHR opsin comprises an amino acid sequence at least 95% identical to the sequence shown in SEQ ID NO:1 and an endoplasmic reticulum (ER) export signal. In some embodiments, the amino acid sequence at least 95% identical to the sequence shown in SEQ ID NO:1 is linked to the ER export signal through a linker. In some embodiments, the ER export signal comprises the amino acid sequence FXYENE (SEQ ID NO:12), where X can be any amino acid. In another embodiment, the ER export signal comprises the amino acid sequence VXXSL (SEQ ID NO:15), where X can be any amino acid. In some embodiments, the ER export signal comprises the amino acid sequence FCYENEV (SEQ ID NO:13). In some embodiments, the NpHR opsin comprises an amino acid sequence at least 95% identical to the sequence shown in SEQ ID NO:1, an ER export signal, and a membrane trafficking signal. In other embodiments, the NpHR opsin comprises, from the N-terminus to the C-terminus, the amino acid sequence at least 95% identical to the sequence shown in SEQ ID NO:1, the ER export signal, and the membrane trafficking signal. In other embodiments, the NpHR opsin comprises, from the N-terminus to the C-terminus, the amino acid sequence at least 95% identical to the sequence shown in SEQ ID NO:1, the membrane trafficking signal, and the ER export signal. In some embodiments, the membrane trafficking signal is derived from the amino acid sequence of the human inward rectifier potassium channel $K_{ir}2.1$. In some embodiments, the membrane trafficking signal comprises the amino acid sequence K S R I T S E G E Y I P L D Q I D I N V (SEQ ID NO:14). In some embodiments, the membrane trafficking signal is linked to the amino acid sequence at least 95% identical to the sequence shown in SEQ ID NO:1 by a linker. In some embodiments, the membrane trafficking signal is linked to the ER export signal through a linker. The linker may comprise any of 5, 10, 20, 30, 40, 50, 75, 100, 125, 150, 175, 200, 225, 250, 275, 300, 400, or 500 amino acids in length. The linker may further comprise a fluorescent protein, for example, but not limited to, a yellow fluorescent protein, a red fluorescent protein, a green fluorescent protein, or a cyan fluorescent protein. In some embodiments, the light-activated opsin further comprises an N-terminal signal peptide. In some embodiments, the light-activated opsin comprises the amino acid sequence of SEQ ID NO:2. In some embodiments, the light-activated protein comprises the amino acid sequence of SEQ ID NO:3.

[0041] In some embodiments, the light-activated opsin is a chimeric protein derived from VChR1 from *Volvox carteri* and ChR1 from *Chlamydomonas reinhardti*. In some embodiments, the chimeric protein comprises the amino acid sequence of VChR1 having at least the first and second transmembrane helices replaced by the corresponding first and second transmembrane helices of ChR1. In other embodiments, the chimeric protein comprises the amino acid sequence of VChR1 having the first and second transmembrane helices replaced by the corresponding first and second transmembrane helices of ChR1 and further comprises at least a portion of the intracellular loop domain located between the second and third transmembrane helices replaced by the corresponding portion from ChR1. In some embodiments, the entire intracellular loop domain between the second and third transmembrane helices of the chimeric light-activated protein can be replaced with the corresponding intracellular loop domain from ChR1. In some embodiments, the light-activated chimeric protein comprises an amino acid sequence at least 90%, 91%, 92%, 93%, 94%, 95%, 96%, 97%, 98%, 99%, or 100% identical to the sequence shown in SEQ ID NO:8 without the signal peptide sequence. In some embodiments, the light-activated chimeric protein comprises an amino acid sequence at least 90%, 91%, 92%, 93%, 94%, 95%, 96%, 97%, 98%, 99%, or 100% identical to the sequence shown in SEQ ID NO:8. C1V1 chimeric light-activated opsins that may have specific amino acid substitutions at key positions throughout the retinal binding pocket of the VChR1 portion of the chimeric polypeptide. In some embodiments, the C1V1 protein has a mutation at amino acid residue E122 of SEQ ID NO:8. In some embodiments, the C1V1 protein has a mutation at amino acid residue E162 of SEQ ID NO:8. In other embodiments, the C1V1 protein has a mutation at both amino acid residues E162 and E122 of SEQ ID NO:8. In some embodiments, each of the disclosed mutant C1V1 chimeric proteins can have specific properties and characteristics for use in depolarizing the membrane of an animal cell in response to light.

[0042] As used herein, a vector comprises a nucleic acid encoding a light-responsive opsin described herein and the nucleic acid is operably linked to a promoter that controls the specific expression of the opsin in the glutamatergic pyramidal neurons. Any vectors that are useful for delivering a nucleic acid to glutamatergic pyramidal neurons may be used. Vectors include viral vectors, such as AAV vectors, retroviral vectors, adenoviral vectors, HSV vectors, and lentiviral vectors. Examples of AAV vectors are AAV1, AAV2, AAV3, AAV4, AAV5, AAV6, AAV7, AAV8, AAV9, AAV10, AAV11, AAV12, AAV13, AAV14, AAV15, and AAV16. A CaMKIIα promoter and any other promoters that can control the expression of the opsin in the glutamatergic pyramidal neurons may be used.

[0043] An "individual" is a mammal, such as a human. Mammals also include, but are not limited to, farm animals, sport animals, pets (such as cats, dogs, horses), primates, mice and rats. An "animal" is a non-human mammal

[0044] As used herein, "treatment" or "treating" or "alleviation" is an approach for obtaining beneficial or desired results including and preferably clinical results. For purposes of this invention, beneficial or desired clinical results include, but are not limited to, one or more of the following: showing observable and/or measurable reduction in one or more signs of the disease (such as anxiety), decreasing symptoms resulting from the disease, increasing the quality of life of those suffering from the disease, decreasing the dose of other medications required to treat the disease, and/or delaying the progression of the disease.

[0045] As used herein, an "effective dosage" or "effective amount" of a drug, compound, or pharmaceutical composition is an amount sufficient to effect beneficial or desired results. For therapeutic use, beneficial or desired results include clinical results such as decreasing one or more symptoms resulting from the disease, increasing the quality of life of those suffering from the disease, decreasing the dose of other medications required to treat the disease, enhancing effect of another medication such as via targeting, and/or delaying the progression of the disease. As is understood in the clinical context, an effective dosage of a drug, compound, or pharmaceutical composition may or may not be achieved in conjunction with another drug, compound, pharmaceutical composition, or another treatment. Thus, an "effective dosage" may be considered in the context of administering one or more therapeutic agents or treatments, and a single agent may be considered to be given in an effective amount if, in conjunction with one or more other agents or treatments, a desirable result may be or is achieved.

[0046] The above overview is not intended to describe each illustrated embodiment or every implementation of the present disclosure.

DETAILED DESCRIPTION AND EXAMPLE EXPERIMENTAL EMBODIMENTS

[0047] The present disclosure is believed to be useful for controlling anxiety states and/or symptoms of anxiety. Specific applications of the present invention relate to optogenetic systems or methods that correlate temporal, spatio and/or cell-type control over a neural circuit associated with anxiety states and/or symptoms thereof. As many aspects of the example embodiments disclosed herein relate to and significantly build on previous developments in this field, the following discussion summarizes such previous developments to provide a solid understanding of the foundation and underlying teachings from which implementation details and modifications might be drawn, including those found in the Examples. It is in this context that the following discussion is provided and with the teachings in the references incorporated herein by reference. While the present invention is not necessarily limited to such applications, various aspects of the invention may be appreciated through a discussion of various examples using this context.

[0048] Anxiety refers to a sustained state of heightened apprehension in the absence of an immediate threat, which in disease states becomes severely debilitating. Embodiments of the present disclosure are directed toward the use of one or more of cell type-specific optogenetic tools with two-photon microscopy, electrophysiology, and anxiety assays to study and develop treatments relating to neural circuits underlying anxiety-related behaviors.

[0049] Aspects of the present disclosure are related to the optogenetic targeting of specific projections of the brain, rather than cell types, in the study of neural circuit function relevant to psychiatric disease.

[0050] Consistent with particular embodiments of the present disclosure, temporally-precise optogenetic stimulation of basolateral amygdala (BLA) terminals in the central nucleus of the amygdala (CeA) are used to produce a

reversible anxiolytic effect. The optogenetic stimulation can be implemented by viral transduction of BLA with a light-responsive opsin, such as ChR2, followed by restricted illumination in downstream CeA.

[0051] Consistent with other embodiments of the present disclosure, optogenetic inhibition of the basolateral amygdala (BLA) terminals in the central nucleus of the amygdala (CeA) are used to increase anxiety-related behaviors. The optogenetic stimulation can be implemented by viral transduction of BLA with a light-responsive opsin, such as eNpHR3.0, followed by restricted illumination in downstream CeA.

[0052] Embodiments of the present disclosure are directed towards the specific targeting of neural cell populations, as anxiety-based effects were not observed with direct optogenetic control of BLA somata. For instance, targeting of specific BLA-CeA projections as circuit elements have been experimentally shown to be sufficient for endogenous anxiety control in the mammalian brain.

[0053] Consistent with embodiments of the present disclosure, the targeting of the specific BLA-CeA projections as circuit elements is based upon a number of factors discussed in more detail hereafter. The amygdala is composed of functionally and morphologically heterogeneous subnuclei with complex interconnectivity. A primary subdivision of the amygdala is the basolateral amygdala complex (BLA), which encompasses the lateral (LA), basolateral (BL) and basomedial (BM) amygdala nuclei (~90% of BLA neurons are glutamatergic). In contrast, the central nucleus of the amygdala (CeA), which is composed of the centrolateral (CeL) and centromedial (CeM) nuclei, is predominantly (~95%) comprised of GABAergic medium spiny neurons. The BLA is ensheathed in dense clusters of GABAergic intercalated cells (ITCs), which are functionally distinct from both local interneurons and the medium spiny neurons of the CeA. The primary output nucleus of the amygdala is the CeM, which, when chemically or electrically excited, is believed to mediate autonomic and behavioral responses that are associated with fear and anxiety via projections to the brainstem. While the CeM is not directly controlled by the primary amygdala site of converging environmental and cognitive information (LA), LA and BLA neurons excite GABAergic CeL neurons, which can provide feed-forward inhibition onto CeM "output" neurons and reduce amygdala output. The BLA-CeL-CeM is a less-characterized pathway suggested to be involved not in fear extinction but in conditioned inhibition. The suppression of fear expression, possibly due to explicit unpairing of the tone and shock, suggested to be related to the potentiation of BLA-CeL synapses.

[0054] BLA cells have promiscuous projections throughout the brain, including to the bed nucleus of the stria terminalis (BNST), nucleus accumbens, hippocampus and cortex. Aspects of the present disclosure relate to methods for selective control of BLA terminals in the CeL, without little or no direct affect/control of other BLA projections. Preferential targeting of BLA-CeL synapses can be facilitated by restricting opsin gene expression to BLA glutamatergic projection neurons and by restricting light delivery to the CeA.

[0055] For instance, control of BLA glutamatergic projection neurons can be achieved with an adeno-associated virus (AAVS) vector carrying light-activated optogenetic control genes under the control of a CaMKIIa promoter. Within the BLA, CaMKIIα is only expressed in glutamatergic pyramidal neurons, not in local interneurons or intercalated cells.

[0056] FIG. **1** shows a system for providing optogenetic targeting of specific projections of thebrain, consistent with an embodiment of the present disclosure. For instance, a beveled guide cannula can be used to direct light, e.g., prevent light delivery to the BLA and allow selective illumination of the CeA. This preferential delivery of light to the CeA projection can be accomplished using stereotaxic guidance along with implantation over the CeL. Geometric and functional properties of the resulting light distribution can be quantified both in vitro and in vivo, e.g., using in vivo electrophysiological recordings to determine light power parameters for selective control of BLA terminals but not BLA cell bodies. Experimental results, such as those described in the Examples, support that such selective excitation or inhibition result in significant, immediate and reversible anxiety-based effects.

[0057] Embodiments of the present disclosure are directed toward the above realization being applied to various ones of the anatomical, functional, structural, and circuit targets identified herein. For instance, the circuit targets can be studied to develop treatments for the psychiatric disease of anxiety. These treatments can include, as non-limiting examples, pharmacological, electrical, magnetic, surgical and optogenetic, or other treatment means.

[0058] FIG. **2** shows a flow diagram for use of an anxiety-based circuit model, consistent with an embodiment of the present disclosure. An optogenetic delivery device, such as a. viral delivery device, is generated **202**. This delivery device can be configured to introduce optically responsive opsins to the target cells and may include targeted promoters for specific cell types. The delivery device can then be stereotaxically (or otherwise) injected **204** into the BLA. A light delivery device can then be surgical implanted **206**. This light delivery device can be configured to provide targeted illumination (e.g., using a directional optical element). The target area is then illuminated **208**. The target area can be, for example, the BLA-CeA. The effects thereof can then be monitored and/or assessed **210**. This can also be used in connection with treatments or drug screening.

[0059] Various embodiments of the present disclosure relate to the use of the identified model for screening new treatments for anxiety. For instance, anxiety can be artificially induced or repressed using the methods discussed herein, while pharmacological, electrical, magnetic, surgical, or optogenetic treatments are then applied and assessed. In other embodiments of the present disclosure, the model can be used to develop an in vitro approximation or simulation of the identified circuit, which can then be used in the screening of devices, reagents, tools, technologies, methods and approaches and for studying and probing anxiety and related disorders. This study can be directed towards, but not necessarily limited to, identifying phenotypes, endophenotypes, and treatment targets.

[0060] Embodiments of the present disclosure are directed toward modeling the BLA-CeL pathway as an endogenous neural substrate for bidirectionally modulating the unconditioned expression of anxiety. Certain embodiments are directed toward other downstream circuits, such as CeA projections to the BNST, for their role in the expression of anxiety or anxiety-related behaviors. For instance, it is believed that corticotropin releasing hormone (CRH) networks in the BNST may be critically involved in modulating

anxiety-related behaviors, as the CeL is a primary source of CRH for the BNST. Other neurotransmitters and neuromodulators may modulate or gate effects on distributed neural circuits, including serotonin, dopamine, acetylcholine, glycine, GABA and CRH. Still other embodiments are directed toward control of the neural circuitry converging to and diverging from this pathway, as parallel or downstream circuits of the BLA-CeL synapse are believed to contribute to the modulation or expression of anxiety phenotypes. Moreover, upstream of the amygdala, this microcircuit is well-positioned to be recruited by top-down cortical control from regions important for processing fear and anxiety, including the prelimbic, infralimbic and insular cortices that provide robust innervation to the BLA and CeL.

[0061] Experimental results based upon the BLA anatomy suggest that the populations of BLA neurons projecting to CeL and CeM neurons are largely non-overlapping. In natural states, the CeL-projecting BLA neurons may excite CeM-projecting BLA neurons in a microcircuit homeostatic mechanism, which can then be used to study underlying anxiety disorders when there are synaptic changes that skew the balance of the circuit to allow uninhibited CeM activation.

[0062] The embodiments and specific applications discussed herein (including the Examples) may be implemented in connection with one or more of the above-described aspects, embodiments and implementations, as well as with those shown in the figures and described below. Reference may be made to the following Example, which is fully incorporated herein by reference. For further details on light-responsive molecules and/or opsins, including methodology, devices and substances, reference may also be made to the following background publications: U.S. Patent Publication No. 2010/0190229, entitled "System for Optical Stimulation of Target Cells" to Zhang et al.; U.S. Patent Publication No. 2010/0145418, also entitled "System for Optical Stimulation of Target Cells" to Zhang et al.; U.S. Patent Publication No. 2007/0261127, entitled "System for Optical Stimulation of Target Cells" to Boyden et al.; and PCT WO 2011/116238, Entitled "Light Sensitive Ion Passing Molecules". These applications form part of the patent document and are fully incorporated herein by reference. Consistent with these publications, numerous opsins can be used in mammalian cells in vivo and in vitro to provide optical stimulation and control of target cells. For example, when ChR2 is introduced into an electrically-excitable cell, such as a neuron, light activation of the ChR2 channelrhodopsin can result in excitation and/or firing of the cell. In instances when NpHR is introduced into an electrically-excitable cell, such as a neuron, light activation of the NpHR opsin can result in inhibition of firing of the cell. These and other aspects of the disclosures of the above-referenced patent applications may be useful in implementing various aspects of the present disclosure.

[0063] While the present disclosure is amenable to various modifications and alternative forms, specifics thereof have been shown by way of example in the drawings and will be described in further detail. It should be understood that the intention is not to limit the disclosure to the particular embodiments and/or applications described. On the contrary, the intention is to cover all modifications, equivalents, and alternatives falling within the spirit and scope of the present disclosure.

EXAMPLES

[0064] Introduction

[0065] Anxiety is a sustained state of heightened apprehension in the absence of immediate threat, which in disease states becomes severely debilitating'. Anxiety disorders represent the most common of the psychiatric diseases (with 28% lifetime prevalence)[2], and have been linked to the etiology of major depression and substance abuse[3-5]. While the amygdala, a brain region important for emotional processing[9-17], has long been hypothesized to play a role in anxiety[18-23], the neural mechanisms which control and mediate anxiety have yet to be identified. Here, we combine cell type-specific optogenetic tools with two-photon microscopy, electrophysiology, and anxiety assays in freely-moving mice to identify neural circuits underlying anxiety-related behaviors. Capitalizing on the unique capability of optogenetics[24-26] to control not only cell types, but also specific connections between cells, we observed that temporally-precise optogenetic stimulation of basolateral amygdala (BLA) terminals in the central nucleus of the amygdala (CeA), resolved by viral transduction of BLA with ChR2 followed by restricted illumination in downstream CeA, exerted a profound, immediate, and reversible anxiolytic effect. Conversely, selective optogenetic inhibition of the same defined projection with eNpHR3.0[25] potently, swiftly, and reversibly increased anxiety-related behaviors. Importantly, these effects were not observed with direct optogenetic control of BLA somata themselves. Together, these results implicate specific BLA-CeA projections as circuit elements both necessary and sufficient for endogenous anxiety control in the mammalian brain, and demonstrate the importance of optogenetically targeting specific projections, rather than cell types, in the study of neural circuit function relevant to psychiatric disease.

[0066] Despite the high prevalence and severity[1] of anxiety disorders, the corresponding neural circuit substrates are poorly understood, impeding the development of safe and effective treatments. Available treatments tend to be inconsistently effective or, in the case of benzodiazepines, addictive and linked to significant side effects including sedation and respiratory suppression that can cause cognitive impairment and death[27, 28]. A deeper understanding of anxiety control mechanisms in the mammalian brain[29, 30] is necessary to develop more efficient treatments that have fewer side-effects. Of particular interest and novelty would be the possibility of recruiting native pathways for anxiolysis.

[0067] The amygdala is critically involved in processing associations between neutral stimuli and positive or negative outcomes, and has also been implicated in processing unconditioned emotional states. While the amygdala microcircuit has been functionally dissected in the context of fear conditioning, amygdalar involvement has been implicated in a multitude of other functions and emotional states, including unconditioned anxiety. The amygdala is composed of functionally and morphologically heterogeneous subnuclei with complex interconnectivity. A primary subdivision of the amygdala is the basolateral amygdala complex (BLA), which encompasses the lateral (LA), basolateral (BL) and basomedial (BM) amygdala nuclei (~90% of BLA neurons are glutamatergic)[33, 34]. In contrast, the central nucleus of the amygdala (CeA), which is composed of the centrolateral (CeL) and centromedial (CeM) nuclei, is predominantly (~95%) comprised of GABAergic medium spiny neurons[35]. The BLA is ensheathed in dense clusters of GABAergic

intercalated cells (ITCs), which are functionally distinct from both local interneurons and the medium spiny neurons of the CeA[36, 37]. The primary output nucleus of the amygdala is the CeM,[32, 35, 38-40] which when chemically or electrically excited mediates autonomic and behavioral responses associated with fear and anxiety via projections to the brainstem6, 12, 32, 35. While the CeM is not directly controlled by the primary amygdala site of converging environmental and cognitive information (LA)[12, 38, 41], LA and BLA neurons excite GABAergic CeL neurons[42] which can provide feed-forward inhibition onto CeM[40, 46] "output" neurons and reduce amygdala output. The BLA-CeL-CeM is a less-characterized pathway suggested to be involved not in fear extinction but in conditioned inhibition, the suppression of fear expression due to explicit unpairing of the tone and shock, due to the potentiation of BLA-CeL synapses[47]. Although fear is characterized to be a phasic state triggered by an external cue, while anxiety is a sustained state that may occur in the absence of an external trigger, we wondered if circuits modulating conditioned inhibition of fear might also be involved in modulating unconditioned inhibition of anxiety.

[0068] Materials and Methods

[0069] Subjects: Male C57BL/6 mice, aged 4-6 weeks at the start of experimental procedures, were maintained with a reverse 12-hr light/dark cycle and given food and water ad libitum. Animals shown in FIGS. **3**A-**3**K, **4**A-**4**F and **5**A-**5**J (mice in the ChR2 Terminals, EYFP Terminals and ChR2 Cell Bodies groups) were all single-housed in a typical high-traffic mouse facility to increase baseline anxiety levels. Each mouse belonged to a single treatment group. Animals shown in FIG. **6**A-**6**P (Bilateral EYFP and eNpHR 3.0 groups) were group-housed in a special low-traffic facility to decrease baseline anxiety levels. Animal husbandry and all aspects of experimental manipulation of our animals were in accordance with the guidelines from the National Institute of Health and have been approved by members of the Stanford Institutional Animal Care and Use Committee.

[0070] Optical Intensity Measurements: Light transmission measurements were conducted with blocks of brain tissue from acutely sacrificed mice. The tissue was then placed over the photodetector of a power meter (ThorLabs, Newton, N.J.) to measure the light power of the laser penetrated the tissue. The tip of a 300 μm diameter optical fiber was coupled to a 473 nm blue laser (OEM Laser Systems, East Lansing, Mich.). To characterize the light transmission to the opposite side of the bevel, the photodetector of the power meter was placed parallel to the beveled cannula. For visualization of the light cone, we used Fluorescein isothiocyanate-dextran (FD150s; Sigma, Saint Louis, Mo.) at approximately 5 mg/ml placed in a cuvette with the optical fibers either with or without beveled cannula shielding aimed perpendicularly over the fluorescein solution. Power density at specific depths were calculated considering both fractional decrease in intensity due to the conical output of light from the optical fiber and the loss of light due to scattering in tissue (Aravanis et al., *J Neural Eng,* 4:S143-156, 2007) (Gradinaru et al., *Neurosci,* 27:14231-14238, 2007). The half-angle of divergence θ_{div} for a multimode optical fiber, which determines the angular spread of the output light, is

$$\theta_{div} = \sin^{-1}\left(\frac{NA_{fib}}{n_{tiz}}\right)$$

where n_{tis} is the index of refraction of gray matter (1.36, Vo-Dinh T 2003, Biomedical Photonics Handbook (Boca Raton, Fla.: CRC Press)) and NA_{fib}(0.37) is the numerical aperture of the optical fiber. The fractional change in intensity due to the conical spread of the light with distance (z) from the fiber end was calculated using trigonometry

$$\frac{I(z)}{I(Z=0)} = \frac{\rho^2}{(z+\rho)^2}, \text{ where } \rho = r\sqrt{\left(\frac{n}{NA}\right)^2 - 1}$$

and r is the radius of the optical fiber (100 pm).

[0071] The fractional transmission of light after loss due to scattering was modeled as a hyperbolic function using empirical measurements and the Kubelka-Munk model [1, 2], and the combined product of the power density at the tip of the fiber and the fractional changes due to the conical spread and light scattering, produces the value of the power density at a specific depth below the fiber.

[0072] Virus construction and packaging: The recombinant AAV vectors were serotyped with AAV5 coat proteins and packaged by the viral vector core at the University of North Carolina. Viral titers were $2\times10e^{12}$ particles/mL, $3\times10e^{12}$ particles/mL, $4\times10e^{12}$ particles/mL respectively for AAV-CaMKIIα-hChR2(H134R)-EYFP, AAV-CaMKIIα-EYFP, and AAV-CaMKIIα-eNpHR 3.0-EYFP. The pAAV-CaMKIIα-eNpHR3.0-EYFP plasmid was constructed by cloning CaMKIIα-eNpHR3.0-EYFP into an AAV backbone using MluI and EcoRI restriction sites. Similarly, The pAAV-CaMKIIα-EYFP plasmid was constructed by cloning CaMKIIα-EYFP into an AAV backbone using MluI and EcoRI restriction sites. The maps are available online at www.optogenetics.org, which are incorporated herein by reference.

[0073] Stereotactic injection and optical fiber placement: All surgeries were performed under aseptic conditions under stereotaxic guidance. Mice were anaesthetized using 1.5-3.0% isoflourane. All coordinates are relative to bregma in mm^3. In all experiments, both in vivo and in vitro, virus was delivered to the BLA only, and any viral expression in the CeA rendered exclusion from all experiments. Cannula guides were beveled to form a 45-55 degree angle for the restriction of the illumination to the CeA. The short side of the beveled cannula guide was placed antero-medially, the long side of the beveled cannula shielded the posterior-lateral portion of the light cone, facing the opposite direction of the viral injection needle. To preferentially target BLA-CeL synapses, we restricted opsin gene expression to BLA glutamatergic projection neurons and restricted light delivery to the CeA. Control of BLA glutamatergic projection neurons was achieved using an adeno-associated virus (AAV5) vector carrying light-activated optogenetic control genes under the control of a CaMKIIα promoter. Within the BLA, CaMKIIα is only expressed in glutamatergic pyramidal neurons, not in local interneurons[4]. Mice in the ChR2 Terminals and EYFP Terminals groups received unilateral implantations of beveled cannulae for the optical fiber (counter-balanced for hemisphere), while mice in the eNpHR 3.0 or respective EYFP group received bilateral

implantations of the beveled cannulae over the CeA (−1.06 mm anteroposterior (AP); ±2.25 mm mediolateral (ML); and −4.4 mm dorsoventral (DV); PlasticsOne, Roanoke, Va.)[3]. Mice in the ChR2 Cell Bodies groups received unilateral implantation of a Doric patchcord chronically implantable fiber (NA=0.22; Doric lenses, Quebec, Canada) over the BLA at (−1.6 mm AP; ±3.1 mm ML; −4.5 mm DV)[3]. For all mice, 0.5 μl of purified AAV_5 was injected unilaterally or bilaterally in the BLA (±3.1 mm AP, 1.6 mm ML, −4.9 mm DV)[3] using beveled 33 or 35 gauge metal needle facing postero-lateral side to restrict the viral infusion to the BLA. 10 μl Hamilton microsyringe (nanofil; WPI, Sarasota, Fla.) were used to deliver concentrated AAV solution using a microsyringe pump (UMP3; WPI, Sarasota, Fla.) and its controller (Micro4; WPI, Sarasota, Fla.). Then, 0.5 μl of virus solution was injected at each site at a rate of 0.1 μl per min. After injection completion, the needle was lifted 0.1 mm and stayed for 10 additional minutes and then slowly withdrawn. One layer of adhesive cement (C&B metabond; Parkell, Edgewood, N.Y.) followed by cranioplastic cement (Dental cement; Stoelting, Wood Dale, Ill.) was used to secure the fiber guide system to the skull. After 20 min, the incision was closed using tissue adhesive (Vetbond; Fisher, Pittsburgh, Pa.). The animal was kept on a heating pad until it recovered from anesthesia. A dummy cap (rat: C312G, mouse: C313G) was inserted to keep the cannula guide patent. Behavioral and electrophysiological experiments were conducted 4-6 weeks later to allow for viral expression.

[0074] In vivo recordings: Simultaneous optical stimulation of central amygdala (CeA) and electrical recording of basolateral amygdala (BLA) of adult male mice previously (4-6 weeks prior) transduced in BLA with AAV-CaMKIIa-ChR2-eYFP viral construct was carried out as described previously (Gradinaru et al., *J Neurosci,* 27:14231-14238, 2007). Animals were deeply anesthetized with isoflurane prior to craniotomy and had negative toe pinch. After aligning mouse stereotaxically and surgically removing approximately 3 mm^2 skull dorsal to amygdala. Coordinates were adjusted to allow for developmental growth of the skull and brain, as mice received surgery when they were 4-6 weeks old and experiments were performed when the mice were 8-10 weeks old (centered at −1.5 mm AP, ±2.75 mm ML)[3], a 1Mohm 0.005-in extracellular tungsten electrode (A-M systems) was stereotactically inserted into the craniotomized brain region above the BLA (in mm −1.65 AP, ±3.35 ML, −4.9 DV)[3]. Separately, a 0.2 N.A. 200 μm core diameter fiber optic cable (Thor Labs) was stereotactically inserted into the brain dorsal to CeA (−1.1 AP, ±2.25 ML, −4.2 DV)[3]. After acquiring a light evoked response, voltage ramps were used to vary light intensity during stimulation epochs (20 Hz, 5 ms pulse width) 2 s in length. After acquiring optically evoked signal, the exact position of the fiber was recorded, the fiber removed from the brain, inserted into a custom beveled cannula, reinserted to the same position, and the same protocol was repeated. In most trials, the fiber/cannula was then extracted from the brain, the cannula removed, and the bare fiber reinserted to ensure the fidelity of the population of neurons emitting the evoked signal. Recorded signals were bandpass filtered between 300 Hz and 20 kHz, AC amplified either 1000× or 10000× (A-M Systems 1800), and digitized (Molecular Devices Digidata 1322A) before being recorded using Clampex software (Molecular Devices). Clampex software was used for both recording field signals and controlling a 473 nm (OEM Laser Systems) solidstate laser diode source coupled to the optrode. Light power was titrated between <1 mW (~14 mW/mm^2) and 28 mW (~396 mW/mm^2) from the fiber tip and measured using a standard light power meter (Thor-Labs). Electrophysiological recordings were initiated approximately 1 mm dorsal to BLA after lowering isoflurane anesthesia to a constant level of 1%. Optrode was lowered ventrally in ~0.1 mm steps until localization of optically evoked signal.

[0075] Behavioral assays: All animals used for behavior received viral transduction of BLA neurons and the implantation enabling unilateral (for ChR2 groups and controls) or bilateral (for eNpHR3.0 groups and controls) light delivery. For behavior, multimode optical fibers (NA 0.37; 300 pm core, BFL37-300; ThorLabs, Newton, N.J.) were precisely cut to the optimal length for restricting the light to the CeA, which was shorter than the long edge of the beveled cannula, but longer than the shortest edge of the beveled cannula. For optical stimulation, the fiber was connected to a 473 nm or 594 nm laser diode (OEM Laser Systems, East Lansing, Mich.) through an FC/PC adapter. Laser output was controlled using a Master-8 pulse stimulator (A.M.P.I., Jerusalem, Israel) to deliver light trains at 20 Hz, 5 ms pulse-width for 473 nm light, and constant light for 594 nm light experiments. All included animals had the center of the viral injection located in the BLA, though there was sometimes leak to neighboring regions or along the needle tract. Any case in which there was any detectable viral expression in the CeA, the animals were excluded. All statistically significant effects of light were discussed, and undiscussed comparisons did not show detectable differences.

[0076] The elevated plus maze was made of plastic and consisted of two light gray open arms (30×5 cm), two black enclosed arms (30×5×30 cm) extending from a central platform (5×5×5 cm) at 90 degrees in the form of a plus. The maze was placed 30 cm above the floor. Mice were individually placed in the center. 1-5 minutes were allowed for recovery from handling before the session was initiated. Video tracking software (BiObserve, Fort Lee, N.J.) was used to track mouse location, velocity and movement of head, body and tail. All measurements displayed were relative to the mouse body. Light stimulation protocols are specified by group. ChR2:BLA-CeA mice and corresponding controls groups (EYFP:BLA-CeA and ChR2:BLA Somata) were singly-housed in a high-stress environment for at least 1 week prior to anxiety assays: unilateral illumination of BLA terminals in the CeA at 7-8 mW (~106 mW/mm^2 at the tip of the fiber, ~6.3 mW/mm2 at CeL and ~2.4 mW/mm^2 at the CeM) of 473 nm light pulse trains (5 ms pulses at 20 Hz). For the ChR2 Cell Bodies group BLA neurons were directly illuminated with a lower light power because illumination with 7-8 mW induced seizure activity, so we unilaterally illuminated BLA neurons at 3-5 mW (~57 mW/mm^2) of 473 nm light pulse trains (5 ms pulses at 20 Hz). For the eNpHR 3.0 and corresponding EYFP group, all mice were group-housed and received bilateral viral injections and bilateral illumination of BLA terminals in the CeA at 4-6 mW (~71 mW/mm^2 at the tip of the fiber, ~4.7 mW/mm^2 at the CeL and ~1.9 mW/mm^2 at the CeM) of 594 nm light with constant illumination throughout the 5-min light on epoch. The 15-min session was divided into 3 5-min epochs, the first epoch there was no light stimulation (off), the second epoch light was delivered as specified above (on), and the third epoch there was no light stimulation (off).

[0077] The open-field chamber (50×50 cm) and the open field was divided into a central field (center, 23 x 23 cm) and an outer field (periphery). Individual mice were placed in the periphery of the field and the paths of the animals were recorded by a video camera. The total distance traveled was analyzed by using the same video-tracking software, Viewer^2 (BiObserve, Fort Lee, N.J.). The open field assessment was made immediately after the elevated-plus maze test. The open field test consisted of an 18-min session in which there were six 3-min epochs. The epochs alternated between no light and light stimulation periods, beginning with a light off epoch. For all analyses and charts where only "off" and "on" conditions are displayed, the 3 "off" epochs were pooled and the 3 "on" epochs were pooled.

[0078] For the glutamate receptor antagonist manipulation, a glutamate antagonist solution consisting of 22.0 mM of NBQX and 38.0 mM of D-APV (Tocris, Ellisville, Mo.) dissolved in saline (0.9% NaCl). 5-15 min before the anxiety assays, 0.3 μl of the glutamate antagonist solution was infused into the CeA via an internal infusion needle, inserted into the same guide cannulae used for light delivery via optical fiber, that was connected to a 10-μl Hamilton syringe (nanofil; WPI, Sarasota, Fla.). The flow rate (0.1 μl per min) was regulated by a syringe pump (Harvard Apparatus, Mass.). Placements of the viral injection, guide cannula and chronically-implanted fiber were histologically verified as indicated in FIGS. **7** and **10**A-**10**F.

[0079] Two-photon optogenetic circuit mapping and ex vivo electrophysiological recording: Mice were injected with AAV5-CaMKIIα-ChR2-EYFP at 4 weeks of age, and were sacrificed for acute slice preparation 4-6 weeks to allow for viral expression. Coronal slices containing the BLA and CeA were prepared to examine the functional connectivity between the BLA and the CeA. Two-photon images and electrophysiological recordings were made under the constant perfusion of aCSF, which contained (in mM): 126 NaCl, 26 $NaHCO_3$, 2.5 KCl, 1.25 NaH_2PO_4, 1 $MgCl_2$, 2 $CaCl_2$, and 10 glucose. All recordings were at 32° C. Patch electrodes (4-6 MOhms) were filled (in min): 10 HEPES, 4 Mg-ATP, 0.5 $MgCl_2$, 0.4 Na_3-GTP, 10 NaCl, 140 potassium gluconate, and 80 Alexa-Fluor 594 hydrazide (Molecular Probes, Eugene Oreg.). Whole-cell patch-clamp recordings were performed in BLA, CeL and CeM neurons, and cells were allowed to fill for approximately 30 minutes before imaging on a modified two-photon microscope (Prairie Microscopes, Madison Wis.) where two-photon imaging, whole-cell recording and optogenetic stimulation could be done simultaneously. Series resistance of the pipettes was usually 10-20 MOhms. Blue light pulses were elicited using a 473 nm LED at ~7 mW/mm^2 (Thorlabs, Newton N.J.) unless otherwise noted. A Coherent Ti-Saphire laser was used to image both ChR2-YFP (940 nm) and Alexa-Fluor 594 (800 nm). A FF560 dichroic with filters 630/69 and 542/27 (Semrock, Rochester N.Y.) was also used to separate both molecules' emission. All images were taken using a 40X/.8 NA LUMPlanFL/IR Objective (Olympus, Center Valley Pa.). In order to isolate fibers projecting to CeL from the BLA and examine responses in the CeM, slices were prepared as described above with the BLA excluded from illumination. Whole-cell recordings were performed in the CeM with illumination from the objective aimed over the CeL. To further ensure activation of terminals from the BLA to CeL was selective, illumination was restricted to a ~125 μm diameter around the center of the CeL. Here, blue light pulses were elicited using an XCite halogen light source (EXPO, Mississauga, Ontario) with a 470/3 filter at 6.5 mW/mm^2 coupled to a shutter (Uniblitz, Rochester N.Y.). For functional mapping, we first recorded from a BLA neuron expressing ChR2 and simultaneously collected electrophysiological recordings and filled the cell with Alexa-Fluor 594 hydrazide dye to allow for two-photon imaging. Two-photon z-stacks were collected at multiple locations along the axon of the filled BLA neuron. We then followed the axon of the BLA neuron projecting to the CeL nucleus and recorded from a CeL neuron in the BLA terminal field. We then simultaneously recorded from a CeL neuron, filled the cell with dye and performed two-photon live imaging before following the CeL neuronal axons to the CeM. We then repeated this procedure in a CeM neuron, but moved the light back to the terminal field in the CeL to mimic the preferential illumination of BLA-CeL synapses with the same stimulation parameters as performed in vivo. Voltage-clamp recordings were made at both −70 mV, to isolate EPSCs, and at 0 mV, to isolate IPSCs. EPSCs were confirmed to be EPSCs via bath application of the glutamate receptor antagonists (n=5), NBQX (22 μM) and AP5 (38 μM), IPSCs were confirmed to be IPSCs via bath application of bicuculline (10 μM; n=2), which abolished them, respectively. We also performed current-clamp recordings when the cell was resting at approximately −70 mV.

[0080] For the characterization of optogenetically-driven antidromic stimulation in BLA axon terminals, animals were injected with AAV5-CaMKIIα-ChR2-EYFP at 4 weeks of age, and were sacrificed for acute slice preparation 4-6 weeks to allow for viral expression. Slice preparation was the same as above. To the aCSF we added 0.1 mM picrotoxin, 10 μM CNQX and 25 μM AP5 (Sigma, St. Louis, Mo.). Whole-cell patch-clamp recordings were performed in BLA neurons and were allowed to fill for approximately 30 minutes before two-photon imaging. Series resistance of the pipettes was usually 10-20 MOhms. All images were taken using a 40X/.8 NA LUMPlanFL/IR Objective (Olympus, Center Valley Pa.). Blue light pulses were elicited using an XCite halogen light source (EXPO, Mississauga, Ontario) with a 470/30 filter at 6.5 mW/mm^2 coupled to a shutter (Uniblitz, Rochester N.Y.). Two-photon z-stacks were collected at multiple locations along the axon of the filled BLA neuron. Only neurons whose axons could be visualized for over ~300 μm diameter towards the CeL nucleus were included for the experiment, and neurons that had processes going in all directions were also excluded. Stimulation on/off axon was accomplished by moving the slice relative to a ~125 μm diameter blue light spot. In order to calibrate the slice for correct expression, whole-cell patch-clamp was performed on a CeL cell and a ~125 μm diameter spot blue pulse was used to ensure that synaptic release from the BLA terminals on to the CeL neuron was reliable.

[0081] For the dissection of direct and indirect projections to CeM, animals were injected with AAV_5-CaMKIIα-ChR2-EYFP at 4 weeks of age, and were sacrificed for acute slice preparation 4-6 weeks to allow for viral expression. Slice preparation was the same as above. Light was delivered through a 40X/.8 NA LUMPlanFL/IR Objective (Olympus, Center Valley Pa.). Prior to whole cell patch clamping in the CeM nucleus, the location of the CeL nucleus was noted in order to revisit it with the light spot restricted to this region. Whole-cell patch-clamp recordings were performed in CeM neurons. Series resistance of the pipettes was usually 10-20

MOhms. Blue light pulses were elicited using a XCite halogen light source (EXPO, Mississauga, Ontario) with a 470/30 filter at 6.5 mW/mm^2 coupled to a shutter (Uniblitz, Rochester N.Y.). During CeM recordings, broad illumination (~425-450 μm in diameter) of BLA terminals in the CeA and 20 Hz, 5 ms light train for 2 s was applied. Voltage-clamp recordings were made at 70 mV and 0 mV to isolate EPSCs and IPSCs respectively. Current-clamp recordings were also made. Then, illumination was moved to the CeL using a restricted light spot ~125 μm in diameter. We again performed voltage clamp recordings at −70 mV and 0 mV and used 20 Hz, 5 ms light train for 2 s. For the CeM neuron spiking inhibition experiments, in current-clamp, we applied the minimal current step required to induce spiking (~60 pA) and simultaneously applied preferential illumination of ChR2-expressing BLA terminals in the CeL with a 20 Hz, 5 ms light train for 2s (mean over 6 sweeps per cell). For the experiments comparing the broad illumination of the BLA terminal field centered in the CeM to selective illumination of BLA-CeL terminals, these conditions were performed in repeated alternation in the same CeM cells (n=7).

[0082] To verify that terminal inhibition did not alter somatic spiking, animals were injected with AAV5-CaMKIIα-eNpHR3.0-EYFP at 4 weeks of age, and were sacrificed for acute slice preparation 4-6 weeks to allow for viral expression. Slice preparation was the same as above. Whole-cell patch-clamp recordings were performed in BLA neurons and were allowed to fill for approximately 30 minutes. Light was delivered through a 40X/.8 NA LUMPlanFL/IR Objective (Olympus, Center Valley Pa.). Whole-cell patch-clamp recordings were performed on BLA neurons. Series resistance of the pipettes was usually 10-20 MOhms. Yellow light pulses were elicited using a XCite halogen light source (EXPO, Mississauga, Ontario) with a 589/24 filter at 6.5 mW/mm^2 coupled to a shutter (Uniblitz, Rochester N.Y.). After patching, an unrestricted light spot (~425-450 microns in diameter) was placed over the BLA soma and a is pulse was applied. Cells were excluded if the current recorded was under 600 pA of hyperpolarizing current and the axon did not travel over ~300 μm towards the CeL nucleus. The light spot was then restricted to ~125 pm in diameter. On and off axon voltage clamp recordings were taken with a is pulse of light. For the current clamp recordings, action potentials were generated by applying 250 pA of current to the cell soma through the patch pipette.

[0083] To demonstrate that selective illumination of eNpHR3.0-expressing BLA terminals reduced the probability of spontaneous vesicle release, animals were injected with AAV5-CaMKIIα-eNpHR3.0-EYFP at 4 weeks of age, and were sacrificed for acute slice preparation 4-6 weeks to allow for viral expression. Slice preparation was the same as above. Whole-cell patch-clamp recordings were performed in central lateral neurons. Light was delivered through a 40X/.8 NA LUMPlanFL/IR Objective (Olympus, Center Valley Pa.). Series resistance of the pipettes was usually 10-20 MOhms. Yellow light pulses were elicited using a XCite halogen light source (EXPO, Mississauga, Ontario) with a 589/24 filter at 6.5 mW/mm^2 coupled to a shutter (Uniblitz, Rochester N.Y.). The light spot was restricted to ~125 μm in diameter. Carbachol was added to the bath at a concentration of 20 ~M. After sEPSC activity increased in the CeL neuron, light pulses were applied ranging in times from 5s to 30 s.

[0084] To demonstrate that selective illumination of eNpHR3.0-expressing BLA terminals could reduce the probability of vesicle release evoked by electrical stimulation, animals were injected with AAVS-CaMKIIα-eNpHR3.0-EYFP at 4 weeks of age, and were sacrificed for acute slice preparation 4-6 weeks to allow for viral expression. Slice preparation was the same as above. A bipolar concentric stimulation probe (FHC, Bowdoin Me.) was placed in the BLA. Whole-cell patch-clamp recordings were performed in CeL neurons. Light was delivered through a 40X/.8 NA LUMPlanFL/IR Objective (Olympus, Center Valley Pa.). Series resistance of the pipettes was usually 10-20 MOhms. Amber light pulses over the central lateral cell were elicited using a XCite halogen light source (EXPO, Mississauga, Ontario) with a 589/24 filter at 6.5 mW/mm^2 coupled to a shutter (Uniblitz, Rochester N.Y.). The light spot was restricted to ~125 μm in diameter. Electrical pulses were delivered for 40 seconds and light was delivered starting at 10 seconds and shut off at 30 seconds in the middle.

[0085] For the anatomical tracing experiments, neurons were excluded when the traced axons were observed to be severed and all BLA neurons included in the anatomical assay (FIGS. **5**A-**5**I) showed spiking patterns typical of BLA pyramidal neurons[18] upon a current step.

[0086] Slice immunohistochemistry: Anesthetized mice were transcardially perfused with ice-cold 4% paraformaldehyde (PFA) in PBS (pH 7.4) 100-110 min after termination of in vivo light stimulation. Brains were fixed overnight in 4% PFA and then equilibrated in 30% sucrose in PBS. 40 μm-thick coronal sections were cut on a freezing microtome and stored in cryoprotectant at 4° C. until processed for immunohistochemistry. Free-floating sections were washed in PBS and then incubated for 30 min in 0.3% Tx100 and 3% normal donkey serum (NDS). Primary antibody incubations were performed overnight at 4° C. in 3% NDS/PBS (rabbit anti-c-fos 1:500, Calbiochem, La Jolla, Calif.; mouse anti-CaMKII 1:500, Abcam, Cambridge, Mass.). Sections were then washed and incubated with secondary antibodies (1:1000) conjugated to Cy3 or Cy5 (Jackson Laboratories, West Grove, Pa.) for 3 hrs at room temperature. Following a 20 min incubation with DAPI (1:50,000) sections were washed and mounted on microscope slides with PVD-DABCO.

[0087] Confocal microscopy and analysis: Confocal fluorescence images were acquired on a Leica TCS SP5 scanning laser microscope using a 20X/0.70NA or a 40X/1.25NA oil immersion objective. Serial stack images covering a depth of 10 μm through multiple sections were acquired using equivalent settings. The Volocity image analysis software (Improvision/PerkinElmer, Waltham, Mass.) calculated the number of c-fos positive cells per field by thresholding c-fos immunoreactivity above background levels and using the DAPI staining to delineate nuclei. All imaging and analysis was performed blind to the experimental conditions.

[0088] Statistics: For behavioral experiments and the ex vivo electrophysiology data, binary comparisons were tested using nonparametric bootstrapped t-tests (paired or unpaired where appropriate)[5], while hypotheses involving more than two group means were tested using linear contrasts (using the "boot" and "lme4" packages in R[6], respectively); the latter were formulated as contrasts between coefficients of a linear mixed-effects model (a "two-way repeated-measures ANOVA") with the fixed effects being the genetic or phar-

macological manipulation and the light treatment (on or off). All hypothesis tests were specified a priori. Subjects were modeled as a random effects. For c-fos quantification comparisons, we used a one-way ANOVA followed by Tukey's multiple comparisons test.

[0089] Plots of the data clearly show a relationship between observation mean and observation variance (that is, they are heteroskedastic; see for example, FIG. **3**E and FIG. **5**J). We found that a standard square-root transformation corrected this well. Additionally, eNpHR3.0 elevated plus maze (EPM) data required detrending by a linear fit over time to account for a decrease in exploration behavior over time. As is standard for a two-way linear mixed effects model (also known as a two-way repeated-measures ANOVA), we model (the square-root corrected value of) the kth observation in the ijth cell (y_{ijk}) as

$$\sqrt{y_{ijk}}=\mu+c_j+t_j+(c:t)_{ij}+b_j+c_{ijk} \quad (1)$$

[0090] where

[0091] μ is the grand mean across all cells (where the ijth "cell" in the collection of observations corresponding to the ith condition and jth treatment)

[0092] c_i is a fixed effect due to the ith animal condition across treatments (for example, a genetic manipulation)

[0093] t_j is a fixed effect due to the jth treatment across conditions (for example, light on or light off)

[0094] $(c:t)_{ij}$ is a fixed effect due to the interaction of the ith condition and jth treatment in the ijth cell

[0095] b_j is a random effect corresponding to animals being used across treatments, and

[0096] e_{ijk} is an independent and identically distributed (i.i.d.) random normal disturbance in the ijkth observation with mean 0 and variance σ^2, and independent of b_j for all j

[0097] Collecting the fixed effects into a 2-way analysis of variance (ANOVA) design matrix $X \in R^{nxp}$, dummy coding the random effects in a sparse matrix $Z \in R^{nxq}$, and letting $\mu=\sqrt{u}$ we can express the model in matrix form as where $ij \in \mathbb{R}$, $b \in \mathbb{R}^q$, and $\varepsilon \in \mathbb{R}$ are observations of random $\bar{y}$, $\mathcal{B}$ and ε respectively and our model assumes

$$\mathcal{B} \sim \mathcal{N}(0, \sigma^2\Sigma)$$

$$\mathcal{N} \sim \mathcal{N}(0, \sigma^2 I), \in \perp \mathcal{B}$$

$$(y)|\mathcal{B}=b) \sim \mathcal{N}(X\beta+Zb, \sigma^2 I) \quad \mathcal{N}$$

where $N(\mu, \Sigma)$ denotes the multivariate Gaussian distribution with mean vector μ and variance-covariance matrix Σ, and $\perp$ indicates that two variables are independent. To estimate the coefficient vectors $\beta \in R^p$, $b \in R^q$, and the variance parameter σ and sparse (block-diagonal) relative variance-covariance matrix $\Sigma \in R^{qxq}$, we use the lme4 package in R written by Douglas Bates and Martin Maechler, which first finds a linear change of coordinates that "spheres" the random effects and then finds the maximum likelihood estimates for β, σ, and Σ using penalized iteratively reweighted least-squares, exploiting the sparsity of the random effects matrix to speed computation. For more details see the documentation accompanying the package in the lme4 repository at http://www.r-project.org/.

[0098] To solve for the maximum likelihood estimates, the design matrix X in equation 2 must be of full column rank. It is well known that this is not the case for a full factorial design matrix with an intercept (as in equation 1), and thus linear combinations ("contrasts") must be used to define the columns of X in order for the fixed-effect coefficients to be estimable. As our designs are balanced (or nearly balanced), we used orthogonal (or nearly orthogonal) Helmert contrasts between the coefficients associated with light on as compared to light off conditions, terminal stimulation as compared to control conditions, and so on, as reported in the main text. Such contrasts allowed us to compare pooled data (e.g., from several sequential light on vs. light off conditions) against each other within a repeated-measures design—yielding improved parameter estimation and test power while accounting for within-animal correlations.

[0099] Results

[0100] BLA cells have promiscuous projections throughout the brain, including to the bed nucleus of the stria terminalis (BNST), nucleus accumbens, hippocampus and cortex[38, 43]. To test whether BLA-CeL synapses could be causally involved in anxiety, it was therefore necessary to develop a method to selectively control BLA terminals in the CeL, without directly affecting other BLA projections. To preferentially target BLA-CeL synapses, we restricted opsin gene expression to BLA glutamatergic projection neurons and restricted light delivery to the CeA. Control of BLA glutamatergic projection neurons was achieved with an adeno-associated virus (AAV5) vector carrying light-activated optogenetic control genes under the control of a CaMKIIα promoter; within the BLA, CaMKIIα is only expressed in glutamatergic pyramidal neurons, not in local interneurons or intercalated cells[48]. To preferentially deliver light to the CeA projection, virus was delivered unilaterally into the BLA under stereotaxic guidance (FIGS. **7** and **8**A-**8**E) along with implantation of a beveled guide cannula over the CeL to prevent light delivery to the BLA and allow selective illumination of the CeA. Geometric and functional properties of the resulting light distribution were quantified both in vitro and in vivo, with in vivo electrophysiological recordings to determine light power parameters for selective control of BLA terminals but not BLA cell bodies (FIGS. **9**A-**9**D).

[0101] To test the hypothesis that the BLA-CeA pathway could implement an endogenous mechanism for anxiolysis, we probed freely-moving mice under projection-specific optogenetic control in two distinct and well-validated anxiety assays: the elevated plus maze and the open field test (FIGS. **3**A-**3**F). Mice display anxiety-related behaviors when exposed to open or exposed spaces, therefore increased time spent in the exposed arms of the elevated plus maze or in the center of the open field chamber indicates reduced anxiety[49, 50]. To test for both induction and reversal of relevant behaviors, we first exposed mice to the elevated plus maze for three 5-min epochs, in which light was delivered during the second epoch only.

[0102] To determine whether the anxiolytic effect we observed would be specific to activation of BLA terminals in the CeA, and not BLA cells in general, we compared mice receiving projection-specific control (in the ChR2:BLA-CeA group; FIG. **3**A to both a negative control group receiving transduction with a control virus given the same pattern of illumination (EYFP:BLA-CeA) and a positive control group transduced with the AAV-CaMKIIα-ChR2-EYFP virus in the BLA with a fiber implanted directly over the BLA (ChR2:BLA Somata). For this group (ChR2:BLA Somata), light stimulation did not elicit the anxiolysis observed in the ChR2:BLA-CeA group (FIG. **3**B-**3**C; indeed, the ChR2:BLA-CeA group spent significantly more

time in open arms (t(42)=8.312; p<0.00001; FIG. **3***b,c*) during light-induced activation of BLA terminals in the CeA , in comparison to controls (EYFP:BLA-CeA and ChR2:BLA Somata groups). The ChR2:BLA-CeA mice also showed an increase in the probability of entering an open arm rather than a closed arm, from the choice point of the center of the maze (FIG. **3**C inset), indicating an increased probability of selecting the normally anxiogenic environment.

[0103] We also probed mice on the open field arena for six 3-minute epochs, again testing for reversibility by alternating between no light (off) and light stimulation (on) conditions. Experimental (ChR2:BLA-CeA) mice displayed an immediate, robust, and reversible light-induced anxiolytic response as measured by the time in center of the open field chamber (FIG. **3**D-**3**E), while mice in the EYFP:BLA-CeA and ChR2:BLA Somata groups did not (FIG. **3**E). Light stimulation did not significantly alter locomotor activity (FIG. **3**F). While there was no detectable difference among groups in the off conditions, there was a significant increase in center time of the open field spent by mice in the ChR2:BLA-CeA group relative to the EYFP:BLA-CeA or ChR2:BLA Somata groups during the on conditions (t(105) =4.96178; p<0.0001 for each contrast). We concluded that selective stimulation of BLA projections to the CeA, but not BLA somata, produces an acute, rapidly reversible anxiolytic effect, supporting the hypothesis that the BLA-CeL-CeM pathway could represent a native microcircuit for anxiety control.

[0104] We next investigated the physiological basis of this light-induced anxiolytic effect. Glutamatergic neurons in the BLA send robust excitatory projections to CeL neurons as well as to CeM neurons[38]; however, not only are the CeM synapses distant from the light source (FIG. **8**A-**8**E), but also any residual direct excitation of these CeM neurons would be expected to result in an anxiogenic, rather than an anxiolytic, effect[12]. However, CeL neurons exert strong inhibition onto these brainstem-projecting CeM output neurons[32, 35, 40], and we therefore hypothesized that illumination of BLA terminals in the CeA could activate BLA-CeL neurons and thereby elicit feed-forward inhibition onto CeM neurons and implement the observed anxiolytic phenomenon.

[0105] To confirm the operation of this optogenetically-defined projection, we undertook in vivo experiments, with light delivery protocols matched to those delivered in the behavioral experiments, and activity-dependent immediate early gene (c-fos) expression analysis as the readout to verify the pattern of neuronal activation (FIG. **3**G-**3**K). Under blinded conditions, we quantified the proportion of neurons in the BLA, CeL and CeM (FIG. **3**I-**3**K) for ChR2:BLA-CeA, EYFP:BLA-CeA and ChR2:BLA Somata groups that expressed EYFP or showed c-fos immunoreactivity. Virus expression under the CaMKIIα promoter in the BLA targeted glutamatergic neurons[47], and we did not observe EYFP expression in local interneurons nor intercalated cells (FIG. **10**A-**10**F). No significant differences among groups were detected in the proportion of EYFP-positive cells within each region (FIG. **3**G-**3**K), but we found a significantly higher proportion of c-fos positive BLA cells in the ChR2:BLA Somata group, relative to ChR2:BLA-CeA or EYFP:BLA-CeA groups (FIG.**3**I;p<0.01 and p<0.05, respectively). There was no detectable difference in c-fos between the ChR2:BLA-CeA and EYFP:BLA-CeA groups, indicating that the beveled cannula shielding effectively prevented direct illumination to BLA cell bodies. A significantly higher proportion of CeL neurons expressed c-fos in the ChR2:BLA-CeA group relative to the EYFP:BLA-CeA group (p<0.05), but not the ChR2:BLA Somata group (FIG. **3**J). Thus, selective illumination of BLA terminals expressing ChR2 in the CeA led to preferential activation of CeL neurons, without activating BLA somata. In the CeM, we found twice as many c-fos positive neurons (relative to total neurons) in the ChR2:BLA Somata group than in the ChR2:BLA-CeA (FIG. **3**K), consistent with anatomical projections, as LA neurons selectively innervate CeL neurons, while neurons in the BL and BM nuclei of the amygdala have monosynaptic projections to both the CeL and the CeM[38, 43, 51]. Together, these data reveal that the in vivo illumination that triggers an acute anxiolytic behavioral phenotype implements selective illumination of BLA-CeL synapses without activating BLA cell bodies.

[0106] To test the hypothesis that selective illumination of BLA terminals in the CeL induces feed-forward inhibition of CeM output neurons, we combined whole-cell patch-clamp recording with live two-photon imaging to visualize the microcircuit while simultaneously probing the functional relationships among these cells during projection-specific optogenetic control (FIG. **4**A-**4**F). While the light-stimulation parameters used in vivo were delivered via a fiber optic and the parameters used in our ex vivo experiments were delivered onto acute slices, we matched the light power density at our target location ~6 mW/mm^2. A two-photon image of the BLA-CeL-CeM circuit is shown in FIG. **4**A, with all three cells imaged from the same slice (FIG.**4**A). The BLA neuron expressing ChR2-EYFP showed robust, high-fidelity spiking to direct illumination with 20 Hz, 5 ms pulses of 473 nm light (FIG. **4**B). A representative trace from a CeL neuron, recorded during illumination of the terminal field of BLA neurons expressing ChR2-EYFP, demonstrates the typical excitatory responses seen in CeL (FIG. **4**C), with population summaries revealing that spiking fidelity was steady throughout the 40-pulse light train and that responding cells include both weakly and strongly-excited CeL cells (n=16; FIG. **4**C). To test whether illumination of BLA-CeL synapses would be functionally significant at the level of blocking spiking in CeM cells due to the robust feed-forward inhibition from CeL neurons, we recorded from CeM neurons while selectively illuminating BLA-CeL synapses (FIG. **4**D). Indeed, we observed potent spiking inhibition ($F_{2,11}$=15.35, p=0.0044) in the CeM due to light stimulation of BLA terminals in the CeL (FIG.**4***d*; spikes per second before (49±9.0), during (1.5±0.87), and after (33±8.4) illumination; mean±s.e.m). Next, FIG. **4**E shows CeM responses recorded during illumination of the terminal field of BLA neurons in the CeM expressing ChR2-EYFP, and the combined excitatory and inhibitory input. Population summaries from voltage-clamp recordings indicated that latencies of EPSCs were shorter than those of the disynaptic IPSCs, as expected, and that the mean IPSC amplitude was greater than mean EPSC amplitude (recorded at 0 and −70 mV, respectively; FIG. **4**E). Importantly, the very same CeM neurons (n=7) yielded net excitation with broad illumination of BLA inputs to the CeM (FIG. **4**E), but displayed net inhibition with selective illumination of BLA inputs to the CeL (FIG. **4**F) in a repeatable fashion with alternation between sites. This demonstrates that the balance of direct

and indirect inputs from the BLA to the CeM can modulate CeM output. Together, these data reveal a structurally- and functionally-identified physiological microcircuit, whereby selective illumination of BLA terminals in the CeA activates BLA-CeL synapses, thus increasing feed-forward inhibition from CeL neurons onto the brainstem-projecting CeM neurons.

[0107] To further elucidate the amygdalar microcircuits underlying this anxiolytic effect, we carefully dissected the anatomical and functional properties governing this phenomenon. While some efforts to map the projections of BLA collaterals in the CeA have been made in the rat, we empirically tested whether overlapping or distinct populations of BLA neurons projected to the CeL and CeM (FIG. **5**A-**5**B). A noteworthy caveat is that we visualized these neurons in ~350 um thick coronal sections and while every attempt was made to exclude neurons in which the axons were severed, we cannot exclude the possibility that this occurred nor can we deny that this induced some sampling bias for BLA neurons closer to the CeA. FIG. **5**A summarizes the anatomical projections of the BLA neurons sampled (n=18) and shows that the 44% of neurons projected to the CeL alone and 17% projected to the CeM alone. However, a minority of BLA cells (n=1;6%), projected to both the CeL and the CeM, one of which sent separate collaterals to the CeL and CeM and one of which sent a collateral that sent branches to the CeL and CeM. FIG. **5**B shows the 2-photon image of each cell sampled, all of which showed spiking patterns typical of BLA pyramidal neurons upon a current step.

[0108] Next, as our c-fos assays suggested that illumination of BLA terminals in the CeL were sufficient to excite CeL neurons, but not BLA neurons themselves, we sought to confirm this hypothesis with whole-cell recordings. With electrical stimulation, depolarization of axon terminals leads to antidromic spiking at the cell soma. However, there has been evidence that optogenetically-induced depolarization functions via a distinct mechanism. To evaluate the properties of optogenetically-induced terminal stimulation in this amygdalar microcircuit, we recorded from BLA pyramidal neurons expressing ChR2 and moved a light spot (~120 μm in diameter) in 100 μm steps from the cell soma, both in a direction over a visually-identified axon collateral and in a direction where there was no axon (FIG. **5**C). The spike fidelity of the BLA neuron given a 20 Hz train of light at each distance from the soma is summarized in FIG. **5**D, while the depolarizing current is summarized in FIG.**5***e*. In all preparations, we confirmed that the light stimulation parameters used were sufficient to elicit high-fidelity spiking at the BLA cell soma (FIG.Sf) and reliable vesicle release at BLA terminals as shown by recordings from a postsynaptic CeL neuron (FIG. **5**G; FIG. **15**). In contrast, when recording from the same BLA neurons with the light spot 300 um away from the cell soma we did not observe reliable action potential induction, regardless of whether we were over an axon (FIG. **5**H) or not (FIG. **5**I). This absence of antidromic spiking was observed even upon bath application of GABA and AMPA receptor antagonists (n=7), thus excluding the possible contribution of local inhibitory constraints. While we demonstrate that optogenetically-induced vesicle release can occur in the absence of antidromic stimulation in BLA pyramidal neurons, it is possible that at antidromic stimulation could be achieved with greater light power density than we used here (~6 mW/mm^2). Thusfar, we have demonstrated that the populations of BLA neurons projecting to the CeL and the CeM are largely distinct and that illumination of BLA-CeL synapses induces vesicle release and CeL excitation without strong activation of BLA somata themselves.

[0109] Finally, we further explored the mechanism with in vivo pharmacological analysis in the setting of projection-specific optogenetic control. To determine whether the anxiolytic effect we observed could be due to the selective activation of BLA-CeL synapses alone, and not BLA fibers passing through the CeA, nor back-propagation of action potentials to BLA cell bodies which then would innervate all BLA projection target regions, we tested whether local glutamate receptor antagonism would attenuate light-induced anxiolytic effects. This question is of substantial interest since lesions in the CeA that alter anxiety are confounded by the likelihood of ablation of BLA projections to the BNST which pass through CeA[6]. We unilaterally transduced BLA neurons with AAV-CaMKIIα-ChR2-EYFP and implanted beveled cannulae to implement selective illumination of BLA terminals in the CeA as before (n=8; FIGS. **8**A-**8**E), and tested mice on the elevated plus maze and open field test. In this case, however, we infused either the glutamate antagonists NBQX and AP5 using the optical fiber guide cannula, or saline control on different trials in the same animals, with trials counter-balanced for order. Confirming a local synaptic mechanism rather than control of fibers of passage, for the same mice and light stimulation parameters, local glutamate receptor antagonism in the CeA abolished light-induced reductions in anxiety on both the elevated plus maze (FIG. **5**K) and the open field test (FIG. **5**J). Importantly, in control experiments, drug treatment did not impair locomotor activity (FIG. **11**), and in acute slices time-locked light-evoked excitatory responses were abolished upon bath application of NBQX and AP5 (FIG. **12**A-**12**C). Together these data indicate that the light-induced anxiolytic effects we observed were caused by the activation of BLA-CeL synapses, and not attributable to BLA projections to distal targets passing through the CeA.

[0110] In a final series of experiments, to determine if endogenous anxiety-reducing processes could be blocked by selectively inhibiting this pathway, we tested whether the selective inhibition of these optogenetically defined synapses could reversibly increase anxiety. We performed bilateral viral transductions of either eNpHR3.0, a light-activated chloride pump which hyperpolarizes neuronal membranes upon illumination with amber light[25], or EYFP alone, both under the CaMKIIa promoter in the BLA, and implanted bilateral beveled guide cannulae to allow selective illumination of BLA terminals in the CeA (FIG.**6***a*; FIG. **13**). eNpHR3.0 expression was restricted to glutamatergic CaMKIIα-positive neurons in the BLA (FIG. **6**B). The eNpHR3.0:BLA-CeA group only showed significantly elevated levels of c-fos expression, relative to the EYFP: BLA-CeA bil and eNpHR 3.0:Soma groups, in the CeM ($p<0.05$; FIGS.**6***c-e*), consistent with the hypothesis that selective inhibition of BLA terminals in the CeA suppresses feed-forward inhibition from CeL neurons to CeM neurons, thus increasing CeM excitability and the downstream processes leading to increased anxiety phenotypes. Importantly, inhibition of BLA somata did not induce an anxiogenic response, likely due to the simultaneous decrease in direct BLA-CeM excitatory input. We also found that the eNpHR3.0:BLA-CeA group showed a significant reduction in open

arm time and probability of open arm entry on the elevated plus maze during light-on epochs, but not light-off epochs, relative to the EYFP and Soma groups (FIGS. **6**F-**6**G), without altering locomotor activity (FIG. **16**). The eNpHR3.0:BLA-CeA group also showed a significant reduction in center time upon illumination with 594 nm light, relative to the EYFP and Soma groups (statistics, p=0.002; FIGS. **6**H-**6**I). Finally, we also demonstrate that selective illumination of eNpHR3.0-expressing axon terminals can reduce the probability of both spontaneously occurring (FIGS. **6**J-**6**L) and evoked (FIGS. **6**M-**6**P) vesicle release, without preventing spiking at the cell soma (FIGS. **14**A-**14**E). These data demonstrate that selective inhibition of BLA terminals in the CeA induces an acute increase in anxiety-like behaviors.

[0111] Conclusions: In these experiments, we have identified the BLA-CeL pathway as an endogenous neural substrate for bidirectionally modulating the unconditioned expression of anxiety. While we identify the BLA-CeL pathway as the critical substrate rather than BLA fibers passing through the CeL, it is likely that other downstream circuits, such as CeA projections to the BNST play an important role in the expression of anxiety or anxiety-related behaviors[4, 6, 13]. Indeed, our findings may support the notion that corticotrophin releasing hormone (CRH) networks in the BNST can be critically involved in modulating anxiety-related behaviors[6, 52], as the CeL is a primary source of CRH for the BNST[53].

[0112] Other neurotransmitters and neuromodulators may modulate or gate effects on distributed neural circuits, including serotonin[54, 55], dopamine[56], acetylcholine[57], glycine[58], GABA[13] and CRH[59]. The neural circuitry converging to and diverging from this pathway will provide many opportunities for modulatory control, as parallel or downstream circuits of the BLA-CeL synapse likely contribute to modulate the expression of anxiety phenotypes[6, 56]. Moreover, upstream of the amygdala, this microcircuit is well-positioned to be recruited by top-down cortical control from regions important for processing fear and anxiety, including the prelimbic, infralimbic and insular cortices that provide robust innervation to the BLA and CeL.[4, 13, 23, 60].

[0113] Our examination of the BLA anatomy suggests that the populations of BLA neurons projecting to CeL and CeM neurons are largely non-overlapping. In natural states, the CeL-projecting BLA neurons may excite CeM-projecting BLA neurons in a microcircuit homeostatic mechanism. This may also represent a potential mechanism underlying anxiety disorders, when there are synaptic changes that skew the balance of the circuit to allow uninhibited CeM activation.

[0114] Together, the data presented here support identification of the BLA-CeL synapse as a critical circuit element both necessary and sufficient for the expression of endogenous anxiolysis in the mammalian brain, providing a novel source of insight into anxiety as well as a new kind of treatment target, and demonstrate the importance of resolving specific projections in the study of neural circuit function relevant to psychiatric disease.

[0115] Although the foregoing invention has been described in some detail by way of illustration and example for purposes of clarity of understanding, the descriptions and examples should not be construed as limiting the scope of the invention.

[0116] All references, publications, and patent applications disclosed herein are hereby incorporated by reference in their entirety.

REFERENCES

[0117] 1. Lieb, R. Anxiety disorders: clinical presentation and epidemiology. *Handb Exp Pharmacol,* 405-432 (2005).

[0118] 2. Kessler, R. C., et al. Lifetime prevalence and age-of-onset distributions of DSM-IV disorders in the National Comorbidity Survey Replication. Arch Gen Psychiatry 62, 593-602 (2005).

[0119] 3. Koob, G. F. Brain stress systems in the amygdala and addiction. Brain Res 1293, 61-75 (2009).

[0120] 4. Ressler, K. J. & Mayberg, H. S. Targeting abnormal neural circuits in mood and anxiety disorders: from the laboratory to the clinic. *Nat Neurosci* 10, 1116-1124 (2007).

[0121] 5. Vanderschuren, L. J. & Everitt, B. J. Behavioral and neural mechanisms of compulsive drug seeking. Eur J Pharmacol 526, 77-88 (2005).

[0122] 6. Davis, M., Walker, D. L., Miles, L. & Grillon, C. Phasic vs sustained fear in rats and humans: role of the extended amygdala in fear vs anxiety. Neuropsychopharmacology 35, 105-135.

[0123] 7. Ehrlich, I., et al. Amygdala inhibitory circuits and the control of fear memory. Neuron 62, 757-771 (2009).

[0124] 8. Han, J. H., et al. Selective erasure of a fear memory. *Science* 323, 1492-1496 (2009).

[0125] 9. Herry, C., et al. Switching on and off fear by distinct neuronal circuits. *Nature* 454, 600-606 (2008).

[0126] 10. LeDoux, J. The emotional brain, fear, and the amygdala. Cell Mol Neurobiol 23, 727-738 (2003).

[0127] 11. Maren, S. & Quirk, G. J. Neuronal signaling of fear memory. Nat Rev Neurosci 5, 844-852 (2004).

[0128] 12. Pare, D., Quirk, G. J. & Ledoux, J. E. New vistas on amygdala networks in conditioned fear. J Neurophysiol 92, 1-9 (2004).

[0129] 13. Shin, L. M. & Liberzon, I. The neurocircuitry of fear, stress, and anxiety disorders. Neuropsychopharmacology 35, 169-191.

[0130] 14. Davis, M. The role of the amygdala in conditioned and unconditioned fear and anxiety. in The Amygdala (ed. A. JP) p. 213-288 (Oxford University Press, Oxford, UK, 2000).

[0131] 15. Killcross, S., Robbins, T. W. & Everitt, B. J. Different types of fear-conditioned behaviour mediated by separate nuclei within amygdala. Nature 388, 377-380 (1997).

[0132] 16. Tye, K. M. & Janak, P. H. Amygdala neurons differentially encode motivation and reinforcement. J Neurosci 27, 3937-3945 (2007).

[0133] 17. Tye, K. M., Stuber, G. D., de Ridder, B., Bonci, A. & Janak, P. H. Rapid strengthening of thalamo-amygdala synapses mediates cue-reward learning. Nature 453, 1253-1257 (2008).

[0134] 18. Bahi, A., Mineur, Y. S. & Picciotto, M. R. Blockade of protein phosphatase 2B activity in the amygdala increases anxiety- and depression-like behaviors in mice. Biol Psychiatry 66, 1139-1146 (2009).

[0135] 19. Davis, M. Are different parts of the extended amygdala involved in fear versus anxiety? *Biol Psychiatry* 44, 1239-1247 (1998).

[0136] 20. Etkin, A., et al. Individual differences in trait anxiety predict the response of the basolateral amygdala to unconsciously processed fearful faces. Neuron 44, 1043-1055 (2004).

[0137] 21. Kahn, N. H., Shelton, S. E. & Davidson, R. J. The role of the central nucleus of the amygdala in mediating fear and anxiety in the primate. J Neurosci 24, 5506-5515 (2004).

[0138] 22. Roozendaal, B., McEwen, B. S. & Chattarji, S. Stress, memory and the amygdala. *Nat Rev* Neurosci (2009).

[0139] 23. Stein, M. B., Simmons, A. N., Feinstein, J. S. & Paulus, M. P. Increased amygdala and insula activation during emotion processing in anxiety-prone subjects. Am J Psychiatry 164, 318-327 (2007).

[0140] 24. Boyden, E. S., Zhang, F., Bamberg, E, Nagel, G. & Deisseroth, K. Millisecond-timescale, genetically targeted optical control of neural activity. Nat Neurosci 8, 1263-1268 (2005).

[0141] 25. Gradinaru, V., at aL Molecular and cellular approaches for diversifying and extending optogenetics. Ce//141, 154-165.

[0142] 26. Nagel, G., at al. Channelrhodopsin-2, a directly light-gated cation-selective membrane channel. Proc Nat/ Acad Sci U S A 100, 13940-13945 (2003).

[0143] 27. Fraser, A. D. Use and abuse of the benzodiazepines. Ther Drug Monit 20, 481-489 (1998).

[0144] 28. Woods, J. H., Katz, J. L. & Winger, G. Benzodiazepines: use, abuse, and consequences. Pharmacol Rev 44, 151-347 (1992).

[0145] 29. Hovatta, I. & Barlow, C. Molecular genetics of anxiety in mice and men. Anti Med 40, 92-109 (2008).

[0146] 30. Hovatta, I., et al. Glyoxalase 1 and glutathione reductase 1 regulate anxiety in mice. *Nature* 438, 662-666 (2005).

[0147] 31. Blanchard, R. J., Yudko, E. B., Rodgers, R. J. & Blanchard, D. C. Defense system psychopharmacology: an ethological approach to the pharmacology of fear and anxiety. Behav Brain Res 58, 155-165 (1993).

[0148] 32. LeDoux, J. E., Iwata, J., Cicchetti, P. & Reis, D. J. Different projections of the central amygdaloid nucleus mediate autonomic and behavioral correlates of conditioned fear. J Neurosci 8, 2517-2529 (1988).

[0149] 33. Carlson, J. lrnmunocytochemical localization of glutamate decarboxylase in the rat basolateral amygdaloid nucleus, with special reference to GABAergic innervation of amygdalostriatal projection neurons. J Comp Neurol 273, 513-526 (1988).

[0150] 34. Smith, Y. & Pare, D. Intra-amygdaloid projections of the lateral nucleus in the cat: PHA-L anterograde labeling combined with postembedding GABA and glutamate immunocytochemistry. *J Comp Neurol* 342, 232-248 (1994).

[0151] 35. McDonald, A. J. Cytoarchitecture of the central amygdaloid nucleus of the rat. *J Comp Neurol* 208, 401-418 (1982).

[0152] 36. Bissiere, S., Humeau, Y. & Luthi, A. Dopamine gates LTP induction in lateral amygdala by suppressing feedforward inhibition. Nat Neurosci 6, 587-592 (2003).

[0153] 37. Marowsky, A., Yanagawa, Y., Obata, K. & Vogt, K. E. A specialized subclass of interneurons mediates dopaminergic facilitation of amygdala function. Neuron 48, 1025-1037 (2005).

[0154] 38. Pitkanen, A. Connectivity of the rat amygdaloid complex. in *The Amygdala* (ed. A. J P) p. 31-99 (Oxford University Press, Oxford, UK, 2000).

[0155] 39. Krettek, J. E. & Price, J. L. Amygdaloid projections to subcortical structures within the basal forebrain and brainstem in the rat and cat. J Comp Neurol 178, 225-254 (1978).

[0156] 40. Petrovich, G. D. & Swanson, L. W. Projections from the lateral part of the central amygdalar nucleus to the postulated fear conditioning circuit. Brain Res 763, 247-254 (1997).

[0157] 41. LeDoux, J. E., Cicchetti, P., Xagoraris, A. & Romanski, L. M. The lateral amygdaloid nucleus: sensory interface of the amygdala in fear conditioning. J Neurosci 10, 1062-1069 (1990).

[0158] 42. Krettek, J. E. & Price, J. L. A description of the amygdaloid complex in the rat and cat with observations on intra-amygdaloid axonal connections. J Comp Neurol 178, 255-280 (1978).

[0159] 43. Petrovich, G. D., Risold, P. Y. & Swanson, L. W. Organization of projections from the basomedial nucleus of the amygdala: a PHAL study in the rat. J Comp Neural 374, 387-420 (1996).

[0160] 44. Pare, D. & Smith, Y. The intercalated cell masses project to the central and medial nuclei of the amygdala in cats. Neuroscience 57, 1077-1090 (1993).

[0161] 45. Likhtik, E., Popa, D., Apergis-Schoute, J., Fidacaro, G.A. & Pare, D. Amygdala intercalated neurons are required for expression of fear extinction. Nature 454, 642-645 (2008).

[0162] 46. Jolkkonen, E. & Pitkanen, A. Intrinsic connections of the rat amygdaloid complex:

[0163] projections originating in the central nucleus. J Comp Neurol 395, 53-72 (1998).

[0164] 47. Amano, T., Unal, C. T. & Pare, D. Synaptic correlates of fear extinction in the amygdala. *Nat Neurosci* 13, 489-494.

[0165] 48. McDonald, A. J., Muller, J. F. & Mascagni, F. GABAergic innervation of alpha type II calcium/calmodulin-dependent protein kinase immunoreactive pyramidal neurons in the rat basolateral amygdala. J Comp Neurol 446, 199-218 (2002).

[0166] 49. Choleris, E., Thomas, A. W., Kavaliers, M. & Prato, F. S. A detailed ethological analysis of the mouse open field test: effects of diazepam, chlordiazepoxide and an extremely low frequency pulsed magnetic field. Neurosci Biobehav Rev 25, 235-260 (2001).

[0167] 50. Pellow, S., Chopin, P., File, S. E. & Briley, M. Validation of open:closed arm entries in an elevated plus-maze as a measure of anxiety in the rat. J Neurosci Methods 14, 149-167 (1985).

[0168] 51. Sah, P. & Lopez De Armentia, M. Excitatory synaptic transmission in the lateral and central amygdala. Ann N YAcad Sci 985, 67-77 (2003).

[0169] 52. Davis, M. & Shi, C. The extended amygdala: are the central nucleus of the amygdala and the bed nucleus of the stria terminalis differentially involved in fear versus anxiety? Ann N YAcad Sci 877, 281291 (1999).

[0170] 53. Sakanaka, M., Shibasaki, T. & Lederis, K. Distribution and efferent projections of corticotropin-releasing factor-like immunoreactivity in the rat amygdaloid complex. Brain Res 382, 213-238 (1986).

[0171] 54. Holmes, A., Yang, R. J., Lesch, K. P., Crawley, J. N. & Murphy, D. L. Mice lacking the serotonin transporter exhibit 5-HT(1A) receptor-mediated abnormalities in tests for anxiety-like behavior. *Neuropsychopharmacology* 28, 2077-2088 (2003).

[0172] 55. Lesch, K. P., et al. Association of anxiety-related traits with a polymorphism in the serotonin transporter gene regulatory region. Science 274, 1527-1531 (1996).

[0173] 56. Graybiel, A. M. & Rauch, S. L. Toward a neurobiology of obsessive-compulsive disorder. *Neuron* 28, 343-347 (2000).

[0174] 57. Picciotto, M. R., Brunzell, D. H. & Caldarone, B. J. Effect of nicotine and nicotinic receptors on anxiety and depression. Neuroreport 13, 1097-1106 (2002).

[0175] 58. Snyder, S. H. & Enna, S. J. The role of central glycine receptors in the pharmacologic actions of benzodiazepines. *Adv Biochem Psychopharmacol,* 81-91 (1975).

[0176] 59. Lesscher, H. M., et al. Amygdala protein kinase C epsilon regulates corticotropin-releasing factor and anxiety-like behavior. Genes Brain Behav 7, 323-333 (2008).

[0177] 60. Milad, M. R., Rauch, S. L., Pitman, R. K. & Quirk, G. J. Fear extinction in rats: implications for human brain imaging and anxiety disorders. Biol Psycho! 73, 61-71 (2006).

SEQUENCES

(NpHR amino acid sequence without the signal peptide):

SEQ ID NO: 1

VTQRELFEFVLNDPLLASSLYINIALAGLSILLFVFMTRGLDDPRAKLIA

VSTILVPVVSIASYTGLASGLTISVLEMPAGHFAEGSSVMLGGEEVDGVV

TMWGRYLTWALSTPMILLALGLLAGSNATKLFTAITFDIAMCVTGLAAAL

TTSSHLMRWFWYAISCACFLVVLYILLVEWAQDAKAAGTADMFNTLKLLT

VVMWLGYPIVWALGVEGIAVLPVGVTSWGYSFLDIVAKYIFAFLLLNYLT

SNESVVSGSILDVPSASGTPADD

(eYFP-NpHR3.0 amino acid sequence):

SEQ ID NO: 2

MTETLPPVTESAVALQAEVTQRELFEFVLNDPLLASSLYINIALAGLSIL

LFVFMTRGLDDPRAKLIAVSTILVPVVSIASYTGLASGLTISVLEMPAGH

FAEGSSVMLGGEEVDGVVTMWGRYLTWALSTPMILLALGLLAGSNATKLF

TAITFDIAMCVTGLAAALTTSSHLMRWFWYAISCACFLVVLYILLVEWAQ

DAKAAGTADMFNTLKLLTVVMWLGYPIVWALGVEGIAVLPVGVTSWGYSF

LDIVAKYIFAFLLLNYLTSNESVVSGSILDVPSASGTPADDAAAKSRITS

EGEYIPLDQIDINVVSKGEELFTGVVPILVELDGDVNGHKFSVSGEGEGD

ATYGKLTLKFICTTGKLPVPWPTLVTTFGYGLQCFARYPDHMKQHDFFKS

AMPEGYVQERTIFFKDDGNYKTRAEVKFEGDTLVNRIELKGIDFKEDGNI

LGHKLEYNYNSHNVYIMADKQKNGIKVNFKIRHNIEDGSVQLADHYQQNT

PIGDGPVLLPDNHYLSYQSALSKDPNEKRDHMVLLEFVTAAGITLGMDEL

YKFCYENEV

-continued

(eYFP-NpHR3.1 amino acid sequence):

SEQ ID NO: 3

MVTQRELFEFVLNDPLLASSLYINIALAGLSILLFVFMTRGLDDPRAKLI

AVSTILVPVVSIASYTGLASGLTISVLEMPAGHFAEGSSVMLGGEEVDGV

VTMWGRYLTWALSTPMILLALGLLAGSNATKLFTAITFDIAMCVTGLAAA

LTTSSHLMRWFWYAISCACFLVVLYILLVEWAQDAKAAGTADMFNTLKLL

TVVMWLGYPIVWALGVEGIAVLPVGVTSWGYSFLDIVAKYIFAFLLLNYL

TSNESVVSGSILDVPSASGTPADDAAAKSRITSEGEYIPLDQIDINVVSK

GEELFTGVVPILVELDGDVNGHKFSVSGEGEGDATYGKLTLKFICTTGKL

PVPWPTLVTTFGYGLQCFARYPDHMKQHDFFKSAMPEGYVQERTIFFKDD

GNYKTRAEVKFEGDTLVNRIELKGIDFKEDGNILGHKLEYNYNSHNVYIM

ADKQKNGIKVNFKIRHNIEDGSVQLADHYQQNTPIGDGPVLLPDNHYLSY

QSASKDPNEKRDHMVLLEFVTAAGITLGMDELYKFCYENEV

(GtR3 amino acid sequence):

SEQ ID NO: 4

ASSFGKALLEFVFIVFACITLLLGINAAKSKAASRVLFPATFVTGIASIA

YFSMASGGGWVIAPDCRQLFVARYLDWLITTPLLLIDLGLVAGVSRWDIM

ALCLSDVLMIATGAFGSLTVGNVKWVWWFFGMCWFLHIIFALGKSWAEAA

KAKGGDSASVYSKIAGITVITWFCYPVVWVFAEGFGNFSVTFEVLIYGVL

DVISKAVFGLILMSGAATGYESI

(ChR2 amino acid sequence):

SEQ ID NO: 5

MDYGGALSAVGRELLFVTNPVVVNGSVLVPEDQCYCAGWIESRGTNGAQT

ASNVLQWLAAGFSILLLMFYAYQTWKSTCGWEEIYVCAIEMVKVILEFFF

EFKNPSMLYLATGHRVQWLRYAEWLLTCPVILIHLSNLTGLSNDYSRRTM

GLLVSDIGTIVWGATSAMATGYVKVIFFCLGLCYGANTFFHAAKAYIEGY

HTVPKGRCRQVVTGMAWLFFVSWGMFPILFILGPEGFGVLSVYGSTVGHT

IIDLMSKNCWGLLGHYLRVLIHEHILIHGDIRKTTKLNIGGTEIEVETLV

EDEAEAGAVP

(SFO amino acid sequence):

SEQ ID NO: 6

MDYGGALSAVGRELLFVTNPVVVNGSVLVPEDQCYCAGWIESRGTNGAQT

ASNVLQWLAAGFSILLLMFYAYQTWKSTCGWEEIYVCAIEMVKVILEFFF

EFKNPSMLYLATGHRVQWLRYAEWLLTSPVILIHLSNLTGLSNDYSRRTM

GLLVSDIGTIVWGATSAMATGYVKVIFFCLGLCYGANTFFHAAKAYIEGY

HTVPKGRCRQVVTGMAWLFFVSWGMFPILFILGPEGFGVLSVYGSTVGHT

IIDLMSKNCWGLLGHYLRVLIHEHILIHGDIRKTTKLNIGGTEIEVETLV

EDEAEAGAVP

(SSFO amino acid sequence):

SEQ ID NO: 7

MDYGGALSAVGRELLFVTNPVVVNGSVLVPEDQCYCAGWIESRGTNGAQT

ASNVLQWLAAGFSILLLMFYAYQTWKSTCGWEEIYVCAIEMVKVILEFFF

EFKNPSMLYLATGHRVQWLRYAEWLLTSPVILIHLSNLTGLSNDYSRRTM

GLLVSAIGTIVWGATSAMATGYVKVIFFCLGLCYGANTFFHAAKAYIEGY

-continued

HTVPKGRCRQVVTGMAWLFFVSWGMFPILFILGPEGFGVLSVYGSTVGHT

IIDLMSKNCWGLLGHYLRVLIHEHILIHGDIRKTTKLNIGGTEIEVETLV

EDEAEAGAVP

(C1V1 amino acid sequence):

SEQ ID NO: 8

MSRRPWLLALALAVALAAGSAGASTGSDATVPVATQDGPDYVFHRAHERM

LFQTSYTLENNGSVICIPNNGQCFCLAWLKSNGTNAEKLAANILQWITFA

LSALCLMFYGYQTWKSTCGWEEIYVATIEMIKFIIEYFHEFDEPAVIYSS

NGNKTVWLRYAEWLLTCPVLLIHLSNLTGLKDDYSKRTMGLLVSDVGCIV

WGATSAMCTGWTKILFFLISLSYGMYTYFHAAKVYIEAFHTVPKGICREL

VRVMAWTFFVAWGMFPVLFLLGTEGFGHISPYGSAIGHSILDLIAKNMWG

VLGNYLRVKIHEHILLYGDIRKKQKITIAGQEMEVETLVAEEED

(C1V1-E122T amino acid sequence):

SEQ ID NO: 9

MSRRPWLLALALAVALAAGSAGASTGSDATVPVATQDGPDYVFHRAHERM

LFQTSYTLENNGSVICIPNNGQCFCLAWLKSNGTNAEKLAANILQWITFA

LSALCLMFYGYQTWKSTCGWETIYVATIEMIKFIIEYFHEFDEPAVIYSS

NGNKTVWLRYAEWLLTCPVLLIHLSNLTGLKDDYSKRTMGLLVSDVGCIV

WGATSAMCTGWTKILFFLISLSYGMYTYFHAAKVYIEAFHTVPKGICREL

-continued

VRVMAWTFFVAWGMFPVLFLLGTEGFGHISPYGSAIGHSILDLIAKNMWG

VLGNYLRVKIHEHILLYGDIRKKQKITIAGQEMEVETLVAEEED

(C1V1-E162T amino acid sequence):

SEQ ID NO: 10

MSRRPWLLALALAVALAAGSAGASTGSDATVPVATQDGPDYVFHRAHERM

LFQTSYTLENNGSVICIPNNGQCFCLAWLKSNGTNAEKLAANILQWITFA

LSALCLMFYGYQTWKSTCGWEEIYVATIEMIKFIIEYFHEFDEPAVIYSS

NGNKTVWLRYATWLLTCPVLLIHLSNLTGLKDDYSKRTMGLLVSDVGCIV

WGATSAMCTGWTKILFFLISLSYGMYTYFHAAKVYIEAFHTVPKGICREL

VRVMAWTFFVAWGMFPVLFLLGTEGFGHISPYGSAIGHSILDLIAKNMWG

VLGNYLRVKIHEHILLYGDIRKKQKITIAGQEMEVETLVAEEED

(C1V1-E122T/E162T amino acid sequence):

SEQ ID NO: 11

MSRRPWLLALALAVALAAGSAGASTGSDATVPVATQDGPDYVFHRAHERM

LFQTSYTLENNGSVICIPNNGQCFCLAWLKSNGTNAEKLAANILQWITFA

LSALCLMFYGYQTWKSTCGWETIYVATIEMIKFIIEYFHEFDEPAVIYSS

NGNKTVWLRYATWLLTCPVLLIHLSNLTGLKDDYSKRTMGLLVSDVGCIV

WGATSAMCTGWTKILFFLISLSYGMYTYFHAAKVYIEAFHTVPKGICREL

VRVMAWTFFVAWGMFPVLFLLGTEGFGHISPYGSAIGHSILDLIAKNMWG

VLGNYLRVKIHEHILLYGDIRKKQKITIAGQEMEVETLVAEEED

SEQUENCE LISTING

<160> NUMBER OF SEQ ID NOS: 15

<210> SEQ ID NO 1
<211> LENGTH: 273
<212> TYPE: PRT
<213> ORGANISM: Natronomonas pharaonis

<400> SEQUENCE: 1

Val Thr Gln Arg Glu Leu Phe Glu Phe Val Leu Asn Asp Pro Leu Leu
1 5 10 15

Ala Ser Ser Leu Tyr Ile Asn Ile Ala Leu Ala Gly Leu Ser Ile Leu
20 25 30

Leu Phe Val Phe Met Thr Arg Gly Leu Asp Asp Pro Arg Ala Lys Leu
35 40 45

Ile Ala Val Ser Thr Ile Leu Val Pro Val Val Ser Ile Ala Ser Tyr
50 55 60

Thr Gly Leu Ala Ser Gly Leu Thr Ile Ser Val Leu Glu Met Pro Ala
65 70 75 80

Gly His Phe Ala Glu Gly Ser Ser Val Met Leu Gly Gly Glu Glu Val
85 90 95

Asp Gly Val Val Thr Met Trp Gly Arg Tyr Leu Thr Trp Ala Leu Ser
100 105 110

Thr Pro Met Ile Leu Leu Ala Leu Gly Leu Leu Ala Gly Ser Asn Ala
115 120 125

Thr Lys Leu Phe Thr Ala Ile Thr Phe Asp Ile Ala Met Cys Val Thr
130 135 140

-continued

```
Gly Leu Ala Ala Ala Leu Thr Thr Ser Ser His Leu Met Arg Trp Phe
145                 150                 155                 160

Trp Tyr Ala Ile Ser Cys Ala Cys Phe Leu Val Val Leu Tyr Ile Leu
                165                 170                 175

Leu Val Glu Trp Ala Gln Asp Ala Lys Ala Ala Gly Thr Ala Asp Met
            180                 185                 190

Phe Asn Thr Leu Lys Leu Leu Thr Val Val Met Trp Leu Gly Tyr Pro
        195                 200                 205

Ile Val Trp Ala Leu Gly Val Glu Gly Ile Ala Val Leu Pro Val Gly
    210                 215                 220

Val Thr Ser Trp Gly Tyr Ser Phe Leu Asp Ile Val Ala Lys Tyr Ile
225                 230                 235                 240

Phe Ala Phe Leu Leu Leu Asn Tyr Leu Thr Ser Asn Glu Ser Val Val
                245                 250                 255

Ser Gly Ser Ile Leu Asp Val Pro Ser Ala Ser Gly Thr Pro Ala Asp
            260                 265                 270

Asp
```

```
<210> SEQ ID NO 2
<211> LENGTH: 559
<212> TYPE: PRT
<213> ORGANISM: Artificial Sequence
<220> FEATURE:
<223> OTHER INFORMATION: Synthetic polypeptide

<400> SEQUENCE: 2

Met Thr Glu Thr Leu Pro Pro Val Thr Glu Ser Ala Val Ala Leu Gln
1               5                   10                  15

Ala Glu Val Thr Gln Arg Glu Leu Phe Glu Phe Val Leu Asn Asp Pro
            20                  25                  30

Leu Leu Ala Ser Ser Leu Tyr Ile Asn Ile Ala Leu Ala Gly Leu Ser
        35                  40                  45

Ile Leu Leu Phe Val Phe Met Thr Arg Gly Leu Asp Asp Pro Arg Ala
    50                  55                  60

Lys Leu Ile Ala Val Ser Thr Ile Leu Val Pro Val Val Ser Ile Ala
65                  70                  75                  80

Ser Tyr Thr Gly Leu Ala Ser Gly Leu Thr Ile Ser Val Leu Glu Met
                85                  90                  95

Pro Ala Gly His Phe Ala Glu Gly Ser Ser Val Met Leu Gly Gly Glu
            100                 105                 110

Glu Val Asp Gly Val Val Thr Met Trp Gly Arg Tyr Leu Thr Trp Ala
        115                 120                 125

Leu Ser Thr Pro Met Ile Leu Leu Ala Leu Gly Leu Leu Ala Gly Ser
    130                 135                 140

Asn Ala Thr Lys Leu Phe Thr Ala Ile Thr Phe Asp Ile Ala Met Cys
145                 150                 155                 160

Val Thr Gly Leu Ala Ala Ala Leu Thr Thr Ser Ser His Leu Met Arg
                165                 170                 175

Trp Phe Trp Tyr Ala Ile Ser Cys Ala Cys Phe Leu Val Val Leu Tyr
            180                 185                 190

Ile Leu Leu Val Glu Trp Ala Gln Asp Ala Lys Ala Ala Gly Thr Ala
        195                 200                 205

Asp Met Phe Asn Thr Leu Lys Leu Leu Thr Val Val Met Trp Leu Gly
```

-continued

```
    210                 215                 220

Tyr Pro Ile Val Trp Ala Leu Gly Val Glu Gly Ile Ala Val Leu Pro
225                 230                 235                 240

Val Gly Val Thr Ser Trp Gly Tyr Ser Phe Leu Asp Ile Val Ala Lys
                245                 250                 255

Tyr Ile Phe Ala Phe Leu Leu Leu Asn Tyr Leu Thr Ser Asn Glu Ser
            260                 265                 270

Val Val Ser Gly Ser Ile Leu Asp Val Pro Ser Ala Ser Gly Thr Pro
        275                 280                 285

Ala Asp Asp Ala Ala Ala Lys Ser Arg Ile Thr Ser Glu Gly Glu Tyr
    290                 295                 300

Ile Pro Leu Asp Gln Ile Asp Ile Asn Val Val Ser Lys Gly Glu Glu
305                 310                 315                 320

Leu Phe Thr Gly Val Val Pro Ile Leu Val Glu Leu Asp Gly Asp Val
                325                 330                 335

Asn Gly His Lys Phe Ser Val Ser Gly Glu Gly Glu Gly Asp Ala Thr
            340                 345                 350

Tyr Gly Lys Leu Thr Leu Lys Phe Ile Cys Thr Thr Gly Lys Leu Pro
        355                 360                 365

Val Pro Trp Pro Thr Leu Val Thr Thr Phe Gly Tyr Gly Leu Gln Cys
    370                 375                 380

Phe Ala Arg Tyr Pro Asp His Met Lys Gln His Asp Phe Phe Lys Ser
385                 390                 395                 400

Ala Met Pro Glu Gly Tyr Val Gln Glu Arg Thr Ile Phe Phe Lys Asp
                405                 410                 415

Asp Gly Asn Tyr Lys Thr Arg Ala Glu Val Lys Phe Glu Gly Asp Thr
            420                 425                 430

Leu Val Asn Arg Ile Glu Leu Lys Gly Ile Asp Phe Lys Glu Asp Gly
        435                 440                 445

Asn Ile Leu Gly His Lys Leu Glu Tyr Asn Tyr Asn Ser His Asn Val
    450                 455                 460

Tyr Ile Met Ala Asp Lys Gln Lys Asn Gly Ile Lys Val Asn Phe Lys
465                 470                 475                 480

Ile Arg His Asn Ile Glu Asp Gly Ser Val Gln Leu Ala Asp His Tyr
                485                 490                 495

Gln Gln Asn Thr Pro Ile Gly Asp Gly Pro Val Leu Leu Pro Asp Asn
            500                 505                 510

His Tyr Leu Ser Tyr Gln Ser Ala Leu Ser Lys Asp Pro Asn Glu Lys
        515                 520                 525

Arg Asp His Met Val Leu Leu Glu Phe Val Thr Ala Ala Gly Ile Thr
    530                 535                 540

Leu Gly Met Asp Glu Leu Tyr Lys Phe Cys Tyr Glu Asn Glu Val
545                 550                 555


<210> SEQ ID NO 3
<211> LENGTH: 542
<212> TYPE: PRT
<213> ORGANISM: Artificial Sequence
<220> FEATURE:
<223> OTHER INFORMATION: Synthetic polypeptide

<400> SEQUENCE: 3

Met Val Thr Gln Arg Glu Leu Phe Glu Phe Val Leu Asn Asp Pro Leu
```

-continued

```
1               5                   10                  15

Leu Ala Ser Ser Leu Tyr Ile Asn Ile Ala Leu Ala Gly Leu Ser Ile
            20                  25                  30

Leu Leu Phe Val Phe Met Thr Arg Gly Leu Asp Asp Pro Arg Ala Lys
        35                  40                  45

Leu Ile Ala Val Ser Thr Ile Leu Val Pro Val Val Ser Ile Ala Ser
    50                  55                  60

Tyr Thr Gly Leu Ala Ser Gly Leu Thr Ile Ser Val Leu Glu Met Pro
65                  70                  75                  80

Ala Gly His Phe Ala Glu Gly Ser Ser Val Met Leu Gly Gly Glu Glu
                85                  90                  95

Val Asp Gly Val Val Thr Met Trp Gly Arg Tyr Leu Thr Trp Ala Leu
            100                 105                 110

Ser Thr Pro Met Ile Leu Leu Ala Leu Gly Leu Leu Ala Gly Ser Asn
        115                 120                 125

Ala Thr Lys Leu Phe Thr Ala Ile Thr Phe Asp Ile Ala Met Cys Val
    130                 135                 140

Thr Gly Leu Ala Ala Ala Leu Thr Thr Ser Ser His Leu Met Arg Trp
145                 150                 155                 160

Phe Trp Tyr Ala Ile Ser Cys Ala Cys Phe Leu Val Val Leu Tyr Ile
                165                 170                 175

Leu Leu Val Glu Trp Ala Gln Asp Ala Lys Ala Ala Gly Thr Ala Asp
            180                 185                 190

Met Phe Asn Thr Leu Lys Leu Leu Thr Val Val Met Trp Leu Gly Tyr
        195                 200                 205

Pro Ile Val Trp Ala Leu Gly Val Glu Gly Ile Ala Val Leu Pro Val
    210                 215                 220

Gly Val Thr Ser Trp Gly Tyr Ser Phe Leu Asp Ile Val Ala Lys Tyr
225                 230                 235                 240

Ile Phe Ala Phe Leu Leu Leu Asn Tyr Leu Thr Ser Asn Glu Ser Val
                245                 250                 255

Val Ser Gly Ser Ile Leu Asp Val Pro Ser Ala Ser Gly Thr Pro Ala
            260                 265                 270

Asp Asp Ala Ala Ala Lys Ser Arg Ile Thr Ser Glu Gly Glu Tyr Ile
        275                 280                 285

Pro Leu Asp Gln Ile Asp Ile Asn Val Val Ser Lys Gly Glu Glu Leu
    290                 295                 300

Phe Thr Gly Val Val Pro Ile Leu Val Glu Leu Asp Gly Asp Val Asn
305                 310                 315                 320

Gly His Lys Phe Ser Val Ser Gly Glu Gly Glu Gly Asp Ala Thr Tyr
                325                 330                 335

Gly Lys Leu Thr Leu Lys Phe Ile Cys Thr Thr Gly Lys Leu Pro Val
            340                 345                 350

Pro Trp Pro Thr Leu Val Thr Thr Phe Gly Tyr Gly Leu Gln Cys Phe
        355                 360                 365

Ala Arg Tyr Pro Asp His Met Lys Gln His Asp Phe Phe Lys Ser Ala
    370                 375                 380

Met Pro Glu Gly Tyr Val Gln Glu Arg Thr Ile Phe Phe Lys Asp Asp
385                 390                 395                 400

Gly Asn Tyr Lys Thr Arg Ala Glu Val Lys Phe Glu Gly Asp Thr Leu
                405                 410                 415
```

-continued

```
Val Asn Arg Ile Glu Leu Lys Gly Ile Asp Phe Lys Glu Asp Gly Asn
            420                 425                 430

Ile Leu Gly His Lys Leu Glu Tyr Asn Tyr Asn Ser His Asn Val Tyr
        435                 440                 445

Ile Met Ala Asp Lys Gln Lys Asn Gly Ile Lys Val Asn Phe Lys Ile
    450                 455                 460

Arg His Asn Ile Glu Asp Gly Ser Val Gln Leu Ala Asp His Tyr Gln
465                 470                 475                 480

Gln Asn Thr Pro Ile Gly Asp Gly Pro Val Leu Leu Pro Asp Asn His
                485                 490                 495

Tyr Leu Ser Tyr Gln Ser Ala Leu Ser Lys Asp Pro Asn Glu Lys Arg
            500                 505                 510

Asp His Met Val Leu Leu Glu Phe Val Thr Ala Ala Gly Ile Thr Leu
        515                 520                 525

Gly Met Asp Glu Leu Tyr Lys Phe Cys Tyr Glu Asn Glu Val
    530                 535                 540


<210> SEQ ID NO 4
<211> LENGTH: 223
<212> TYPE: PRT
<213> ORGANISM: Guillardia theta

<400> SEQUENCE: 4

Ala Ser Ser Phe Gly Lys Ala Leu Leu Glu Phe Val Phe Ile Val Phe
1               5                   10                  15

Ala Cys Ile Thr Leu Leu Leu Gly Ile Asn Ala Ala Lys Ser Lys Ala
            20                  25                  30

Ala Ser Arg Val Leu Phe Pro Ala Thr Phe Val Thr Gly Ile Ala Ser
        35                  40                  45

Ile Ala Tyr Phe Ser Met Ala Ser Gly Gly Gly Trp Val Ile Ala Pro
    50                  55                  60

Asp Cys Arg Gln Leu Phe Val Ala Arg Tyr Leu Asp Trp Leu Ile Thr
65                  70                  75                  80

Thr Pro Leu Leu Leu Ile Asp Leu Gly Leu Val Ala Gly Val Ser Arg
                85                  90                  95

Trp Asp Ile Met Ala Leu Cys Leu Ser Asp Val Leu Met Ile Ala Thr
            100                 105                 110

Gly Ala Phe Gly Ser Leu Thr Val Gly Asn Val Lys Trp Val Trp Trp
        115                 120                 125

Phe Phe Gly Met Cys Trp Phe Leu His Ile Ile Phe Ala Leu Gly Lys
    130                 135                 140

Ser Trp Ala Glu Ala Ala Lys Ala Lys Gly Gly Asp Ser Ala Ser Val
145                 150                 155                 160

Tyr Ser Lys Ile Ala Gly Ile Thr Val Ile Thr Trp Phe Cys Tyr Pro
                165                 170                 175

Val Val Trp Val Phe Ala Glu Gly Phe Gly Asn Phe Ser Val Thr Phe
            180                 185                 190

Glu Val Leu Ile Tyr Gly Val Leu Asp Val Ile Ser Lys Ala Val Phe
        195                 200                 205

Gly Leu Ile Leu Met Ser Gly Ala Ala Thr Gly Tyr Glu Ser Ile
    210                 215                 220
```

-continued

<210> SEQ ID NO 5
<211> LENGTH: 310
<212> TYPE: PRT
<213> ORGANISM: Artificial Sequence
<220> FEATURE:
<223> OTHER INFORMATION: Synthetic polypeptide

<400> SEQUENCE: 5

Met Asp Tyr Gly Gly Ala Leu Ser Ala Val Gly Arg Glu Leu Leu Phe
1 5 10 15

Val Thr Asn Pro Val Val Val Asn Gly Ser Val Leu Val Pro Glu Asp
20 25 30

Gln Cys Tyr Cys Ala Gly Trp Ile Glu Ser Arg Gly Thr Asn Gly Ala
35 40 45

Gln Thr Ala Ser Asn Val Leu Gln Trp Leu Ala Ala Gly Phe Ser Ile
50 55 60

Leu Leu Leu Met Phe Tyr Ala Tyr Gln Thr Trp Lys Ser Thr Cys Gly
65 70 75 80

Trp Glu Glu Ile Tyr Val Cys Ala Ile Glu Met Val Lys Val Ile Leu
85 90 95

Glu Phe Phe Phe Glu Phe Lys Asn Pro Ser Met Leu Tyr Leu Ala Thr
100 105 110

Gly His Arg Val Gln Trp Leu Arg Tyr Ala Glu Trp Leu Leu Thr Cys
115 120 125

Pro Val Ile Leu Ile His Leu Ser Asn Leu Thr Gly Leu Ser Asn Asp
130 135 140

Tyr Ser Arg Arg Thr Met Gly Leu Leu Val Ser Asp Ile Gly Thr Ile
145 150 155 160

Val Trp Gly Ala Thr Ser Ala Met Ala Thr Gly Tyr Val Lys Val Ile
165 170 175

Phe Phe Cys Leu Gly Leu Cys Tyr Gly Ala Asn Thr Phe Phe His Ala
180 185 190

Ala Lys Ala Tyr Ile Glu Gly Tyr His Thr Val Pro Lys Gly Arg Cys
195 200 205

Arg Gln Val Val Thr Gly Met Ala Trp Leu Phe Phe Val Ser Trp Gly
210 215 220

Met Phe Pro Ile Leu Phe Ile Leu Gly Pro Glu Gly Phe Gly Val Leu
225 230 235 240

Ser Val Tyr Gly Ser Thr Val Gly His Thr Ile Ile Asp Leu Met Ser
245 250 255

Lys Asn Cys Trp Gly Leu Leu Gly His Tyr Leu Arg Val Leu Ile His
260 265 270

Glu His Ile Leu Ile His Gly Asp Ile Arg Lys Thr Thr Lys Leu Asn
275 280 285

Ile Gly Gly Thr Glu Ile Glu Val Glu Thr Leu Val Glu Asp Glu Ala
290 295 300

Glu Ala Gly Ala Val Pro
305 310

<210> SEQ ID NO 6
<211> LENGTH: 310
<212> TYPE: PRT
<213> ORGANISM: Artificial Sequence
<220> FEATURE:
<223> OTHER INFORMATION: Synthetic polypeptide

-continued

<400> SEQUENCE: 6

```
Met Asp Tyr Gly Gly Ala Leu Ser Ala Val Gly Arg Glu Leu Leu Phe
1               5                   10                  15

Val Thr Asn Pro Val Val Val Asn Gly Ser Val Leu Val Pro Glu Asp
            20                  25                  30

Gln Cys Tyr Cys Ala Gly Trp Ile Glu Ser Arg Gly Thr Asn Gly Ala
        35                  40                  45

Gln Thr Ala Ser Asn Val Leu Gln Trp Leu Ala Ala Gly Phe Ser Ile
    50                  55                  60

Leu Leu Leu Met Phe Tyr Ala Tyr Gln Thr Trp Lys Ser Thr Cys Gly
65                  70                  75                  80

Trp Glu Glu Ile Tyr Val Cys Ala Ile Glu Met Val Lys Val Ile Leu
                85                  90                  95

Glu Phe Phe Phe Glu Phe Lys Asn Pro Ser Met Leu Tyr Leu Ala Thr
            100                 105                 110

Gly His Arg Val Gln Trp Leu Arg Tyr Ala Glu Trp Leu Leu Thr Ser
        115                 120                 125

Pro Val Ile Leu Ile His Leu Ser Asn Leu Thr Gly Leu Ser Asn Asp
    130                 135                 140

Tyr Ser Arg Arg Thr Met Gly Leu Leu Val Ser Asp Ile Gly Thr Ile
145                 150                 155                 160

Val Trp Gly Ala Thr Ser Ala Met Ala Thr Gly Tyr Val Lys Val Ile
                165                 170                 175

Phe Phe Cys Leu Gly Leu Cys Tyr Gly Ala Asn Thr Phe Phe His Ala
            180                 185                 190

Ala Lys Ala Tyr Ile Glu Gly Tyr His Thr Val Pro Lys Gly Arg Cys
        195                 200                 205

Arg Gln Val Val Thr Gly Met Ala Trp Leu Phe Phe Val Ser Trp Gly
    210                 215                 220

Met Phe Pro Ile Leu Phe Ile Leu Gly Pro Glu Gly Phe Gly Val Leu
225                 230                 235                 240

Ser Val Tyr Gly Ser Thr Val Gly His Thr Ile Ile Asp Leu Met Ser
                245                 250                 255

Lys Asn Cys Trp Gly Leu Leu Gly His Tyr Leu Arg Val Leu Ile His
            260                 265                 270

Glu His Ile Leu Ile His Gly Asp Ile Arg Lys Thr Thr Lys Leu Asn
        275                 280                 285

Ile Gly Gly Thr Glu Ile Glu Val Glu Thr Leu Val Glu Asp Glu Ala
    290                 295                 300

Glu Ala Gly Ala Val Pro
305                 310
```

<210> SEQ ID NO 7
<211> LENGTH: 310
<212> TYPE: PRT
<213> ORGANISM: Artificial Sequence
<220> FEATURE:
<223> OTHER INFORMATION: Synthetic polypeptide

<400> SEQUENCE: 7

```
Met Asp Tyr Gly Gly Ala Leu Ser Ala Val Gly Arg Glu Leu Leu Phe
1               5                   10                  15
```

-continued

```
Val Thr Asn Pro Val Val Val Asn Gly Ser Val Leu Val Pro Glu Asp
            20                  25                  30

Gln Cys Tyr Cys Ala Gly Trp Ile Glu Ser Arg Gly Thr Asn Gly Ala
        35                  40                  45

Gln Thr Ala Ser Asn Val Leu Gln Trp Leu Ala Ala Gly Phe Ser Ile
    50                  55                  60

Leu Leu Leu Met Phe Tyr Ala Tyr Gln Thr Trp Lys Ser Thr Cys Gly
65                  70                  75                  80

Trp Glu Glu Ile Tyr Val Cys Ala Ile Glu Met Val Lys Val Ile Leu
                85                  90                  95

Glu Phe Phe Phe Glu Phe Lys Asn Pro Ser Met Leu Tyr Leu Ala Thr
            100                 105                 110

Gly His Arg Val Gln Trp Leu Arg Tyr Ala Glu Trp Leu Leu Thr Ser
        115                 120                 125

Pro Val Ile Leu Ile His Leu Ser Asn Leu Thr Gly Leu Ser Asn Asp
    130                 135                 140

Tyr Ser Arg Arg Thr Met Gly Leu Leu Val Ser Ala Ile Gly Thr Ile
145                 150                 155                 160

Val Trp Gly Ala Thr Ser Ala Met Ala Thr Gly Tyr Val Lys Val Ile
                165                 170                 175

Phe Phe Cys Leu Gly Leu Cys Tyr Gly Ala Asn Thr Phe Phe His Ala
            180                 185                 190

Ala Lys Ala Tyr Ile Glu Gly Tyr His Thr Val Pro Lys Gly Arg Cys
        195                 200                 205

Arg Gln Val Val Thr Gly Met Ala Trp Leu Phe Phe Val Ser Trp Gly
    210                 215                 220

Met Phe Pro Ile Leu Phe Ile Leu Gly Pro Glu Gly Phe Gly Val Leu
225                 230                 235                 240

Ser Val Tyr Gly Ser Thr Val Gly His Thr Ile Ile Asp Leu Met Ser
                245                 250                 255

Lys Asn Cys Trp Gly Leu Leu Gly His Tyr Leu Arg Val Leu Ile His
            260                 265                 270

Glu His Ile Leu Ile His Gly Asp Ile Arg Lys Thr Thr Lys Leu Asn
        275                 280                 285

Ile Gly Gly Thr Glu Ile Glu Val Glu Thr Leu Val Glu Asp Glu Ala
    290                 295                 300

Glu Ala Gly Ala Val Pro
305                 310


<210> SEQ ID NO 8
<211> LENGTH: 344
<212> TYPE: PRT
<213> ORGANISM: Artificial Sequence
<220> FEATURE:
<223> OTHER INFORMATION: Synthetic polypeptide

<400> SEQUENCE: 8

Met Ser Arg Arg Pro Trp Leu Leu Ala Leu Ala Leu Ala Val Ala Leu
1               5                   10                  15

Ala Ala Gly Ser Ala Gly Ala Ser Thr Gly Ser Asp Ala Thr Val Pro
            20                  25                  30

Val Ala Thr Gln Asp Gly Pro Asp Tyr Val Phe His Arg Ala His Glu
        35                  40                  45
```

-continued

```
Arg Met Leu Phe Gln Thr Ser Tyr Thr Leu Glu Asn Asn Gly Ser Val
    50                  55                  60

Ile Cys Ile Pro Asn Asn Gly Gln Cys Phe Cys Leu Ala Trp Leu Lys
65                  70                  75                  80

Ser Asn Gly Thr Asn Ala Glu Lys Leu Ala Ala Asn Ile Leu Gln Trp
                85                  90                  95

Ile Thr Phe Ala Leu Ser Ala Leu Cys Leu Met Phe Tyr Gly Tyr Gln
            100                 105                 110

Thr Trp Lys Ser Thr Cys Gly Trp Glu Glu Ile Tyr Val Ala Thr Ile
        115                 120                 125

Glu Met Ile Lys Phe Ile Ile Glu Tyr Phe His Glu Phe Asp Glu Pro
    130                 135                 140

Ala Val Ile Tyr Ser Ser Asn Gly Asn Lys Thr Val Trp Leu Arg Tyr
145                 150                 155                 160

Ala Glu Trp Leu Leu Thr Cys Pro Val Leu Leu Ile His Leu Ser Asn
                165                 170                 175

Leu Thr Gly Leu Lys Asp Asp Tyr Ser Lys Arg Thr Met Gly Leu Leu
            180                 185                 190

Val Ser Asp Val Gly Cys Ile Val Trp Gly Ala Thr Ser Ala Met Cys
        195                 200                 205

Thr Gly Trp Thr Lys Ile Leu Phe Phe Leu Ile Ser Leu Ser Tyr Gly
    210                 215                 220

Met Tyr Thr Tyr Phe His Ala Ala Lys Val Tyr Ile Glu Ala Phe His
225                 230                 235                 240

Thr Val Pro Lys Gly Ile Cys Arg Glu Leu Val Arg Val Met Ala Trp
                245                 250                 255

Thr Phe Phe Val Ala Trp Gly Met Phe Pro Val Leu Phe Leu Leu Gly
            260                 265                 270

Thr Glu Gly Phe Gly His Ile Ser Pro Tyr Gly Ser Ala Ile Gly His
        275                 280                 285

Ser Ile Leu Asp Leu Ile Ala Lys Asn Met Trp Gly Val Leu Gly Asn
    290                 295                 300

Tyr Leu Arg Val Lys Ile His Glu His Ile Leu Leu Tyr Gly Asp Ile
305                 310                 315                 320

Arg Lys Lys Gln Lys Ile Thr Ile Ala Gly Gln Glu Met Glu Val Glu
                325                 330                 335

Thr Leu Val Ala Glu Glu Glu Asp
            340


<210> SEQ ID NO 9
<211> LENGTH: 344
<212> TYPE: PRT
<213> ORGANISM: Artificial Sequence
<220> FEATURE:
<223> OTHER INFORMATION: Synthetic polypeptide

<400> SEQUENCE: 9

Met Ser Arg Arg Pro Trp Leu Leu Ala Leu Ala Leu Ala Val Ala Leu
1               5                   10                  15

Ala Ala Gly Ser Ala Gly Ala Ser Thr Gly Ser Asp Ala Thr Val Pro
            20                  25                  30

Val Ala Thr Gln Asp Gly Pro Asp Tyr Val Phe His Arg Ala His Glu
        35                  40                  45
```

-continued

```
Arg Met Leu Phe Gln Thr Ser Tyr Thr Leu Glu Asn Asn Gly Ser Val
    50                  55                  60

Ile Cys Ile Pro Asn Asn Gly Gln Cys Phe Cys Leu Ala Trp Leu Lys
65                  70                  75                  80

Ser Asn Gly Thr Asn Ala Glu Lys Leu Ala Ala Asn Ile Leu Gln Trp
                85                  90                  95

Ile Thr Phe Ala Leu Ser Ala Leu Cys Leu Met Phe Tyr Gly Tyr Gln
            100                 105                 110

Thr Trp Lys Ser Thr Cys Gly Trp Glu Thr Ile Tyr Val Ala Thr Ile
        115                 120                 125

Glu Met Ile Lys Phe Ile Ile Glu Tyr Phe His Glu Phe Asp Glu Pro
    130                 135                 140

Ala Val Ile Tyr Ser Ser Asn Gly Asn Lys Thr Val Trp Leu Arg Tyr
145                 150                 155                 160

Ala Glu Trp Leu Leu Thr Cys Pro Val Leu Leu Ile His Leu Ser Asn
                165                 170                 175

Leu Thr Gly Leu Lys Asp Asp Tyr Ser Lys Arg Thr Met Gly Leu Leu
            180                 185                 190

Val Ser Asp Val Gly Cys Ile Val Trp Gly Ala Thr Ser Ala Met Cys
        195                 200                 205

Thr Gly Trp Thr Lys Ile Leu Phe Phe Leu Ile Ser Leu Ser Tyr Gly
    210                 215                 220

Met Tyr Thr Tyr Phe His Ala Ala Lys Val Tyr Ile Glu Ala Phe His
225                 230                 235                 240

Thr Val Pro Lys Gly Ile Cys Arg Glu Leu Val Arg Val Met Ala Trp
                245                 250                 255

Thr Phe Phe Val Ala Trp Gly Met Phe Pro Val Leu Phe Leu Leu Gly
            260                 265                 270

Thr Glu Gly Phe Gly His Ile Ser Pro Tyr Gly Ser Ala Ile Gly His
        275                 280                 285

Ser Ile Leu Asp Leu Ile Ala Lys Asn Met Trp Gly Val Leu Gly Asn
    290                 295                 300

Tyr Leu Arg Val Lys Ile His Glu His Ile Leu Leu Tyr Gly Asp Ile
305                 310                 315                 320

Arg Lys Lys Gln Lys Ile Thr Ile Ala Gly Gln Glu Met Glu Val Glu
                325                 330                 335

Thr Leu Val Ala Glu Glu Glu Asp
            340


<210> SEQ ID NO 10
<211> LENGTH: 344
<212> TYPE: PRT
<213> ORGANISM: Artificial Sequence
<220> FEATURE:
<223> OTHER INFORMATION: Synthetic polypeptide

<400> SEQUENCE: 10

Met Ser Arg Arg Pro Trp Leu Leu Ala Leu Ala Leu Ala Val Ala Leu
1               5                   10                  15

Ala Ala Gly Ser Ala Gly Ala Ser Thr Gly Ser Asp Ala Thr Val Pro
            20                  25                  30

Val Ala Thr Gln Asp Gly Pro Asp Tyr Val Phe His Arg Ala His Glu
        35                  40                  45
```

-continued

```
Arg Met Leu Phe Gln Thr Ser Tyr Thr Leu Glu Asn Asn Gly Ser Val
    50                  55                  60

Ile Cys Ile Pro Asn Asn Gly Gln Cys Phe Cys Leu Ala Trp Leu Lys
65                  70                  75                  80

Ser Asn Gly Thr Asn Ala Glu Lys Leu Ala Ala Asn Ile Leu Gln Trp
                85                  90                  95

Ile Thr Phe Ala Leu Ser Ala Leu Cys Leu Met Phe Tyr Gly Tyr Gln
            100                 105                 110

Thr Trp Lys Ser Thr Cys Gly Trp Glu Glu Ile Tyr Val Ala Thr Ile
        115                 120                 125

Glu Met Ile Lys Phe Ile Ile Glu Tyr Phe His Glu Phe Asp Glu Pro
    130                 135                 140

Ala Val Ile Tyr Ser Ser Asn Gly Asn Lys Thr Val Trp Leu Arg Tyr
145                 150                 155                 160

Ala Thr Trp Leu Leu Thr Cys Pro Val Leu Leu Ile His Leu Ser Asn
                165                 170                 175

Leu Thr Gly Leu Lys Asp Asp Tyr Ser Lys Arg Thr Met Gly Leu Leu
            180                 185                 190

Val Ser Asp Val Gly Cys Ile Val Trp Gly Ala Thr Ser Ala Met Cys
        195                 200                 205

Thr Gly Trp Thr Lys Ile Leu Phe Phe Leu Ile Ser Leu Ser Tyr Gly
    210                 215                 220

Met Tyr Thr Tyr Phe His Ala Ala Lys Val Tyr Ile Glu Ala Phe His
225                 230                 235                 240

Thr Val Pro Lys Gly Ile Cys Arg Glu Leu Val Arg Val Met Ala Trp
                245                 250                 255

Thr Phe Phe Val Ala Trp Gly Met Phe Pro Val Leu Phe Leu Leu Gly
            260                 265                 270

Thr Glu Gly Phe Gly His Ile Ser Pro Tyr Gly Ser Ala Ile Gly His
        275                 280                 285

Ser Ile Leu Asp Leu Ile Ala Lys Asn Met Trp Gly Val Leu Gly Asn
    290                 295                 300

Tyr Leu Arg Val Lys Ile His Glu His Ile Leu Leu Tyr Gly Asp Ile
305                 310                 315                 320

Arg Lys Lys Gln Lys Ile Thr Ile Ala Gly Gln Glu Met Glu Val Glu
                325                 330                 335

Thr Leu Val Ala Glu Glu Glu Asp
            340


<210> SEQ ID NO 11
<211> LENGTH: 344
<212> TYPE: PRT
<213> ORGANISM: Artificial Sequence
<220> FEATURE:
<223> OTHER INFORMATION: Synthetic polypeptide

<400> SEQUENCE: 11

Met Ser Arg Arg Pro Trp Leu Leu Ala Leu Ala Leu Ala Val Ala Leu
1               5                   10                  15

Ala Ala Gly Ser Ala Gly Ala Ser Thr Gly Ser Asp Ala Thr Val Pro
            20                  25                  30

Val Ala Thr Gln Asp Gly Pro Asp Tyr Val Phe His Arg Ala His Glu
        35                  40                  45
```

-continued

```
Arg Met Leu Phe Gln Thr Ser Tyr Thr Leu Glu Asn Asn Gly Ser Val
    50                  55                  60

Ile Cys Ile Pro Asn Asn Gly Gln Cys Phe Cys Leu Ala Trp Leu Lys
65                  70                  75                  80

Ser Asn Gly Thr Asn Ala Glu Lys Leu Ala Ala Asn Ile Leu Gln Trp
                85                  90                  95

Ile Thr Phe Ala Leu Ser Ala Leu Cys Leu Met Phe Tyr Gly Tyr Gln
            100                 105                 110

Thr Trp Lys Ser Thr Cys Gly Trp Glu Thr Ile Tyr Val Ala Thr Ile
        115                 120                 125

Glu Met Ile Lys Phe Ile Ile Glu Tyr Phe His Glu Phe Asp Glu Pro
    130                 135                 140

Ala Val Ile Tyr Ser Ser Asn Gly Asn Lys Thr Val Trp Leu Arg Tyr
145                 150                 155                 160

Ala Thr Trp Leu Leu Thr Cys Pro Val Leu Leu Ile His Leu Ser Asn
                165                 170                 175

Leu Thr Gly Leu Lys Asp Asp Tyr Ser Lys Arg Thr Met Gly Leu Leu
            180                 185                 190

Val Ser Asp Val Gly Cys Ile Val Trp Gly Ala Thr Ser Ala Met Cys
        195                 200                 205

Thr Gly Trp Thr Lys Ile Leu Phe Phe Leu Ile Ser Leu Ser Tyr Gly
    210                 215                 220

Met Tyr Thr Tyr Phe His Ala Ala Lys Val Tyr Ile Glu Ala Phe His
225                 230                 235                 240

Thr Val Pro Lys Gly Ile Cys Arg Glu Leu Val Arg Val Met Ala Trp
                245                 250                 255

Thr Phe Phe Val Ala Trp Gly Met Phe Pro Val Leu Phe Leu Leu Gly
            260                 265                 270

Thr Glu Gly Phe Gly His Ile Ser Pro Tyr Gly Ser Ala Ile Gly His
        275                 280                 285

Ser Ile Leu Asp Leu Ile Ala Lys Asn Met Trp Gly Val Leu Gly Asn
    290                 295                 300

Tyr Leu Arg Val Lys Ile His Glu His Ile Leu Leu Tyr Gly Asp Ile
305                 310                 315                 320

Arg Lys Lys Gln Lys Ile Thr Ile Ala Gly Gln Glu Met Glu Val Glu
                325                 330                 335

Thr Leu Val Ala Glu Glu Glu Asp
            340


<210> SEQ ID NO 12
<211> LENGTH: 6
<212> TYPE: PRT
<213> ORGANISM: Artificial Sequence
<220> FEATURE:
<223> OTHER INFORMATION: Synthetic peptide
<220> FEATURE:
<221> NAME/KEY: Misc_feature
<222> LOCATION: (2)...(2)
<223> OTHER INFORMATION: X is any amino acid

<400> SEQUENCE: 12

Phe Xaa Tyr Glu Asn Glu
1               5


<210> SEQ ID NO 13
```

-continued

<211> LENGTH: 7
<212> TYPE: PRT
<213> ORGANISM: Artificial Sequence
<220> FEATURE:
<223> OTHER INFORMATION: Synthetic peptide

<400> SEQUENCE: 13

Phe Cys Tyr Glu Asn Glu Val
1 5

<210> SEQ ID NO 14
<211> LENGTH: 20
<212> TYPE: PRT
<213> ORGANISM: Artificial Sequence
<220> FEATURE:
<223> OTHER INFORMATION: Synthetic peptide

<400> SEQUENCE: 14

Lys Ser Arg Ile Thr Ser Glu Gly Glu Tyr Ile Pro Leu Asp Gln Ile
1 5 10 15

Asp Ile Asn Val
20

<210> SEQ ID NO 15
<211> LENGTH: 5
<212> TYPE: PRT
<213> ORGANISM: Artificial Sequence
<220> FEATURE:
<223> OTHER INFORMATION: Synthetic peptide
<220> FEATURE:
<221> NAME/KEY: Misc_feature
<222> LOCATION: (2)...(2)
<223> OTHER INFORMATION: Xaa is any amino acid
<220> FEATURE:
<221> NAME/KEY: Misc_feature
<222> LOCATION: (3)...(3)
<223> OTHER INFORMATION: Xaa is any amino acid

<400> SEQUENCE: 15

Val Xaa Xaa Ser Leu
1 5

1.-**31**. (canceled)

32. A method for alleviating anxiety in an individual, the method comprising:

(a) administering directly into the brain of the individual an effective amount of a recombinant expression vector comprising a nucleic acid encoding a light-responsive opsin that comprises an amino acid sequence having at least 90% amino acid sequence identity to any one of SEQ ID NOs:6-11, wherein the nucleic acid is operably linked to a promoter that controls the specific expression of the opsin in the glutamatergic pyramidal neurons of the basolateral amygdala (BLA), wherein the opsin is expressed in the glutamatergic pyramidal neurons of the BLA, wherein the opsin is an opsin that induces depolarization by light;

(b) implanting a beveled cannula over the centrolateral nucleus (CeL) to prevent light delivery to the BLA somata; and

(c) delivering light from a light delivery device ensheathed in the beveled cannula to selectively illuminate the opsin in the glutamatergic pyramidal neurons in the central nucleus of the amygdala (CeA) to alleviate anxiety.

33. The method of claim **32**, comprising selectively illuminating the centrolateral nuclei (CeL) to alleviate anxiety.

34. The method of claim **32**, wherein the opsin comprises an amino acid sequence having at least 95% amino acid sequence identity to the amino acid sequence set forth in any one of SEQ ID NOs:6-11.

35. The method of claim **32**, wherein the opsin comprises an amino acid sequence having at least 90% amino acid sequence identity to the amino acid sequence set forth in SEQ ID NO:6.

36. The method of claim **32**, wherein the opsin comprises an amino acid sequence having at least 90% amino acid sequence identity to the amino acid sequence set forth in SEQ ID NO:7.

37. The method of claim **32**, wherein the opsin comprises an amino acid sequence having at least 90% amino acid sequence identity to the amino acid sequence set forth in SEQ ID NO:8.

38. The method of claim **32**, wherein the opsin comprises an amino acid sequence having at least 90% amino acid sequence identity to the amino acid sequence set forth in SEQ ID NO:9.

39. The method of claim **32**, wherein the opsin comprises an amino acid sequence having at least 90% amino acid sequence identity to the amino acid sequence set forth in SEQ ID NO:10.

40. The method of claim **32**, wherein the opsin comprises an amino acid sequence having at least 90% amino acid sequence identity to the amino acid sequence set forth in SEQ ID NO:11.

41. The method of claim **32**, wherein the recombinant vector is an adeno-associated vector, a retroviral vector, an adenoviral vector, or a lentiviral vector.

42. The method of claim **32**, wherein the promoter is a CaMKIIa promoter.

43. The method of claim **32**, wherein said light delivery device comprises an optical fiber.

44. The method of claim **32**, wherein the beveled cannula is beveled to form a 45-55-degree angle for the restriction of the illumination to the CeA.

45. The method of claim **44**, wherein the beveled cannula guide comprises a long side that shields the posterior-lateral portion of the light delivery device.

46. The method of claim **32**, further comprising delivering one or more of a pharmacological agent, an electrical stimulus, or a magnetic stimulus to the individual.

* * * * *